

1. Report No. FHWA/TX-85/73+319-1F		2. Government Accession No.		3. Recipient's Catalog No.	
4. Title and Subtitle Synthetic Fibers in Asphalt Paving Mixtures				5. Report Date November, 1984	
				6. Performing Organization Code	
				8. Performing Organization Report No. Research Report 319-1F	
7. Author(s) Joe W. Button and Thomas G. Hunter				10. Work Unit No. (TRAIS)	
9. Performing Organization Name and Address Texas State Department of Highways and Public Transportation; Transportation Planning Division P. O. Box 5051 Austin, Texas 78763				11. Contract or Grant No. Study No. 2-9-82-319	
				13. Type of Report and Period Covered Final - September, 1984 November, 1984	
12. Sponsoring Agency Name and Address Texas Transportation Institute The Texas A&M University System College Station, Texas 77843				14. Sponsoring Agency Code	
				15. Supplementary Notes Research performed in cooperation with DOT, FHWA. Research Study Title: Evaluation of Synthetic Fibers in Asphalt Pavements.	
16. Abstract <p>Laboratory and field tests were performed to evaluate eight types of chopped synthetic fibers as additives to reduce cracking in hot mixed asphalt concrete. Laboratory tests included Hveem and Marshall stability, resilient modulus, indirect tension, flexural and tensile fatigue, creep and resistance to moisture damage. Thin overlays were placed in East and West Texas and observed for periods of one and two years, respectively.</p> <p>Laboratory tests showed that fibers added flexibility to a paving mixture and improved resistance to crack propagation; however, they also increased compaction requirements. There was no significant difference in the performance of any of the eight different fibers.</p> <p>Based on review of literature and early field performance data, the cost effectiveness of fibers as an additive to reduce cracking in asphalt paving mixtures appears questionable.</p>					
17. Key Words Chopped Synthetic Fibers, Asphalt Paving Mixtures, Resistance to Crack Propagation.			18. Distribution Statement No restriction. This document is available to the public through the National Technical Information Service, 5285 Port Royal Road, Springfield, Virginia 22161.		
19. Security Classif. (of this report) Unclassified		20. Security Classif. (of this page) Unclassified		21. No. of Pages 160	22. Price

SYNTHETIC FIBERS
IN
ASPHALT PAVING MIXTURES

by

Joe W. Button
Associate Research Engineer

and

Thomas G. Hunter
Research Associate

Research Report 319-1F
Research Study 2-9-82-319

Sponsored by

State Department of Highways and Public Transportation
In cooperation with
U. S. Department of Transportation, Federal Highway Administration

November 1984

TEXAS TRANSPORTATION INSTITUTE
The Texas A&M University System
College Station, Texas

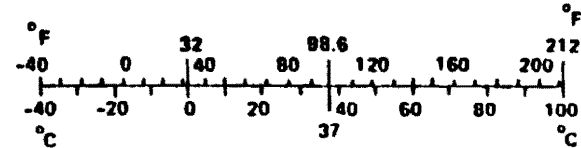
METRIC CONVERSION FACTORS

Approximate Conversions to Metric Measures

Symbol	When You Know	Multiply by	To Find	Symbol
LENGTH				
in	inches	2.5	centimeters	cm
ft	feet	30	centimeters	cm
yd	yards	0.9	meters	m
mi	miles	1.6	kilometers	km
AREA				
in ²	square inches	6.5	square centimeters	cm ²
ft ²	square feet	0.09	square meters	m ²
yd ²	square yards	0.8	square meters	m ²
mi ²	square miles	2.6	square kilometers	km ²
	acres	0.4	hectares	ha
MASS (weight)				
oz	ounces	28	grams	g
lb	pounds	0.45	kilograms	kg
	short tons (2000 lb)	0.9	tonnes	t
VOLUME				
tsp	teaspoons	5	milliliters	ml
Tbsp	tablespoons	15	milliliters	ml
fl oz	fluid ounces	30	milliliters	ml
c	cups	0.24	liters	l
pt	pints	0.47	liters	l
qt	quarts	0.95	liters	l
gal	gallons	3.8	liters	l
ft ³	cubic feet	0.03	cubic meters	m ³
yd ³	cubic yards	0.76	cubic meters	m ³
TEMPERATURE (exact)				
°F	Fahrenheit temperature	5/9 (after subtracting 32)	Celsius temperature	°C

Approximate Conversions from Metric Measures

Symbol	When You Know	Multiply by	To Find	Symbol
LENGTH				
mm	millimeters	0.04	inches	in
cm	centimeters	0.4	inches	in
m	meters	3.3	feet	ft
m	meters	1.1	yards	yd
km	kilometers	0.6	miles	mi
AREA				
cm ²	square centimeters	0.16	square inches	in ²
m ²	square meters	1.2	square yards	yd ²
km ²	square kilometers	0.4	square miles	mi ²
ha	hectares (10,000 m ²)	2.5	acres	
MASS (weight)				
g	grams	0.035	ounces	oz
kg	kilograms	2.2	pounds	lb
t	tonnes (1000 kg)	1.1	short tons	
VOLUME				
ml	milliliters	0.03	fluid ounces	fl oz
l	liters	2.1	pints	pt
l	liters	1.06	quarts	qt
l	liters	0.26	gallons	gal
m ³	cubic meters	35	cubic feet	ft ³
m ³	cubic meters	1.3	cubic yards	yd ³
TEMPERATURE (exact)				
°C	Celsius temperature	9/5 (then add 32)	Fahrenheit temperature	°F



* 1 in = 2.54 (exactly). For other exact conversions and more detailed tables, see NBS Misc. Publ. 286, Units of Weights and Measures, Price \$2.25, SD Catalog No. C13.10:286.

ACKNOWLEDGEMENTS

The authors wish to express their appreciation to Texas SDHPT personnel for their interest and willingness to participate in this research program. The efforts of Kenneth W. Fults (District 11) and Roger G. Welsch, Bobby R. Lindley and Walter L. Plumlee (District 8) are gratefully acknowledged.

Technical guidance for the investigation was provided by Paul E. Krugler of D-9.

Fibers for the test pavements, technical assistance and laboratory data were furnished by Hercules, Inc. Fibers for the test pavement in District 11 were furnished by Kapejo, Inc.

This report was edited by Professor Bob M. Gallaway of the Texas Transportation Institute.

Laboratory testing was conducted by O. Chris Cook and Thomas G. Hunter.

The manuscript was typed by Cathy Roberts, Karen Carroll, Janet Jamison and Bea Cullen.

IMPLEMENTATION STATEMENT

The findings of this study do not warrant widespread use of synthetic fibers in hot mixed asphalt concrete (HMAC) to reduce cracking. However, continued experimentation with fibers in asphalt mixtures is encouraged since certain laboratory test results show significant benefits when fibers are used.

Design of paving mixtures containing fibers may be performed in the usual manner. Addition of fibers in a batch plant is simple. Addition of fibers in a drum mix plant requires equipment modifications. A new specification for HMAC should address the increased compaction requirements of the paving mixtures containing fibers.

DISCLAIMER

The contents of this report reflect the views of the authors who are responsible for the opinions, findings, and conclusions presented herein. The contents do not necessarily reflect the official views or policies of the Federal Highway Administration. This report does not constitute a standard, specification, or regulation.

There was no invention or discovery conceived or first actually reduced to practice in the course of or under this contract, including any art, method, process, machine, manufacture, design or composition of matter, or any new and useful improvement thereof, or any variety of plant which is or may be patentable under the patent laws of the United States of America or any foreign country.

TABLE OF CONTENTS

	<u>Page</u>
METRIC CONVERSION FACTORS.	ii
ACKNOWLEDGEMENTS	iii
IMPLEMENTATION STATEMENT	iv
INTRODUCTION	1
LITERATURE REVIEW.	3
DESCRIPTION OF MATERIALS	5
Asphalt Cement	5
Aggregate.	5
Fibers	5
DESCRIPTION OF EXPERIMENTAL PROGRAM.	7
General.	7
Mixing	7
Resilient Modulus.	8
Indirect Tension Test.	8
Freeze-Thaw Moisture Treatment	9
Flexural Fatigue Test.	9
Resistance to Thermally Induced Reflection Cracking.	10
Direct Compression Tests	11
Incremental Static Loading.	12
1000 Second Creep Test.	13
Dynamic Test.	13
LABORATORY TEST RESULTS AND DISCUSSION	14
General.	14
Determination of Optimum Asphalt Content	15
Gyratory Compacted Specimens	16
Air Voids	16
Hveem Stability	16
Marshall.	17
Resilient Modulus	18
Tensile Properties.	18
Moisture Susceptibility	19

TABLE OF CONTENTS (continued)

	<u>Page</u>
Flexural Fatigue	20
Resistance to Thermal Reflection Cracking.	22
Direct Compression (Creep and Permanent Deformation)	23
Time-Temperature Superposition.	23
Permanent Deformation	24
Predicted Pavement Performance Using VESYS IIM	25
Computer Inputs and Assumptions	26
Results of Predicted Performance.	26
Sensitivity to Permanent Deformation - Shell Method.	27
FIELD PROJECTS	30
District 8	30
Preconstruction	30
Construction.	30
District 11.	31
Construction.	32
Performance	33
CONCLUSIONS AND RECOMMENDATIONS.	34
Conclusions.	34
Recommendations.	36
REFERENCES	86
APPENDIX A - Data from Tests Performed to Determine Optimum Asphalt Content	91
APPENDIX B - Results of Tests on Gyrotory and Marshall Compacted Specimens	113
APPENDIX C - Data from Flexural Fatigue Testing.	122
APPENDIX D - Data from Overlay Tester.	130
APPENDIX E - Data from Direct Compression Tests.	139
APPENDIX F - Test Results from Field Projects.	144

INTRODUCTION

For decades, engineers have recognized that the low tensile strength of asphalt concrete is a serious weakness and often the source of performance problems that develop in asphalt concrete pavements. The current concern with tensile properties involves the failures associated with reflective and thermal-type cracking on bituminous concrete pavements and overlays. Reflection cracking is the propagation of cracks and/or joints in an existing surface or layer through a new overlay. Thermal cracking is the result of stresses induced by rapid drops in temperature. In response to these types of problems, research has been directed toward improving the tensile properties of asphalt concrete. One method which demonstrated merit involves reinforcement of the paving mixture with fibers.

Standardized methods for using fibers in asphalt pavements need to be defined based on an understanding of the interactions that occur as a result of the introduction of the fibers. These methods should include types of fibers that can be used successfully, amount of fiber to use, ways to introduce fibers in the mix and any construction techniques that need to be modified.

The primary objectives of the research are to (1) determine types of fibers that may be used successfully (2) determine optimum amount of fiber to use and (3) assess the differences in mixtures produced with and without fibers. Secondary objectives include determination of effective methods of introducing fibers into the paving mixture with both batch and drum mix plants and installing and monitoring field sections containing both polyester and polypropylene fibers.

The research study was composed of both laboratory and field experiments. The laboratory phase investigated asphalt mixtures with and without fibers over a range of temperatures using standardized laboratory methods along with the more advanced fatigue and creep tests. The field study was performed on pavement projects in Abilene and Lufkin, Texas with the cooperation of the Texas State Department of Highways and Public Transportation. Both polypropylene and

polyester fibers were used in the test pavements. A description of the materials used in the study, the tests methods utilized, the testing program and the results are presented.

LITERATURE REVIEW

The value of fiber reinforcement of construction materials was recognized more than 3000 years ago when Egyptian building specifications required the Hebrews to add straw during the fabrication of their bricks (1).

Busching, Elliott and Reyneveld (2) prepared an extensive review of the literature associated with reinforced asphalt concrete paving in 1970. At that time, most of the reinforcement used had been continuous rather than particulate. Particulate fibers used included asbestos (3-9), cotton (2) and fiberglass (2). Continuous reinforcement in the form of welded wire, synthetic yarns and fabrics has been used sporadically and in modest amounts in the United States for over 30 years.

Busching and Antrim (10) performed a limited series of tests on sand asphalt mixtures containing randomly oriented chopped fiberglass roving and yarn. Data from these tests indicate that randomly oriented chopped strand fiberglass, in amounts up to one percent by weight of the mixture, decreased mixture stiffness and caused cracks to propagate. Busching and Antrim (10) indicated that the release of strain energy from the elastic fiber to the sand asphalt matrix was responsible for the resulting deterioration.

Puzinauskas (3) reported that asphalt cement viscosity and hence mixture stiffness can be improved by the addition of randomly dispersed asbestos fibers. In addition, the asbestos demonstrated effectiveness in improving the low temperature cracking properties of asphalt concrete mixture. Asbestos is a natural fiber with suitable properties; however, the Environmental Protection Agency now considers asbestos fibers a health hazard, hence, these fibers are no longer used.

Synthetic fibers offer promise as a replacement for asbestos as reinforcement in asphalt paving mixtures as their properties can be tailored to the needs of the paving mixture. Because of the above foreseen benefits, polyester and polypropylene fibers were developed as alternatives to asbestos.

With the advent of these new materials, laboratory studies were initiated by universities and state departments of transportation to evaluate properties of asphalt paving mixtures containing fibers (11-20).

In addition to these laboratory studies, several field evaluations were also performed; some were in conjunction with the aforementioned laboratory studies (21-39). Other state departments of transportation have also conducted field studies but have not published results. These include Michigan, Maryland, Oregon, Illinois, New Hampshire, Minnesota, and Ohio.

Based on a review of the above literature and personal communication with state DOT personnel, it is apparent that fibers are being considered for use as reinforcement of asphalt paving mixtures. To date, most of the research has evaluated only one type of fiber at a time and not compared different types of fibers or different concentrations of fibers. The results of tensile tests have shown that the addition of fibers produces a more flexible mixture and thus one that is more resistant to cracking (13-16,18,20). The increased flexibility is manifested by greater elongation at failure without a significant decrease in tensile strength. This corresponds to an increase in the energy required to fail the sample (21-39). Field tests have shown that states in the north, with colder climates, exhibited better results with fibers than the states in the south. It is apparent that synthetic fibers in hot mixed asphalt concrete will often reduce reflective cracking. However, fibers have not been established as a cost effective construction alternative.

DESCRIPTION OF LABORATORY MATERIALS

Asphalt Cement

An AC-20 paving grade asphalt cement was selected for use in the asphalt-aggregate mixtures tested in this study. This asphalt was produced by the American Petrofina (Cosden) refinery located near Big Spring, Texas. It is normally considered to be highly temperature susceptible. It also exhibits above average hardening after heating as compared to other paving grade asphalts. This asphalt is produced from domestic crudes and, therefore, exhibits very uniform physical and chemical properties. It is successfully used in the western portion of the State of Texas.

Laboratory tests were performed to determine the basic physical characteristics (Table 1) of the asphalt cement.

Aggregate

Aggregates were obtained from stockpiles at Young Brothers' Asphalt Mix Plant in Bryan, Texas. A sub-rounded, siliceous gravel, was mixed with field sand and limestone crusher fines to obtain the desired gradation. Gradations of the individual aggregates are presented on Table 2 along with the percentage of each used in the blend. Table 2 also contains the sieve analysis of the combined aggregates used to produce the project design gradation. Design of the mixture was in compliance with Texas State Department of Highways and Public Transportation (SDHPT) Item 340 Type D (Fine Graded Surface Course) specifications for mineral aggregates for paving mixtures. A graphical presentation of the Type D specification limits and the project design gradation are given in Figure 1.

Fibers

Tests were conducted using ten different types of fibers with a wide variety of properties (Table 3). These fibers were composed of polypropylene, polyester, aramid, fiber glass, asbestos, a combination of polypropylene and aramid, and a fiber product consisting of volitals cellulose, starch, and ash. Polyester and polypropylene fibers are by far the most widely used in paving applications and

have, as a result, been subjected to the most laboratory and field research. This is primarily due to their lower relative cost.

Nominal diameter of the fibers is usually given as denier. Denier is the weight in grams of 9,000 meters of a single filament. Denier is not a good comparative measure of fiber diameter because it depends on the density of the fibrous material.

The fibers tested in this study and their suppliers/manufacturers are given below.

<u>Fiber</u>	<u>Supplier/Manufacturer</u>
Fiber Pave 3010	Hercules Incorporated Wilmington, Delaware
BoniFiber B	Kapejo, Incorporated Wilmington, Delaware
Hoechst	Hoechst Fiber Industries Spartanburg, South Carolina
Forta Fiber ES-6	Forta Fiber Incorporated Grove City, Pennsylvania
Phillips	Phillips Fiber Corporation Greenville, South Carolina
Kevlar 29	E.I. DuPont DeNemours & Co. Wilmington, Delaware
Kayocel 10-D50	American Fillers & Abrasives, Inc. Bangor, Michigan
Fiber Glass	Owens-Corning Granville, Ohio
Asbestos	Unknown

DESCRIPTION OF EXPERIMENTAL PROGRAM

General

Analysis of the fiber reinforced asphalt concrete included both laboratory and field evaluations. The laboratory test program consisted of six integrated phases (Figure 2 through 6). The test program was designed to: a) determine mixture designs (Figure 2), b) characterize, in detail, mixtures containing the two most widely used fibers (Figure 3) and c) characterize, in brief, several other fiber mixtures (Figure 4). This was accomplished using not only standard laboratory tests but also certain more advanced tests such as flexural fatigue, tensile fatigue (Figure 5) and creep and permanent deformation (Figure 6). A total of 16 different mixtures was fabricated and tested. Results of these tests on the Hercules FP 3010 polypropylene fibers were used with the VESYS IIM structural subsystem to predict field performance and with the Shell Method to predict rutting.

The field evaluation was performed in two different locations. One location was the hot, dry climate of Abilene, Texas and while the other location was the warm, moist climate of Lufkin, Texas. Only polypropylene fibers were used in Abilene; whereas, both polypropylene and polyester fibers were used in Lufkin. Control sections containing no fibers were installed at both locations to provide valid evaluation of the fibers.

Several of the tests listed in Figures 2 through 6 are widely used standardized methods; however, the fiber mixing procedures, resilient modulus, indirect tensile, flexural fatigue and direct compression tests and moisture treatment method are not widely used and will, therefore, be briefly discussed below.

Mixing

As mentioned earlier, three different aggregates were blended to produce the project design gradation. Asphalt cement and the aggregate were each heated to 280^oF. Fibers were blended with the dry aggregate prior to mixing with the asphalt cement. When the appropriate quantity of asphalt cement was added, the mixture was

manually blended for about two minutes using the back side of a large preheated metal spoon. (Fibers clung to the wire whip of the mechanical mixer.) The standard Texas SDHPT mixing trowel should work well with fiber mixtures. When blending was completed (all aggregate particles coated with asphalt cement), the mixture was placed in an oven at 260⁰F for about 20 to 30 minutes to bring it to the appropriate compaction temperature. Temperatures above 290⁰F may damage polypropylene fibers.

Resilient Modulus

The resilient modulus (M_R) test (40) is described in detail in ASTM Method D 4123-82. It is a nondestructive test which measures mixture stiffness of cylindrical specimens 2-inches in height and 4-inches in diameter at a given temperature. It was determined using the Mark III Resilient Modulus Device developed by Schmidt. A diametral load of approximately 72 pounds was applied for a duration of 0.1 seconds while monitoring the diametral deformation perpendicular to the loaded plane. The load is normally reduced to about 20 pounds for tests performed at 100⁰F or higher to prevent damage to the specimen. Resilient modulus measured over a range of temperatures is used to estimate mixture temperature susceptibility (41,42,43). Resilient modulus of asphalt concrete before and after exposure to moisture has been shown to give reasonable predictions of moisture susceptibility (44,45).

Indirect Tension Test

The indirect tension test employs the indirect method of measuring mixture tensile properties (Figure 7). The 2-inch high and 4-inch diameter cylindrical specimens were loaded diametrically at a constant rate of deformation until complete failure occurred. Diametral deformation perpendicular to the loaded plane was monitored in order to quantify mixture stiffness. The tests were conducted at temperatures of 0, 33 and 77⁰F and deformation rates of 0.02, 0.2 and 2-inches per minute.

This test was used to evaluate the sensitivity to moisture of mixtures containing fibers. A ratio of tensile strength before and after exposure to moisture is becoming widely accepted as a measure of an asphalt mixture's resistance to moisture damage (41,46,47).

Freeze-Thaw Moisture Treatment

Moisture treatment consisted of vacuum saturating the specimens at an absolute pressure of 26 inches of mercury, wrapping them in plastic wrap to retain the moisture, freezing them at 0⁰F for 15 hours followed by a 24-hour period at 140⁰F. The specimens were then brought to the appropriate temperature and tested in accordance with the test program.

Flexural Fatigue Test

Beam fatigue tests were performed to provide information for prediction of the fatigue life of pavements. Fatigue cracking of pavements is caused by repeated wheel loads and will appear as cracks in the wheel path. These cracks will have a pattern similar to that of "chicken wire" or "alligator skins".

The VESYS IIM computer model (48) was used to predict pavement fatigue life. Required input includes elastic properties of the pavement materials and stress versus fatigue life or strain versus fatigue life relationships which can be obtained from laboratory beam fatigue tests.

Flexural fatigue characteristics of asphalt concrete mixtures with and without fibers were determined with the test equipment shown in Figure 8. This equipment is a larger scale model of a device originally developed by Deacon (49). Asphalt concrete beams 3 x 3 x 15-inches are tested. Loads are applied at the third points of the tested portion of the beam, four inches on center, with one inch wide steel blocks. The applied load is measured by a load transducer and continuously recorded on an oscillographic recorder. Beam deflection is measured at the center using a linear variable differential transformer (LVDT) and also recorded on the two channel oscillographic recorder. The machine is operated in the load control mode with a

half-sine wave form at a frequency of 100 cycles per minute (1.67 Hz) and a load duration of 0.1 seconds. A reverse load is applied at the end of each load cycle to insure that the specimen will return to its original at-rest position after each cycle. It is necessary to periodically tighten the specimen loading and holding clamps as a result of plastic flow of the asphalt concrete. Upon rupture of the specimen, limit switches shut off the testing machine, and a cycle counter indicates the number of cycles to complete rupture.

Resistance to Thermally Induced Reflection Cracking

The "overlay tester", developed at Texas A&M University (50), is essentially a displacement controlled fatigue testing machine designed to initially produce a small initial crack (due to tension) in a test specimen and then continue to induce repetitive longitudinal displacements at the base of the crack which causes the crack to propagate upward through the specimen (Figure 9).

An asphalt concrete beam with dimensions of approximately 3 x 3 x 15-inches is attached by epoxy to two rigid aluminum plates on the overlay tester. One is fixed; the other is regulated to oscillate at a displacement of ostensibly 0.07-inch and a rate of 6 cycles per minute. (The displacement during a given test ranged from some minimum value at the start, say about 0.05-inch, to a maximum of 0.07 near the end of a test. This device is in the developmental stage and this shortcoming is being resolved.) The initial movement is outward which causes tensile stresses at the bottom center of the specimen.

Tests were conducted at 77°F and 33°F. Load was measured by a strain gage load transducer and displacement of the moving plate was monitored by a linear variable differential transformer (LVDT). Load as a function of displacement was recorded on an X-Y recorder. An example of recorded data is given in Appendix C, Figure C1. The length of the crack in the specimen was periodically measured on the two sides. The machine was allowed to oscillate until complete specimen failure. Failure is defined as that cycle at which the load supported by the specimen showed no further decrease after an additional approximately 200 displacement cycles. This usually

occurred about the same time the crack propagated completely through the specimen. Ideally, complete failure would be defined as the cycle at which the load approached zero, however, with those specimens containing fibers, a measurable load was supported by the fibers even after the asphalt concrete specimen was completely cracked.

This process is intended to simulate the cyclic stressing of a pavement due to periodic thermal variations. Results obtained with this apparatus should prove very useful in predicting pavement service life extension produced by systems purported to reduce reflection cracking.

Direct Compression Tests

Unconfined direct axial compression testing is required to provide input to the VESYS IIM computer program (48) to aid in predicting plastic deformation (rutting) within the pavement layer.

Direct compression testing including incremental static loading, 1,000 second creep loading and dynamic haversine loading was performed using an MTS Model 810 Materials Testing System. This is a closed-loop servohydraulic system capable of stress, strain or position control. It is equipped with a digital wave form generator to control dynamic tests and an environmental chamber to accurately control test temperature. Two linear variable differential transformers (LVDT) attached to the sample were used to measure sample deformation (Figure 10). The gage length was 4-inches. An X-Y plotter was used to record the axial load applied to the test specimen and the corresponding axial deformation experienced by the specimen.

Compaction of the 4-inch diameter and 8-inch height cylindrical test specimens was accomplished using the intermediate compactive effort as specified in the VESYS Users Manual (48) and the Cox kneading compactor. Sixty tamping blows were applied at 250 pounds per square inch compactor foot pressure. Then a 1,000 pounds per square inch static load was applied at a rate of 0.05-inches per minute to provide a flat, level surface at the top of the specimen. The double plunger method was used to insure uniform compaction on each end of the specimen.

Two preliminary specimens (one control and one with fibers) were made to determine whether air void contents were acceptable using the materials and compaction procedures described above. These were weighed in air and water to determine bulk specific gravity then sacrificed in order to determine maximum specific gravity. Air void contents were found to be acceptable.

A total of nine control specimens and eighteen fiber specimens were prepared and subjected to the direct compression tests. Six each of the fiber test specimens contained 4.6, 4.85 and 5.1 percent asphalt. Control specimens, which contained no fibers, were prepared using 4.6 percent asphalt cement by weight of total mixture. Two each of the six fiber specimens and three each of the control specimens were tested at temperatures of 40, 70 and 100°F.

After a test specimen reached the appropriate test temperature, it was placed in the controlled temperature cabinet and centered under the loading apparatus. The LVDT's were attached and the electronic measuring equipment was adjusted and balanced. In order to condition the specimen, three ramp loads of 20 psi were applied and held for 10 minutes duration. Following a 10-minute unload period, the electronic measuring equipment was readjusted.

Incremental Static Loading. The incremental static loading portion of the test was performed to determine certain parameters required for input into the VESYS IIM computer program. It was performed in the following manner.

1. Apply one ramp load of 20 psi to the specimen as quickly as possible and hold loading for 0.1 second. Release the load and measure total permanent deformation after two minutes of unload.

2. Apply a second ramp load to the specimen at the same stress level used above and hold for one second. Release the load and measure the total permanent deformation after two minutes of unload.

3. Apply a third ramp load to the specimen at the same level and hold for 10 seconds. Release the load and measure the total permanent deformation after two minutes of unload or when rebound becomes negligible.

4. Apply a fourth ramp load to the specimen at the level used above and hold for 100 seconds. Release the load and measure the total permanent deformation remaining after four minutes of unload or when rebound becomes negligible.

1000 Second Creep Test. A second series of tests were conducted to measure creep compliance of the mixtures. The 1,000 second creep test was performed in the following manner.

5. Apply a fifth ramp load to the same specimen at the level used above and hold for 1,000 seconds. Measure the magnitude of the creep deformation during loading after 0.03, 0.1, 1.0, 3.0, 10, 30, 100 and 1,000 seconds. Release the load and measure the total permanent deformation after eight minutes of unload or when rebound becomes negligible; this value is also the final reading for the incremental static loading portion of the test.

Dynamic Test. Repeated haversine loading tests were performed to quantify accumulated strain during a period of dynamic loading. The test was performed in accordance with the following.

6. Re-zero LVDT's.

7. Apply repeated haversine loading to the specimen at 70⁰F such that each load application has a magnitude equal to the stress level used above and each load application has a load duration of a 0.1 second. A 0.9-second rest period follows each load application. A minimum of 1,000 load applications are applied and the accumulated deformations at 1, 10, 100, 200 and 1,000 repetitions are recorded. Record the peak-to-peak strain at the 200th cycle.

8. Release the load after 1000 repetitions, record the rebound after 15 minutes and remove the specimen.

LABORATORY TEST RESULTS AND DISCUSSION

General

Because of the wide range of specific gravities of the fibers, it was decided to add the fibers to the paving mixture on an equal volume basis. For example, the specific gravity of the polyester (1.38) is approximately one and one-half times the specific gravity of polypropylene (0.91) and if mixed on an equal weight basis there would be a large disparity between the volume of fibers in the mixtures. It was hoped that using this method would provide a more equitable evaluation of the properties imparted to the asphalt mixture by the different types of fibers. (It may have been most desirable to add fibers on an equal surface area basis and possibly use the same asphalt content for all fiber mixtures.)

Hercules and BoniFiber products were selected for detailed study because they have been most widely used in paving applications and they were used in the field study which will be described later. The Hercules (polypropylene) fiber mixtures were prepared at concentrations of 0.1, 0.2 and 0.4 percent fibers by weight of mixture. The BoniFiber (polyester) mixtures were prepared at concentrations of 0.15, 0.3 and 0.6 percent fibers by weight of mixture. These six weight percentages yielded three pairs of mixtures containing three different quantities of fibers on a volume percentage basis. The other fiber mixtures were prepared by adding fibers on a volume percentage basis equal to the middle concentration of the three pairs. Additionally, Forta-Fibre was tested at the concentration that the manufacturer recommends (0.05 percent).

Kevlar is composed of aramid which has a modulus (9×10^6 psi) near that of glass (10×10^6 psi). The modulus of the other fiber materials ranges from 500,000 to 1,000,000. Kevlar fibers were tested to observe the effects of a very high modulus synthetic fiber on the properties of an asphalt paving mixture. The high cost of this product will likely preclude its widespread use.

Previous research on asbestos fibers in asphalt concrete (3-9) has shown some favorable results. However, asbestos is not widely used because of the associated health hazard. Past research using fiberglass in asphalt paving mixtures (10) has generally shown unfavorable results, nevertheless, these two fibrous materials were included in this study to provide bases for comparison in addition to the control specimens.

The mixture codes used subsequently in the text, tables and figures are identified in Table 4.

Determination of Optimum Asphalt Content

A combination of the method presented in the Texas State Department of Highways and Public Transportation's (SDHPT) Construction Bulletin C-14 and the Hveem and Marshall mix design procedures was used in determining the optimum asphalt contents (Figure 2). It appears that any of the standard mix design methods can be used satisfactorily with fiberized mixtures. All the test specimens in this program, were compacted using the Texas SDHPT gyratory compactor. A summary of the findings is listed in Appendix A, Table A1. Tests were performed to determine optimum asphalt content for twelve of the sixteen mixtures evaluated in this study. The four fiber mixtures not tested include F.05, KO, AS, and FG. These were added late in the study and the optimum asphalt content was selected based on prior experience with the other mixtures. Subsequent testing of these four mixtures indicates the asphalt content selected was reasonably close to the amount that would have been determined by design. Test results for the mixtures at the various asphalt contents are listed in Tables A2 through A13. Graphical representations of the test results are shown in Figures A1 through A16.

When fibers are introduced into an asphalt paving mixture, additional asphalt is necessary to coat the fibers. (This is similar to the addition of very fine aggregate.) The proper quantity of asphalt for consistent coating of all particles is different not only for different concentrations but also for different fibers. This will

likely be due to the variation in surface area of the different types of fibers. Figure 11 is a bar graph showing the optimum asphalt contents selected for the sixteen mixtures used in this study. Observation of the Hercules (H) and the BoniFiber (B) specimens reveals that optimum asphalt content increases with fiber concentration.

Gyratory Compacted Specimens

Approximately 300 specimens were mixed and compacted using the Texas gyratory shear compactor at the optimum asphalt contents determined earlier. Figure 3 shows the laboratory test program for the control mixtures and those mixtures containing the polypropylene (Hercules) and the polyester (BoniFibers) fibers. Figure 4 shows the laboratory test plan for the other nine fiber mixtures. A summary of the test results is given in Appendix B, Table B1.

Air Voids. It is seen in Figures A1 through A4 that the addition of any fibers in an asphalt paving mixture will increase the resulting air void content when asphalt content and compactive effort remain constant. Furthermore, Figures A1 and A2 show that as the quantity of fibers increases, the amount of air voids also increases. This is important from the standpoint of achieving a desired pavement density, since the mixtures with fibers will require more compactive effort than a mixture without fibers. The comparatively low specific gravity of the synthetic fibers will also have a net effect of decreasing (slightly) compacted mixture density. All test specimens were prepared using the same compactive effort. Figure 12 shows that the mixtures containing fibers exhibited more air voids than the control mixture, even though all of them except mixture F.05 contained more asphalt cement than the control mixture.

Hveem Stability. This particular mixture was chosen because it has a relatively low stability but is, nevertheless, regularly used in paving applications. It should be pointed out that the stabilities of all mixtures (Figure 13) are below the value of 35 as specified for paving mixtures by the Texas SDHPT. Figures A5 through A8 show that, with the exception of 0.15 percent BoniFibers, the addition of fibers

generally results in a significant decrease in Hveem stability. Furthermore, analysis of variance and Duncan's multiple range test ($\alpha = 0.05$) indicates that, for all practical purposes, the decrease in Hveem stability of the mixtures containing fibers is not significant. Hveem stability is more closely related to asphalt content than the presence or type of fibers. That is, Hveem stability generally decreases as the design asphalt content of the various mixtures increases. No consistent relationship between Hveem stability and air void content is evident.

Marshall Test. Marshall stability (Figure 14) inherently exhibits considerable variability. Figures A9 through A12 show that Marshall stability may either increase or decrease when fibers are added. However, decreases in Marshall stability were not large except when the larger quantities of fibers were added. Analysis of variance and Duncan's multiple range test ($\alpha = 0.05$) indicates that only mixture H.2 has significantly greater Marshall stability than the control mixture. Further, Marshall stabilities of all other mixtures are not significantly different from the control mixture. Although air void content and asphalt content varied from mixture to mixture, there were no indications that either of these factors caused the differences in Marshall stability. It appears that, in general, certain fibers in well designed asphalt paving mixtures can be used to increase Marshall stability.

These data show that while fibers increase the optimum asphalt content, they also decrease the mixture's sensitivity to asphalt content. This is an important consideration. Some paving mixtures, particularly those composed of mostly rounded particles (such as the one used in this study) are often quite sensitive to asphalt content. This can pose problems in the field, since absolute control of binder content at a plant is impossible. If fibers prove to be cost effective for other reasons, the fact that they decrease sensitivity of a mixture to asphalt content is an added benefit.

Statistical analyses showed that more than one-half the fiber mixtures exhibited a significantly greater Marshall flow (Figure 15 and Figures A13 through A16) than the control specimens ($\alpha = 0.05$).

This is an important observation in that high Marshall flow is indicative of a mixture containing excessive asphalt. The reader is reminded that these specimens were prepared using the gyratory compactor, therefore, the Marshall values are valid only for comparison with similarly prepared specimens.

Resilient Modulus. Resilient modulus (M_R) tests were performed at five temperatures ranging from -10°F to 104°F . Results of these tests are summarized in Table B1. Figures 16 through 20 show that those mixtures containing fibers generally exhibit lower moduli at temperatures above 77°F ; but at the lower temperatures, there are no consistent differences in the moduli of the mixtures. The fiber mixtures in Figure 20 showed significantly lower values of M_R at -10 and 33°F . These three fiber mixtures were tested about three months later than the control and all the other fiber mixtures and the validity of the direct comparison of these data is questionable.

Resilient modulus is sensitive to binder content and viscosity and air void content, particularly at higher temperatures. It is postulated that if all mixtures had been compacted to the same void content, these test results would have been different. That is, there would have been no appreciable difference in M_R of any of the mixtures at any of the temperatures. Fiber mixtures H.2, P-15 and F had comparatively low void contents reasonably close to the void content of the control mixture. These mixtures also exhibited M_R values reasonably close to those of the control mix at all temperatures.

Resilient modulus can be used to indicate mixture temperature susceptibility (40) (slope of M_R versus temperature curve). Test results show that, generally, the addition of fibers has little effect on mixture temperature susceptibility.

Tensile Properties. Indirect tension tests were performed at 77°F and two inches per minute on all mixtures. Results are summarized on Table B1, Appendix B. Figures 21 and 22 show that tensile strength is generally lower and tensile strain at failure is higher for the fiber mixtures when compared to the control mixture. Statistical analyses showed that tensile strength of nine of the fiber mixtures was not significantly different ($\alpha = 0.05$) from the control specimen.

Further, tensile strain at failure of seven of the fiber mixtures was significantly greater than that of the control mixture.

Indirect tensile tests were performed on mixtures containing BoniFibers and Hercules fibers at three concentrations and the control mixtures at temperatures of 0, 33 and 77⁰F and loading rates of 0.02, 0.2 and 2 inches per minute. Results of these tests are summarized on Tables B2 through B5. At a loading rate of 0.02 inches per minute, tensile strength of the mixtures increases almost linearly as temperature decreases (Figure 23 and 24). However, at loading rates of 0.2 and 2 inches per minute, tensile strength reaches a maximum at a temperature of approximately 30⁰F (Figures 25 through 28). It is believed that this asphalt mixture became brittle at a temperature near 30⁰F which resulted in poor tensile properties at lower temperatures. The indirect tensile test does not measure pure uniaxial tension and the degree of change from uniaxial tension varies with loading rate and test temperature. It appears that a number of factors were working together to produce the results observed.

Figures 23 through 28 show that, overall, the addition of fibers causes a slight reduction in tensile strength of the mixture at temperatures from 0 to 77⁰F. Figures B1 through B6 show that the opposite is true for tensile strain (elongation) at failure. This is likely due in part to the additional asphalt as well as the fibers in these mixtures.

If tensile strain at failure can be increased while not appreciably reducing the tensile strength, a paving mixture will be more flexible. This combination of properties may mean that more energy is required to produce a crack (due to tension) in a pavement, that is, the pavement may give longer service life. Unfortunately, these indirect tension test results did not show a significant advantage when fibers were added.

Moisture Susceptibility. Indirect tensile tests and resilient modulus tests were conducted before and after the specimens were exposed to the Lottman freeze-thaw moisture treatment. Ratios of mixture properties before and after moisture treatment were computed (Table B5) in accordance with the following equations:

$$\text{Tensile Strength Ratio} = \frac{\text{Tensile Strength After Moisture Treatment}}{\text{Tensile Strength Before Moisture Treatment}}$$

and

$$\text{Resilient Modulus Ratio} = \frac{\text{Resilient Modulus After Moisture Treatment}}{\text{Resilient Modulus Before Moisture Treatment}}$$

The ratios are compared in Figures 29 and 30.

The indirect tensile test is normally considered to be more sensitive to moisture damage than the resilient modulus test. Statistical analyses showed that all the mixtures containing fibers except one (B.15) exhibited significantly greater tensile strength ratios ($\alpha = 0.05$) than the control specimens. Similar analyses showed that two fiber mixtures (H.1 and H.4) exhibited significantly greater resilient modulus ratios than the control specimens. Resilient modulus ratios of the remaining mixtures were not significantly different from that of the control mixture from a statistical standpoint. Generally, the mixtures containing fibers are less susceptible to moisture induced damage than the mixture without fibers.

It is important to remember that the mixtures containing fibers had greater asphalt contents and yet greater void contents than the control mixture. Regarding resistance to moisture damage, these two parameters would be expected to oppose one another. It is surmised, therefore, that the additional asphalt in the fiber mixtures increased the film thickness on the aggregate particles thus affording additional protection from moisture.

Flexural Fatigue

Flexural fatigue tests were performed on control mixtures and mixtures containing Bonifiber, Hercules and Kevlar fibers.

Peak stress, initial bending strain (bending strain at the 200th cycle), initial stiffness modulus and estimated total input energy were calculated for each fatigue test specimen in accordance with the formulae (17) given in Appendix C. A statistical summary of the test results is given in Table C1. Tables C2 through C5 give test results for the individual specimens.

Three specimens at each test condition were tested in this experiment. Fatigue tests were conducted at 68⁰F and three stress levels to determine the relationships between applied stress and bending strain and the number of load applications to failure. These relationships along with regression equations and coefficients of determination are given in Figure 31.

The equation format normally used to describe flexural fatigue results is:

$$N_f = K_1 \left(\frac{1}{\epsilon}\right)^{K_2}$$

where N_f = number of load repetitions to failure,
 ϵ = initial bending strain (@ 200th load cycle) and
 K_1 and K_2 = regression constants.

All of the fatigue test beams were prepared using the same compaction procedure. It should be pointed out that the air void contents of the fiber specimens were 1 to 4 percentage points greater than those of the control specimens (Table C1). This is significant, in that for a given mixture, fatigue performance will usually suffer when air void content is increased. Considering these factors, it appears that fibers have the potential to increase fatigue performance of asphalt concrete paving mixtures provided adequate compaction is achieved. Test results indicate that fiber mixtures will provide about the same fatigue performance as the control mixture at low strain levels; but, at high strain levels, the fiber mixtures will provide superior fatigue performance. That is, for major highways with stiff bases and subgrades, fibers in the asphalt concrete surface course may not provide benefits relative to fatigue performance. However, for secondary roads with weak bases and subgrades and thin pavement surfaces, the addition of fibers and asphalt to the surface course may be a viable alternative for increasing service life.

Mixtures containing the Kevlar fibers exhibited slightly better fatigue performance than the other mixtures. Kevlar fibers are composed of aramid which has a much greater modulus than either polypropylene or polyester.

Resistance to Thermal Reflection Cracking

The overlay test measures a materials resistance to crack propagation. Tests were performed at 33 and 77⁰F on control mixtures and mixtures containing Bonifiber, Hercules and Kevlar fibers. A summary of the overlay test results is given on Table D1. Test results for individual specimens are given on Table D2 and Figures D3 through D10. Typical recordings of load versus deformation are shown in Appendix D, Figure D1.

Averages of the number of cycles to failure are compared on the bar chart in Figure 32. Under the test conditions employed, the addition of fibers to this mixture increases the number of cycles to failure by a factor greater than two. Figure 33 and 34 show that, after the initial loading cycles, the mixtures containing fibers supported a greater peak load for a greater number of repetitions at both 33 and 77⁰F. This, of course, is indicative of significantly greater resistance to crack propagation by the fiber mixtures as compared to the control mixture. Statistical techniques revealed that there were no significant differences in the number of cycles to failure between the three fiber mixtures.

The reader is reminded that asphalt content for the fiber mixtures was greater than that of the control mixture. Improved resistance to crack propagation by the fiber mixtures may be at least partially due to the additional asphalt. However, air void content was also generally greater for fiber mixtures. Greater void content normally has negative effects on tensile properties of asphalt concrete. Nevertheless, the addition fibers did improve resistance to crack propagation in this mixture. The test results indicate that the addition of synthetic fibers and asphalt cement to a paving mixture will improve resistance to thermally induced reflection cracking.

Figure D1 shows that fibers will span small cracks in asphalt concrete and support a small load. These asphalt coated fibers may, for a while, impede intrusion of moisture into successive pavement layers.

Figure D2 shows typical cracking patterns of specimens with and without fibers. Specimens containing fibers cracked over a wider area

than those without fibers. This demonstrates the load spreading ability of the fibers.

Direct Compression (Creep and Permanent Deformation)

Direct compression tests were performed on the control mixture and three mixtures containing 0.3 percent Hercules (polypropylene) fibers with 4.6, 4.85 and 5.1 percent asphalt (20).

Direct compression tests include incremental static loading, 1,000 second creep test and repeated haversine loading (dynamic test) for 1,000 cycles. These tests were performed in accordance with the VESYS IIM Users manual (48). Physical properties of the 4-inch diameter and 8-inch height cylindrical test specimens used in this phase of work are given in Table E1, Appendix E. Results of the direct compression tests are summarized in Tables E2, E3 and E4.

Creep compliance curves for the fiber mixtures are compared with those of the control mixture in Figures 35, 36 and 37. Figure 35 shows that the fiber mixture containing the lowest asphalt content (4.6 percent) has about the same compliance as the control mixture at 70 and 100°F but is less compliant than the control mixture at 40°F. As the asphalt content is increased, the fiber mixtures become more compliant than the control mixtures at 70 and 100°F but exhibit about the same compliance as the control mixtures at 40°F (Figures 36 and 37). At lower temperatures, when asphalt cement becomes more elastic, an asphalt paving mixture is less sensitive to asphalt content in this test mode. As the temperature increases, the binder viscosity decreases and the material becomes more viscoelastic which causes an asphalt paving mixture to become more sensitive to asphalt content. This may, in part, explain why the fiber mixtures with the higher asphalt contents exhibit greater compliance than the control mixtures at the higher temperatures.

Time-Temperature Superposition. Viscoelastic pavement response is, of course, influenced by temperature. The VESYS IIM computer program has the capacity to handle material properties as a function of temperature. A computer variable, BETA, relates the time-temperature shift factor, a_T , to the temperature variable for the pavement materials. The relationship is expressed as:

$$\log a_T = \beta(T_0 - T)$$

where a_T = time-temperature shift factor at temperature T ,
 β = BETA = slope of the $\log a_T$ vs. T plot,
 T_0 = reference temperature of master curve and
 T = temperature at which creep test is performed.

The time-temperature shift factor is determined by:

$$a_T = \frac{t}{t_0}$$

where t = time to obtain a given value of a material property
at temperature T and
 t_0 = time to obtain the same value of the material
property at the reference temperature, T_0 .

Table 5 shows that BETA increases when fibers are added to this mixture and that BETA further increases with asphalt content. With all other conditions the same, a larger value of BETA usually indicates the properties of a mixture are more sensitive to changes in temperature. The values of BETA for all four mixtures are within the range established as typical for asphalt concrete by previous research (48,51,52).

Permanent Deformation. The specimens used on the creep tests were also used for permanent deformation or permanent strain testing. Accumulated permanent strain, versus number of load applications from the incremental static and dynamic loading tests are plotted in Figures 38 and 39, respectively. The plots indicate that, generally, permanent deformation of the fiber mixtures is about the same as that of the control mixture at higher temperatures where rutting is a concern. At lower temperatures fibers appear to reduce permanent strain.

Data from these tests were used in accordance with the VESYS IIM Users Manual (48) to determine the values of ALPHA () and GNU () (Table 5). These values are input data for the VESYS structural subsystem.

A value of zero for ALPHA indicates a constant incremental increase in strain with each load application at a given value of GNU. A positive value of ALPHA indicates the fractional change in strain per load application decreases with each load applied. The values of ALPHA computed for these mixtures were below the range considered typical (0.63 to 0.83) for asphalt concrete mixtures (51) and as a result, produced unacceptable results from the VESYS IIM computer program. Therefore, in order to apply the VESYS IIM computer program, the values of ALPHA at 70°F were adjusted upward using the following formula:

$$\alpha_{\text{adjusted}} = \alpha \left(\frac{\alpha - 0}{0.4} \right)$$

When the adjusted values of ALPHA were used, reasonable results were obtained.

GNU is a much more difficult parameter to which one can attach physical significance as it is directly dependent on the slope and intercept of the line drawn on the log-log plot and on the inverse of the strain. GNU for asphalt concrete surfaces can be quite variable with values often exceeding 1.5 (51). Problematic rutting is generally associated with relatively higher values of GNU. Table 5 shows that, generally, GNU increases with temperature, so does rutting.

Predicted Pavement Performance Using VESYS IIM

The VESYS IIM computer program (48) was used to predict performance of hypothetical highway pavements made using Hercules fibers at three different asphalt contents. In addition, performance of two hypothetical pavements made using the same mixture without fibers were also predicted by the program.

The primary purpose of this analysis was to evaluate the performance of the laboratory prepared fiber mixtures when used as a surface course on a pavement. A secondary purpose was to evaluate the actual performance in terms of criteria such as rut depth, slope variance, cracking and present serviceability index.

Computer Inputs and Assumptions. Two different pavement structures were selected for use in the study. Pavement surface thicknesses of 2-inches and 6-inches were used. The 2-inch surface represents a thin pavement and the 6-inch surface represents a thick pavement. The literature (53) indicates that asphalt concrete displays linear viscoelastic response only for short loading times, low stresses and low temperatures and that air void contents have a significant influence. The range of stress levels evaluated in the testing program was not adequate to establish linearity. However, since duration of the repeated loadings considered in the VESYS structural analysis are very short, the asphalt materials were assumed to be linearly viscoelastic. The surface layer was assigned the previously discussed values of K_1 and K_2 from the fatigue tests and ALPHA, GNU, and creep compliance from the direct compression tests.

Each pavement was supported by a 10-inch base. The base was assumed to have an elastic modulus of 50,000 psi which is typical of crushed limestone bases in Texas when the base to subgrade modulus ratio is approximately two. The subgrade was assumed to have a modulus of 20,000 psi which is typical of a hard clay. A relatively hard base and subgrade were employed in order to accent any rutting which may occur in the asphalt pavement.

Each pavement was evaluated in a cool, moderate and warm climate. Generally, the cool climatic region is approximately 10⁰F cooler than the moderate region which, in turn, is approximately 20⁰F cooler than the warm region. Average temperature of the warm region ranges from 40 to 95⁰F. The previously discussed time-temperature shift factors were used in the VESYS analysis to evaluate the effects of temperature on creep properties of the four mixtures and the resultant effects on pavement performance.

Results of Predicted Performance. Results from the factorial predictive performance analysis are given in Figures 40 through 43. The numbers within these figures indicate rankings of the mixtures by order of decreasing performance. The mixture assigned Number 1 exhibited the best pavement performance in that particular category; the mixture assigned Number 4 exhibited the worst performance. That

is, in Figure 40, best to worst performance based on serviceability index of the thick pavement with a hard clay subgrade in a cool climate is as follows: (1) Fibers + 4.6 percent asphalt, (2) Fibers + 4.85 percent asphalt, (3) Control and (4) Fibers + 5.1 percent asphalt.

The best single summary of relative performance as a function of mixture type is Figure 40. This is because present serviceability index is a function of slope variance (roughness), rut depth and cracking.

Figures 44 through 47 show the relative pavement performance as a function of time for a thick surface and a hard subgrade at the moderate climate. The thick surface and hard subgrade were selected to accentuate the properties of the binder in the surface course.

Results from the VESYS IIM computer program show that the fiber mixtures containing 4.6 and 4.85 percent asphalt and the control mixtures perform similarly and that the fiber mixture containing 5.1 percent asphalt performs rather poorly. From an overall performance standpoint, the fiber mixtures containing 4.6 and 4.85 percent asphalt perform best. From the standpoint of cracking, the control mixture generally performs best.

Sensitivity to Permanent Deformation - Shell Method (20)

The permanent deformation or rutting potential of asphalt concrete mixtures containing Hercules fibers was evaluated using the Shell Method (54). This method uses a relationship between mixture stiffness and bitumen or binder stiffness as the basis for rut depth predictions.

The bitumen or binder stiffness is, of course, a function of the temperature and duration of load application. Shell researchers have defined stiffness as being composed of three components: elastic, viscoelastic and viscous. Only the viscous component is nonrecoverable and thus leads to permanent deformation. It can be easily shown that as load duration increases (at a constant temperature) the viscous component of stiffness will ultimately predominate and a correspondingly greater percentage of permanent

deformation will result. Due to the time-temperature interdependency of asphalt cement, an analogous condition occurs at a constant load duration as temperature increases.

Shell researchers have shown that the viscosity of bitumen can be predicted from the Shell nomograph by calculating the stiffness at very long durations of loading. The viscosity is then a function of the product of stiffness and duration of loading. This relationship verifies that, for a selected temperature, once a certain duration of loading is exceeded, viscosity is the sole contributor to stiffness. This may be expressed mathematically as :

$$\eta = \left(\frac{1}{3} \lim_{t \rightarrow \infty} S_{bit}\right)t$$

where η is viscosity in lb. sec./in.², S_{bit} is binder stiffness and t is load duration.

Shell research has further established that the irreversible deformation of bitumen proceeds linearly in relation to time at a constant temperature. This implies that, for the determination of the viscous component of binder stiffness, $S_{bit, visc.}$, in a cycle loading test, the loading times are allowed to be superimposed. Thus,

$$S_{bit, visc.} = \frac{Nt_w}{3\eta}$$

when N is the number of load applications of duration, t_w . If temperature is varied during the period of loading then,

$$S_{bit, visc.} = \frac{3}{t_w \sum_{i=1}^N \frac{(N)}{\eta} T_i}$$

where T_i is the temperature during period i .

The mixture stiffness, S_{mix} , was calculated from constant stress creep testing performed in accordance with the VESYS IIM User's Manual (48). Tests were performed at 40, 70 and 100°F at load durations ranging from 0.01 to 1,000 seconds. These data were used to predict an S_{mix} for each combination of t and T . These values were matched

with S_{bit} computed for corresponding values of t and T to develop the S_{bit} versus S_{mix} curve, Figure 48.

Figure 48 presents the S_{bit} versus S_{mix} relationships for the control mixture and the fiber mixtures tested. Permanent deformation (rutting) becomes critical at very low values of S_{bit} which corresponds to critical combinations of t and T . From the relative position and slope, q , of the curves, it is clear that:

1. At 4.6 percent binder the addition of fibers produces a stiffer mix, less susceptible to permanent deformation than the control mix.

2. At higher binder contents (4.85 and 5.1 percent) the potential for permanent deformation is increased as indicated by both the position and slope of the curves.

3. The position of all the curves in Figure 48 indicate that the mixes are reasonably resistant to large permanent deformations. This is illustrated by comparing the actual curves in Figure 48 with hypothetical S_{bit} versus S_{mix} curves which represents 1/4-inch deformation produced by one million load applications (100 psi contact pressure) at mean annual air temperatures of 86°F and 77°F.

Figures 49, 50 and 51 compare rut depths over a range of load applications and at mean annual air temperatures (MAAT) of 86°F and 77°F. In each figure, a specific mixture containing fibers is compared with the control mixture containing no fibers.

The trend toward a dramatic increase in permanent deformation with increased binder content for the fiber mixes is obvious. At 5.1 percent binder in the fiber mix, the deformation potential is quite nonlinear (Figure 51); and very slight binder increases beyond this point will result in excessive deformations.

FIELD PROJECTS

Two field trials using fibers in hot mixed asphalt concrete were installed in Districts 8 and 11. Descriptions of these installations with traffic and weather conditions are given in Table 6.

District 8

A 13.1 mile section of US 83 (State Project CSB 33-5-53) just north of Abilene was overlaid with hot mixed asphalt concrete in November, 1982. A two mile (approximately) section of this project at the south end on the northbound side was designated as a test section for Hercules FP3010 fibers. A one mile (approximately) section in the southbound lanes from Hawley to the Clear Fork Brazos River bridge was designated as the control section.

Preconstruction. The existing pavement structure in the test section and the control section consisted of a 9-6-9-inch jointed concrete pavement 20 feet wide. Two foot shoulders consisted of 9-inches of flexible base. All had been overlaid with approximately 1-inch of hot mixed asphalt concrete (HMAC) to produce a 24-foot wide pavement which subsequently had a seal coat applied. Transverse cracks and joints in the concrete pavement had reflected through the HMAC and the seal coat. Typical cracking patterns in are shown in Figure F1, Appendix F. Some of the cracks/joints were spalling and were 3 to 4-inches wide at the surface.

This field test project is located on a straight section of a rural divided highway in gently rolling hills. Excellent drainage is provided.

Construction. All cracks and joints in the fiber test section were filled with Hercules Extrudamat. This is a fiber reinforced asphalt cement crack/joint sealing material. Extrudamat was applied using a wand with an eight inch diameter horizontal disc on the pavement surface. The disc aids in forcing the sealant down into the crack and spreads it in a strip about eight inches wide along the crack on the pavement surface. The strip of Extrudamat was about one half inch thick. Cracks/joints in control section were not filled with Extrudamat.

A drum mix plant was used to produce the paving mixture containing fibers. Hercules, Inc. furnished a special device to meter and blend the fibers into the asphalt cement prior to entering the drum. The remainder of the paving operation was performed in the usual manner using conventional equipment.

The control section consisted of an overlay of 1 1/2-inches of Item 340 Type D HMAC composed of crushed limestone, field sand and AC-10. The fiber test section was overlaid with 1-inch of the same material containing 0.3 percent by weight Hercules polypropylene fibers. Gradations of the individual aggregates and the project design gradation is given in Table F1. Asphalt properties are given in Table F2. Design curves for the fiber and control mixtures are plotted in Figures F2 and F3. Design asphalt contents for the control and fiber mixtures were 6.1 and 6.8 percent, respectively.

It was determined by District 8 personnel that the cost per ton of HMAC was \$13.00 for the control mixture and \$25.50 for the fiber mixture. This does not include the cost of the fiber-asphalt crack sealing material. The reader is reminded that the fiber mixture was placed at two-thirds the thickness of the control mixture.

Performance. This field experiment was not designed such that performance of the fiber mixture and the control mixture could be compared on an equal basis. A mixture of fibers in asphalt was used to seal the cracks under the fiber mixture but not under the control mixture. Thickness of the fiber mix overlay is 1-inch and thickness of the control mix overlay is 1 1/2-inch. However, the advantages of the fibers are manifested after each winter in service (Figure 52). The fibers in the mixture and/or the crack sealer appear to aid in reducing reflection cracking. In the spring of 1984, reflected cracks in both sections were sealed using a crumb rubber-asphalt sealer.

District 11

A 4.7 mile portion of SH 94 beginning at Loop 287 near the city limits of Lufkin and extending westward was totally reconstructed (Project EACF 1151(1)) in the spring of 1983. Four pavement test sections were built which included synthetic fibers in the surface course. Control sections with no fibers were also installed to

provide a basis for comparison. The fibers used in these tests were furnished at no cost by Hercules, Inc. and Kapejo, Inc.

Construction. The pavement cross section consists of the following layers: (1) 1 1/2-inches of Item 340 Type D modified surface course, (2) 3-inches of Item 292 Type A asphalt stabilized base course, placed in two 1 1/2-inch lifts, (3) a seal coat, (4) 8-inches of cement treated base, with a cement content of 125 pounds per cubic yard and (5) 6-inches of lime treated subgrade soil, with a lime content of 20 pounds per cubic yard or 4 percent. The pavement shoulders consists of the same lime treated subgrade and cement treated base as the roadway but the surface course is 4 1/2-inches of Item 292 Type A placed in three 1 1/2-inch lifts. A brief description of the test section location and materials used in the surface course is given on Table 6.

Both in the laboratory and in the field, the control mixtures and the two mixtures containing Hercules fibers contained 8.5 percent asphalt; whereas, the mixtures containing BoniFibers contained 9.0% asphalt. Lightweight aggregate produces such a harsh mix that fibers do not significantly affect optimum asphalt content. Mixtures were designed by District 11 personnel in accordance with standard SDHPT procedures. Detailed information on the aggregates and mixture design are given on Tables F3 through F5 and Figures F4 through F9 in Appendix F. These figures show that fibers have the capacity to improve mixture properties and reduce mixture sensitivity to asphalt content.

A CMI 7 foot by 30 foot drum mix plant was used to produce the asphalt paving mixtures. The holding hopper for the fibers was a fertilizer spreader unit. This is a slant sided hopper with a metal chain belt feed system in the bottom. The fibers were fed by this system into a vane feeder then into a Barber-Greene fine feeds blower system. This blower propelled the fibers into the rear of the drum mix plant through a 4-inch diameter pipe. The exit of this pipe was located inside the drum about 12-inches downstream of the asphalt cement injection point. This apparatus functioned reasonably well in transferring the fibers into the drum. Occasionally, the fibers clogged in the vane feeder. This was apparently a result of the close

tolerances of the steel vanes. Larger tolerances and/or flexible vanes would probably alleviate this problem. Generally, the fibers appeared to have been adequately dispersed in the mix; however, some clumps of fibers were noticed, particularly in the BoniFiber product.

Four fiber test sections approximately 1000 feet in length and one lane in width were installed in the outermost eastbound lane. Three of the fiber test sections contained Hercules FP3010 1/4-inch fibers and one contained 1/4-inch BoniFibers B. A fiber-asphalt crack sealer (Hercules Extrudamat) was used to seal cracks (due to shrinkage of soil cement) in the surface of the Type A mix in one of the Hercules fiber test sections prior to application of the Type D mix. Locations of the test pavements are given below:

<u>Pavement Description</u>	<u>Location</u>
0.3 % Hercules	Sta 184+10 - 192+34
Control	Sta 192+25 - 197+60
0.2% Hercules + Extrudamat	Sta 197+60 - 208+50
Control	Sta 208+50 - 229+10
0.2% Hercules	Sta 229+10 - 240+20
Control	Sta 240+20 - 246+00
0.17% BoniFibers	Sta 291+80 - 318+60

(Fiber contents are given in percent by weight of total mixture.)

Performance. Shrinkage cracks in the soil cement reflected through the asphalt stabilized base course prior to placement of the Type D surface course which contained the fibers. Consequently, these cracks reflected through the surface course within three to six months after construction. Cracks in the control sections appeared about 1 to 2 months before those in the fiber test sections. After six months the fiber sections and the control sections had about the same appearance. After 19 months in service, there are no visually detectable differences in the fiber test sections and the control sections.

CONCLUSIONS AND RECOMMENDATIONS

Asphalt paving mixtures containing several types of synthetic fibers were evaluated in a logical sequence of laboratory tests. The effects of fibers on mixture stability, strength, stiffness, tensile properties and resistance to cracking and plastic deformation and moisture damage were assessed. Data from one fiber mixture was utilized in a computer program to predict the effects on pavement performance parameters such as cracking, rutting and roughness. Fibers were installed in field test pavements and have been observed for up to 19 months.

Based on results of these tests and review of existing literature the following conclusions are offered.

Conclusions

1. The addition of fibers to an asphalt paving mixture will normally require (or allow) a slight increase in the optimum design asphalt content. This increase in asphalt content is, of course, dependent upon the quantity and surface area per unit weight of fibers added and the type and gradation of the aggregate.

2. Generally, Hveem and Marshall stability of a paving mixture is not significantly increased or decreased by the addition of synthetic fibers. More than one half the fiber mixtures tested exhibited greater Marshall flow than the control specimens. This is due, in part, to the additional asphalt and air voids in the fiber mixtures.

3. Fibers in an asphalt concrete mixture will decrease the sensitivity to asphalt cement content. That is, stability of a given fiber mixture will not decrease as rapidly as the nonfiber mixture when asphalt content exceeds the optimum.

4. A given dense graded asphalt paving mixture containing synthetic fibers will require more compactive effort to produce a pavement density equal to that normally obtained without fibers.

5. Of those tested, no single type of fiber appears to consistently impart substantially better or worse properties to the asphalt paving mixture than any other type of fiber.

6. According to results from resilient modulus tests, stiffness of the fiber mixtures is not appreciably different from that of the control mixture at any temperature from -10⁰F to 100⁰F.

7. Indirect tension tests revealed that, overall, the addition of fibers to a paving mixture will cause a slight decrease in tensile strength and a slight increase in tensile strain (elongation) at failure. The increased tensile strain at failure is likely due at least partly to the additional asphalt as well as the fibers in these mixtures and shows that fibers and additional asphalt add flexibility or extensibility to asphalt concrete.

8. Generally, a mixture containing fibers is less susceptible to moisture induced damage than a similar mixture containing no fibers. It is surmised that, even though the fiber mixtures had greater void contents than the control mixture, the additional asphalt in the fiber mixtures increased the film thickness on the aggregate particles thus affording greater protection from moisture.

9. Based on a limited number of constant-stress flexural fatigue tests, it appears that synthetic fibers have the potential to increase fatigue performance of asphalt concrete paving mixtures. Fibers appear to be most beneficial at high strain levels.

10. Laboratory tests on fiber and nonfiber asphalt mixtures at 33 and 77⁰F indicate that fiber mixtures will exhibit significantly greater resistance to crack propagation at relatively high strain levels. Apparently, the fibers aid in distributing the stresses away from the crack site.

11. Based on predicted pavement performance using mathematical models, properly designed asphalt paving mixtures containing fibers have the potential to increase overall pavement service life. Further, fiber mixtures exhibited the capacity to reduce rutting but not cracking in an asphalt pavement.

12. Observation of the two field test pavements showed that, in one instance, fibers appeared to reduce reflection cracking, but in the other, fibers had little effect on reflection cracking. Review of field tests conducted by other agencies indicates that synthetic fibers in hot mixed asphalt concrete will often reduce reflective

cracking. However, fibers have not been established as a cost effective construction alternative.

13. Fibers can be successfully employed in drum mix plants using modified fines feeding equipment. Fibers can also be mixed in the asphalt cement before it is introduced into the drum, this process, however, requires special equipment.

Recommendations

1. Continue annual evaluation of asphalt test pavements containing fibers and fiber-asphalt crack sealer. This is the only method whereby realistic cost-benefit ratios can be established.

2. Mix temperature should not exceed 290⁰F when polypropylene fibers are used.

3. Fiber and nonfiber mixtures tested in this study were prepared using the same compactive effort. Laboratory tests should be performed on fiber and nonfiber mixtures that are compacted to the same air void content. This is not an easy task but appears to be a less biased approach for measuring the effects of the different fibers. Properties of the fiberized mixtures would have probably compared more favorably with the control mixture if all had been compacted to the same void content.

Table 1. Physical Properties of AC-20 from American Petrofina
Big Spring, Texas (Cosden)

Properties	Test Results
Viscosity, 77°F, poises	2.5 x 10 ⁶
Viscosity, 140°F, poises	1,910
Viscosity, 275°F, poises	3.10
Penetration, 39.2°F, (200g/60s)	13
Penetration, 77°F, (100g/5s)	45
Softening Point, Ring and Ball, °F	119
Specific Gravity, 60°F	1.041
<u>Thin Film Oven Test</u>	
Viscosity, 140°F, poises	4,290
Penetration, 77°F, dmm	32
Percent Penetration Retained	71
<u>Rolling Thin Film Oven Test</u>	
Viscosity, 140°F, poises	5,350
Penetration, 77°F, dmm	29
Percent Penetration Retained	64

Table 2. Individual Components of the Project Design Gradation.

Sieve Sizes	Aggregate Gradation				
	Siliceous Gravel	Field Sand	Limestone Crushes Fines	Combined Gradation	DSHPT Type D Specification
Passing 1/2-inch sieve	100	100	100	100	100
Passing 3/8"-inch sieve	100	100	100	100	85-100
Passing 3/8", retained on No. 4	49	0	0	35	21-53
Passing No. 4, retained on No. 10	46	0	6	34	11-32
Total retained on No. 10	95	0	6	69	54-74
Passing No. 10, retained on No. 40	3	1	42	11	6-32
Passing No. 40, retained on No. 80	1	49	17	9	4-27
Passing No. 80, retained on No. 200	0	42	16	7	3-27
Passing No. 200 sieve	1	8	19	4	1-8
Percent Combined	70 + 10 + 20 = 100 weight percent				

Table 3. Physical Properties of Fibers.

Fiber	Composition	Diameter, Denier*	Length, inches	Specific Gravity
Hercules-Fiber Pave 3010	Polypropylene	3-5	0.39	0.91
BoniFiber-B	Polyester	4-6	0.25	1.38
Hoechst	Polyester	1.5	0.5	1.38
Forta Fibre-ES-6	80%-Polypropylene+ 20%-Aramid	**	1.5	1.00***
Phillips-15	Polypropylene	15	0.5	0.91
Phillips-60	Polypropylene	60	0.5	0.91
Kevlar	Aramid	1.5	0.5	1.44
Fiber Glass	Fiber Glass	**	0.22	2.50
Asbestos-Gooch	Asbestos	**	**	2.50
Kayocel-10-D50	Volitals Cellulose, Starch, and Ash	**	**	1.37

* Denier is defined as the weight in grams of 9,000 meters of a fiber.

** Not known or not applicable.

*** Composite specific gravity.

Table 4. Specimen Code Identification.

Identification	Specimen Code
Control	C
Hercules Fiber Pave 3010, 0.1 percent	H.1
Hercules Fiber Pave 3010, 0.2 percent	H.2
Hercules Fiber Pave 3010, 0.4 percent	H.4
BoniFiber-B, 0.15 percent	B.15
BoniFiber-B, 0.3 percent	B.3
BoniFiber-B, 0.6 percent	B.6
Hoechst Fiber, 0.3 percent	HTZ
Forta Fibre-ES-6, 0.22 percent	F
Forta Fibre, 0.05 percent	F.05
Phillips Fiber, 60 denier, 0.2 percent	P-60
Phillips Fiber, 15 denier, 0.2 percent	P-15
Kevlar Fiber, 0.31 percent	K
Kayocel Fiber-10-D50, 0.30 percent	KO
Asbestos, 0.55 percent	AS
Fiber Glass Fiber, 0.55 percent	FG

* Percentage of Fibers given by Weight of Total Mix.

Table 5. Permanent Deformation Parameters Used in VESYS IIM Analysis.

Mixture Tested	BETA (β)	Test Temperature, °F	ALPHA (α)	GNU (μ)
Control	0.088	40	0.49	0.080
		70	0.31	0.083
		100	0.54	0.088
4.6% Asphalt	0.094	40	0.42	0.052
		70	0.27	0.050
		100	0.44	0.111
4.85% Asphalt	0.094	40	0.13	0.004
		70	0.13	0.025
		100	0.58	0.190
5.1% Asphalt	0.102	40	0.50	0.04
		70	0.38	0.14
		100	0.55	0.16

Table 6. Summary of Field Projects Containing Fibers.

Item	Location	
	North of Abilene	Westside Lufkin
Highway Designation District Number County (Number) Control-Section No. No. Lanes/Direction	US 83 8 Jones (128) 33-5-53 2/North	SH 94 11 Angelina (3) 319-4-47 2/East
Pavement Structure Layer 1 (Top) Layer 2 Layer 3 Layer 4 Layer 5	(Existing) Seal Coat 1" HMAC 9-6-0 JCP+Flex Base Shoulders Subbase -	(New Construction) 1 1/2" 340 Type D 4" 292 Type A Seal Coat 8" Soil Cement 6" Lime Stab. Base
HMAC Overlay/Surface Asphalt Type & Grade Asphalt Source Aggr. Type	Type D Overlay AC-10 Cosden, Big Spring Crushed Limestone + Field Sand	Type D Surface AC-20 Texaco, Port Neches Lightweight + Course Sand + Fine Sand
Traffic Data ADT Percent Trucks ATHWLD Percent Tandem Axles Equiv. 18k axle loads*	7500 11 12,700 80% of ATHWLD 3.7x10 ⁶	10,000 5 11,400 90% of ATHWLD 1.6x10 ⁶
Temperature Mean Daily Max, °F Mean Daily Min, °F Mean Degree Days **	95 (Aug.) 31 (Jan.) 2641	95 (July) 38 (Jan.) 2044
Annual Ave. Precipitation Rainfall, in. Ice and Snow, in.	23 5	45 0.8

* Applications in one direction expected for a 20 year design period.

** One degree-day represents one day with a mean air temperature one degree above 65°F. Thus, 10 degree days may result when the air temperature is 66°F for 10 days or when the air temperature is 75°F for 1 day.

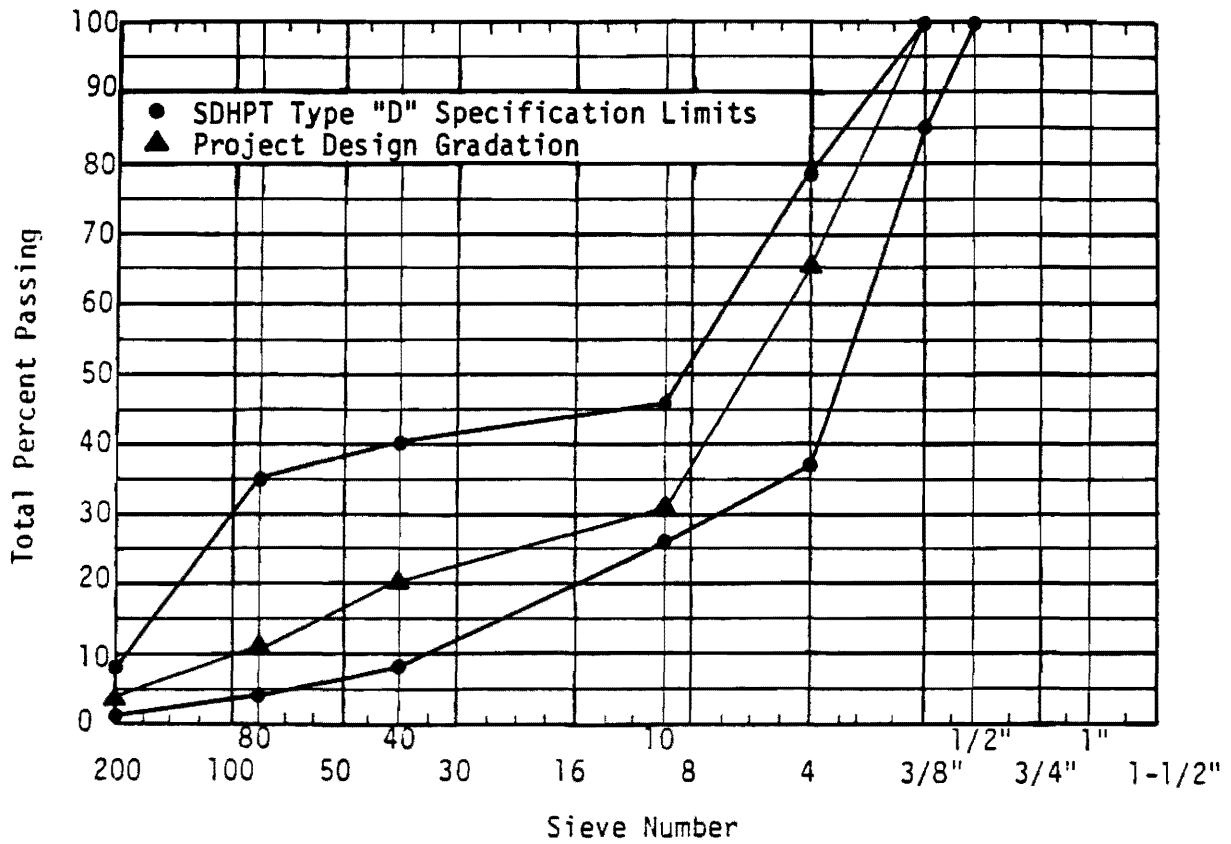


Figure 1. Project Design Gradation Specification Limits.

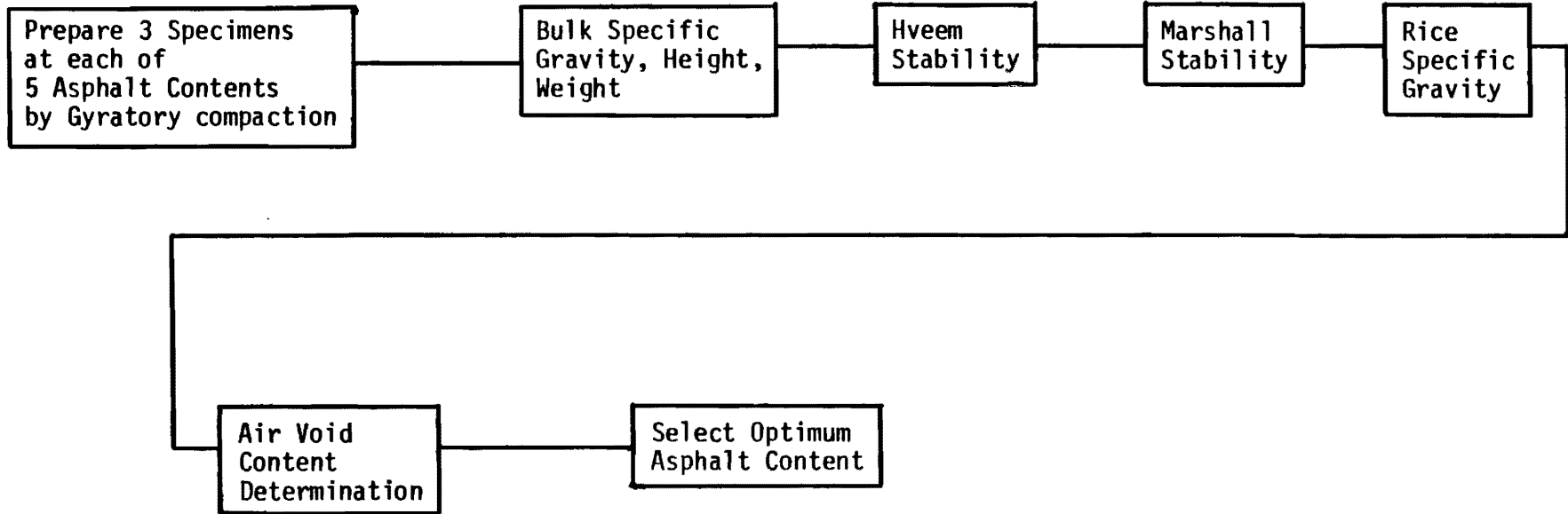


Figure 2. Test Plan for Determining Optimum Asphalt Content.

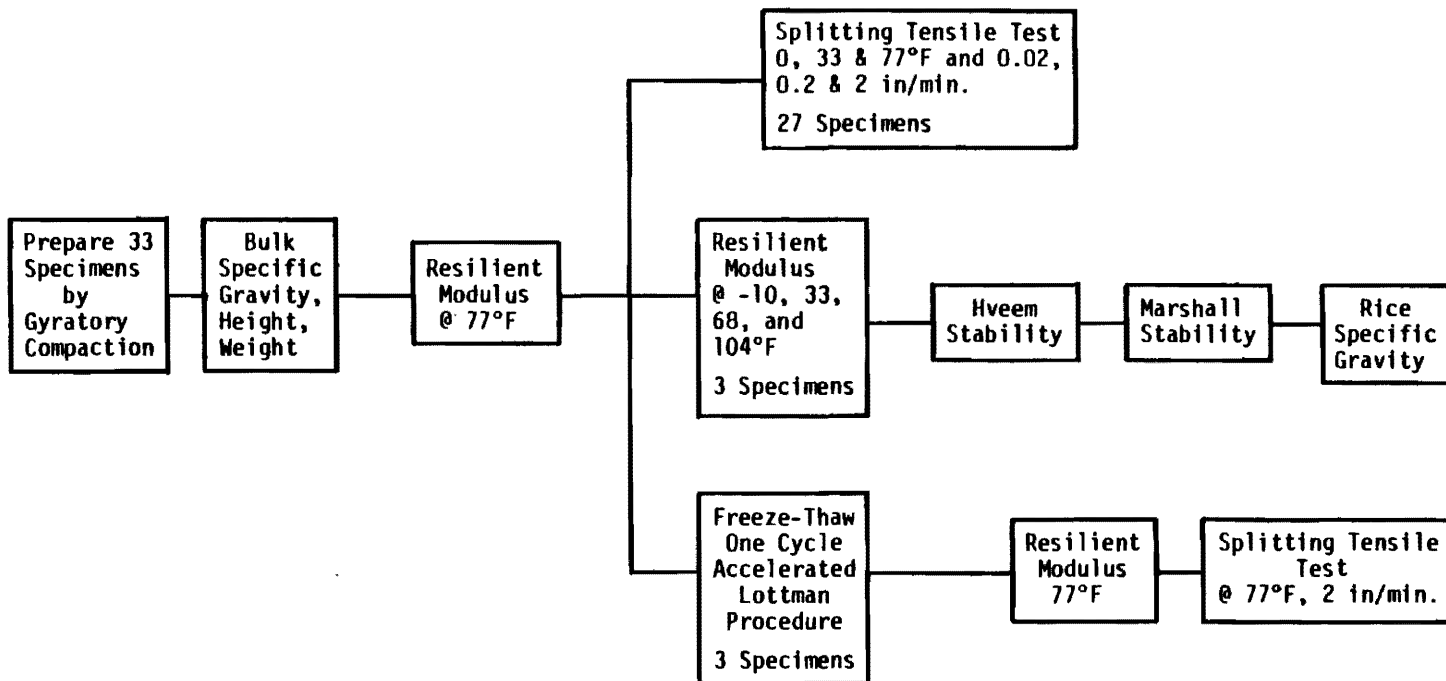


Figure 3. Test Plan for Gyratory Compacted Specimens of Control, Hercules, and BoniFiber Mixtures.

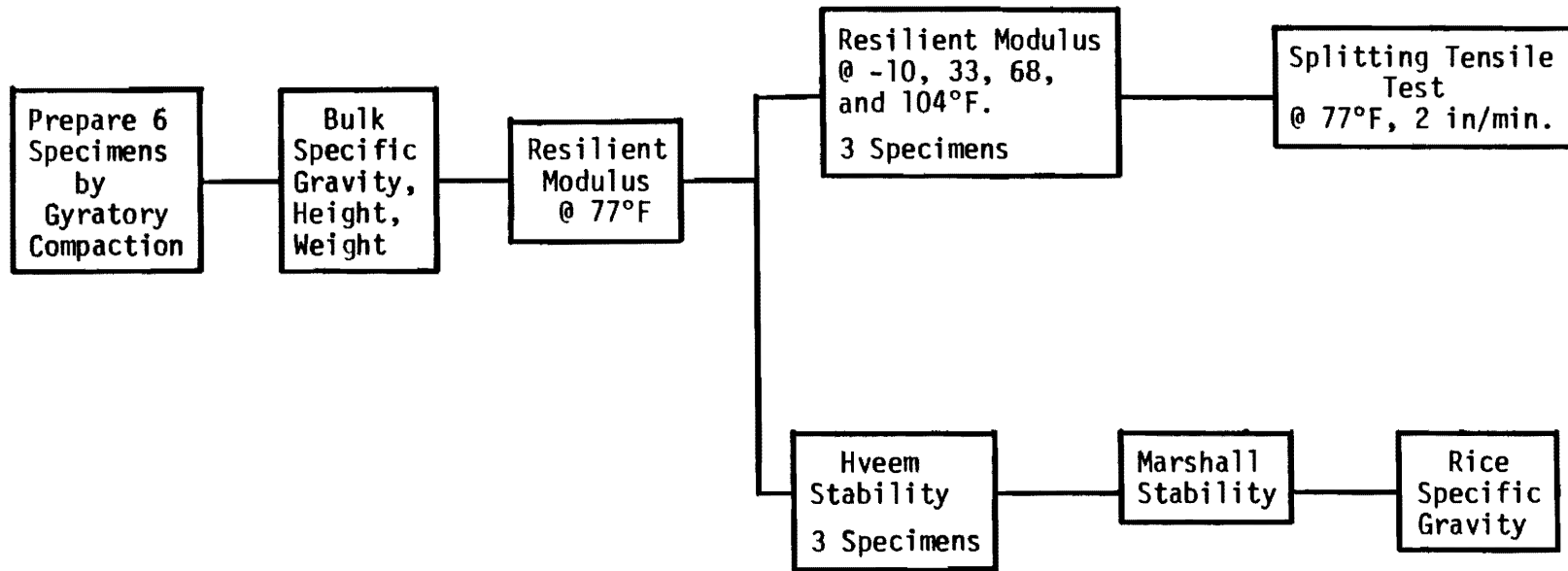


Figure 4. Test Plan for Gyratory Compacted Specimens of Hoechst, Forta Fibre, Phillips, Kevlar, Kayocel, Asbestos and Fiber Glass Mixtures.

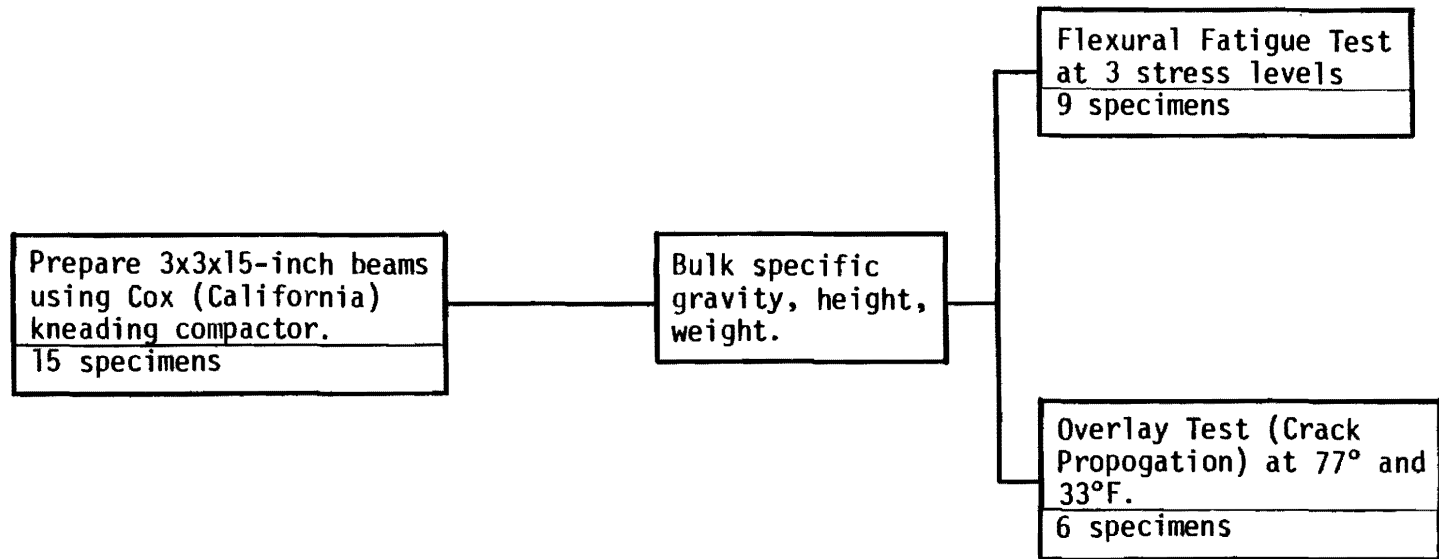


Figure 5. Test Plan Associated with Flexural Fatigue Tests and Determination of Resistance to Thermal Cracking (Hercules, Bonifiber and Kevlar).

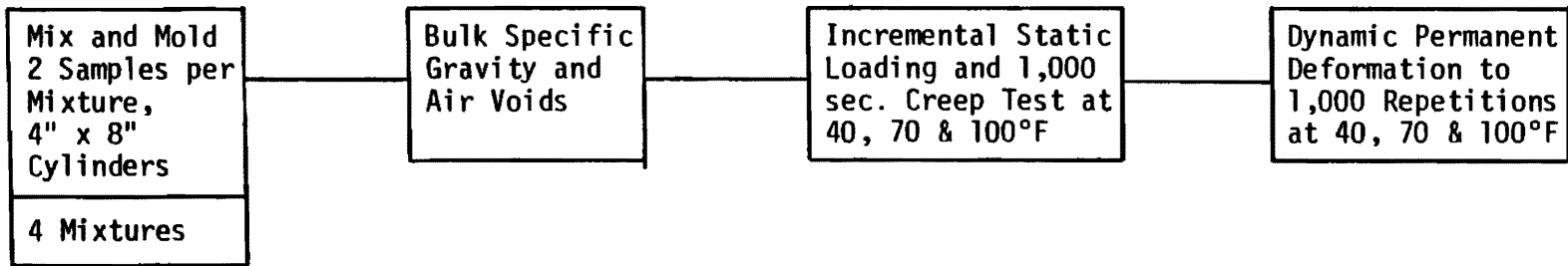
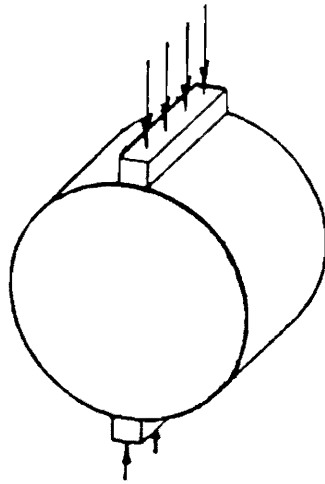
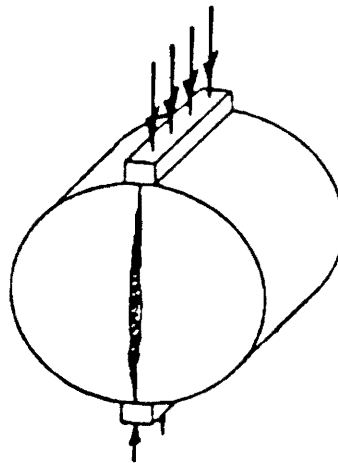


Figure 6. Permanent Deformation and Creep Test Program.

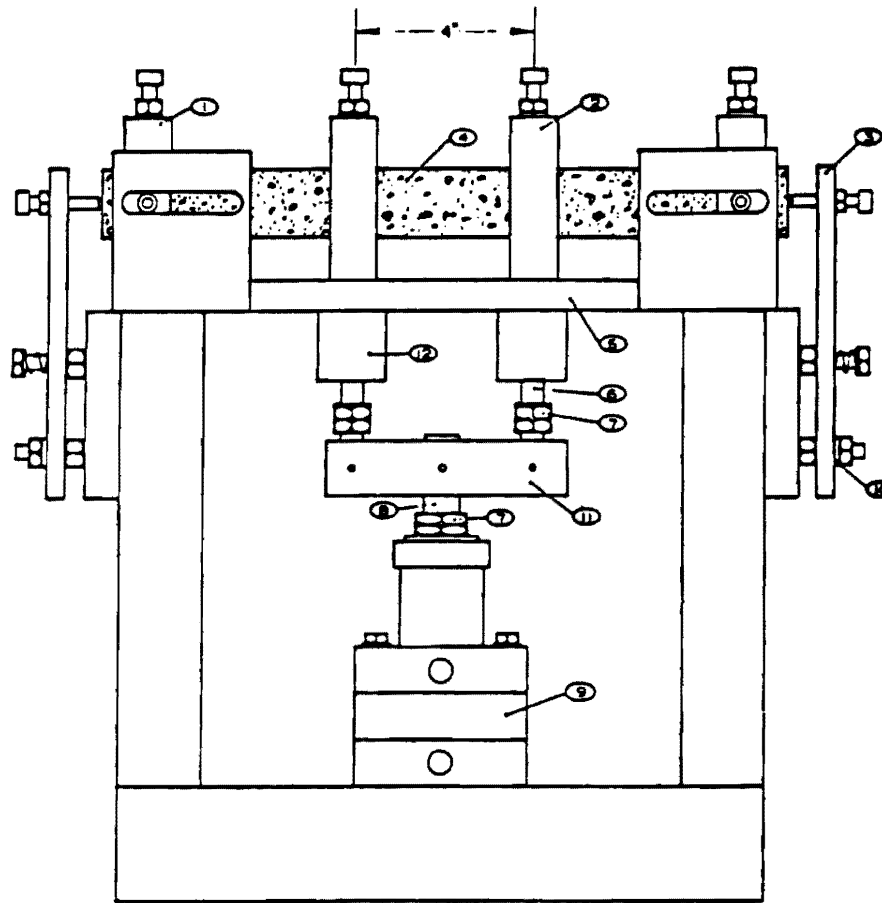


(a) Load Configuration



(b) Failure

Figure 7. Load Configuration and Failure Mode of Indirect Tensile Test Specimen.



- Key:
- | | | |
|-------------------|----------------|--------------------------------------|
| 1. Reaction clamp | 5. Base plate | 9. Double-acting, Bellofram cylinder |
| 2. Load clamp | 6. Loading rod | 10. Rubber washer |
| 3. Restrainer | 7. Stop nut | 11. Lead bar |
| 4. Specimen | 8. Piston rod | 12. Thomson ball bushing |

Figure 8. Schematic of Flexural Fatigue Test Apparatus.

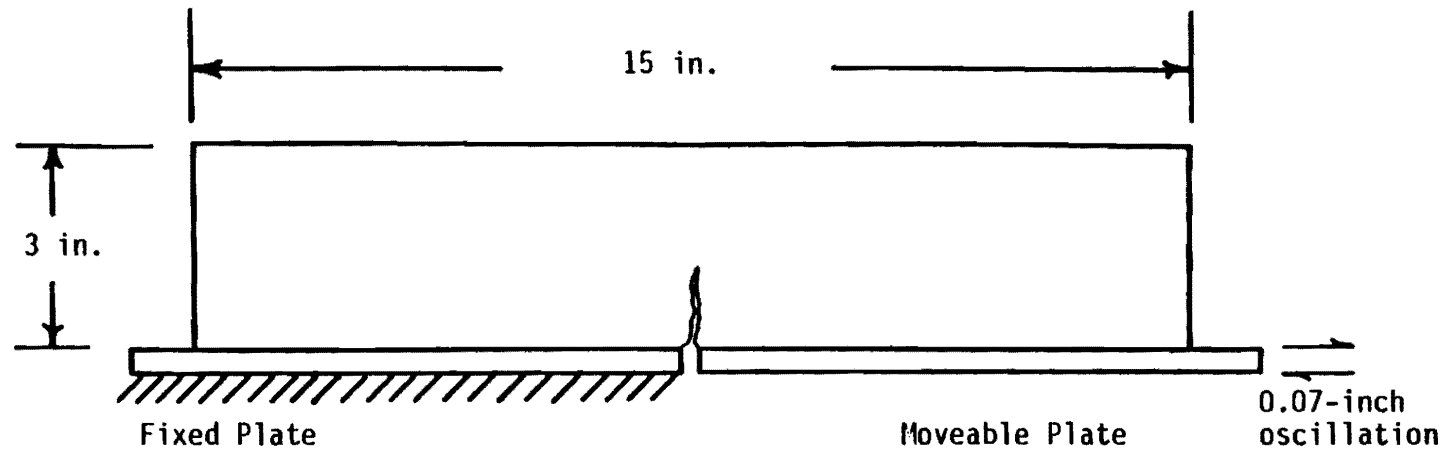


Figure 9. Schematic diagram of test specimen and TTI Overlay Tester.

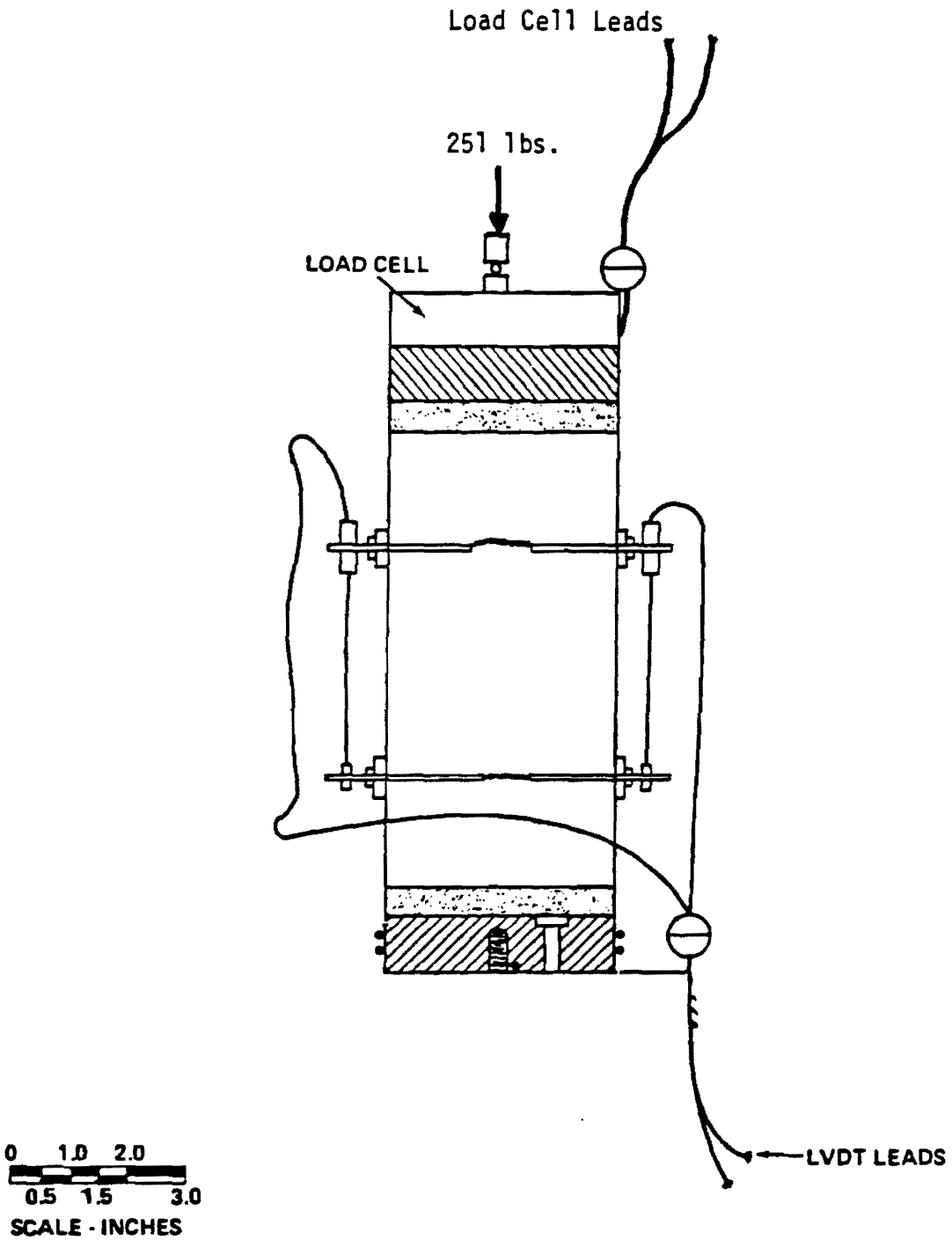


Figure 10. Configuration for Direct Compression Testing of Cylindrical Specimens (Creep and Permanent Deformation).

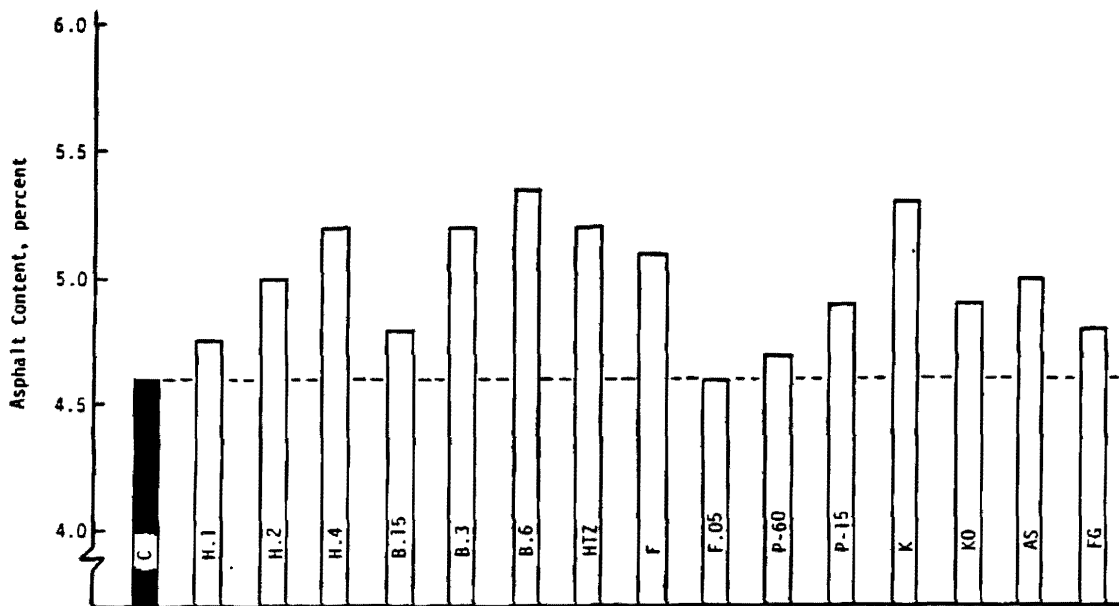


Figure 11. Optimum Asphalt Cement Content for Gyratory Compacted Specimens.

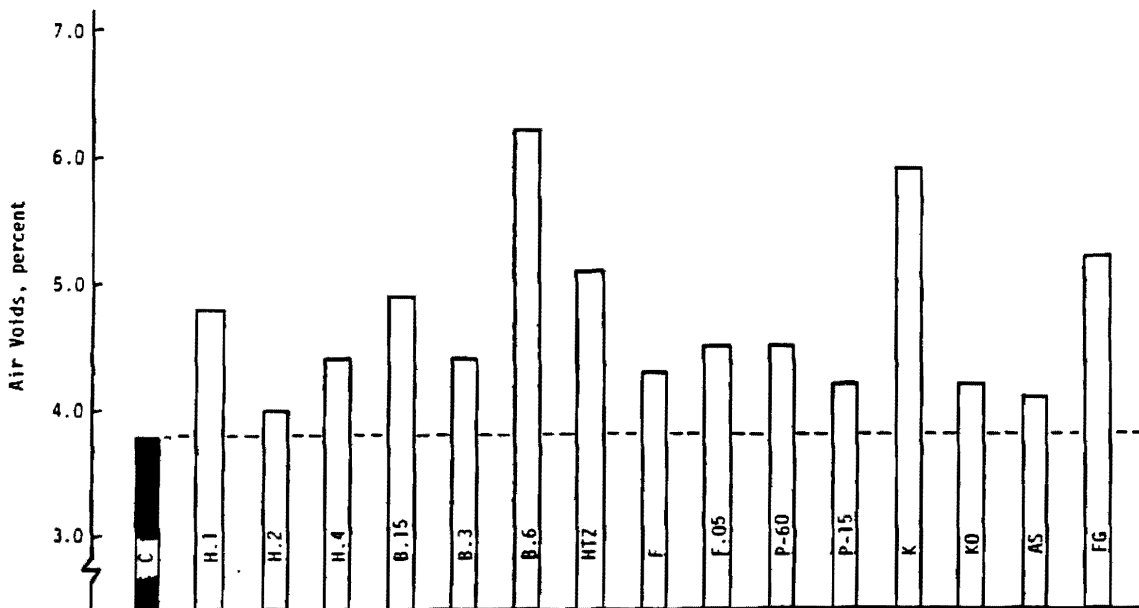


Figure 12. Percent Air Voids at Optimum Asphalt Content for Gyratory Compacted Specimens.

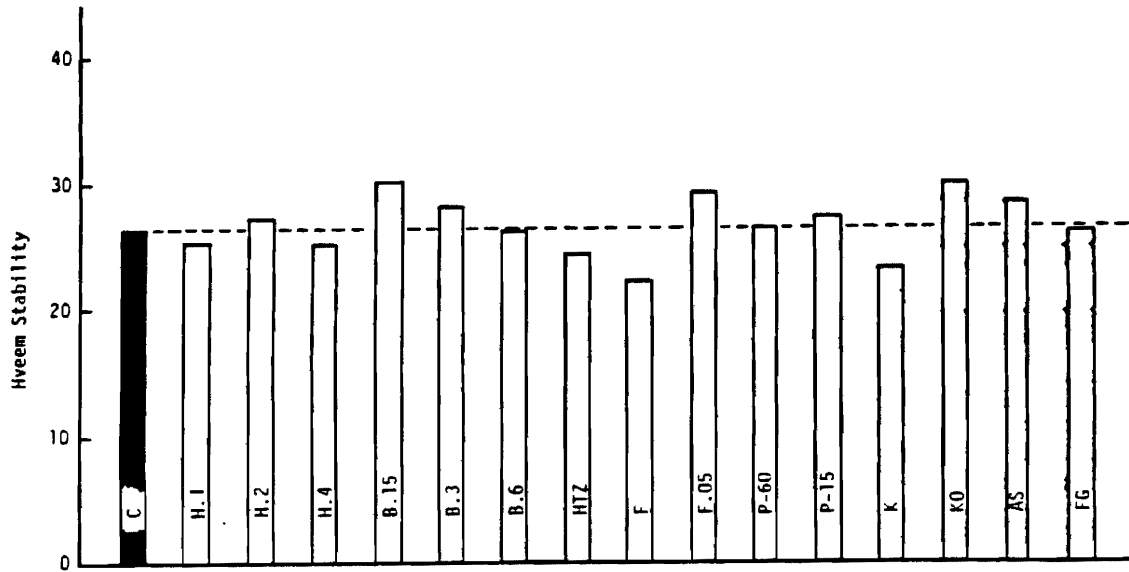


Figure 13. Hveem Stability at Optimum Asphalt Content for Gyratory Compacted Specimens.

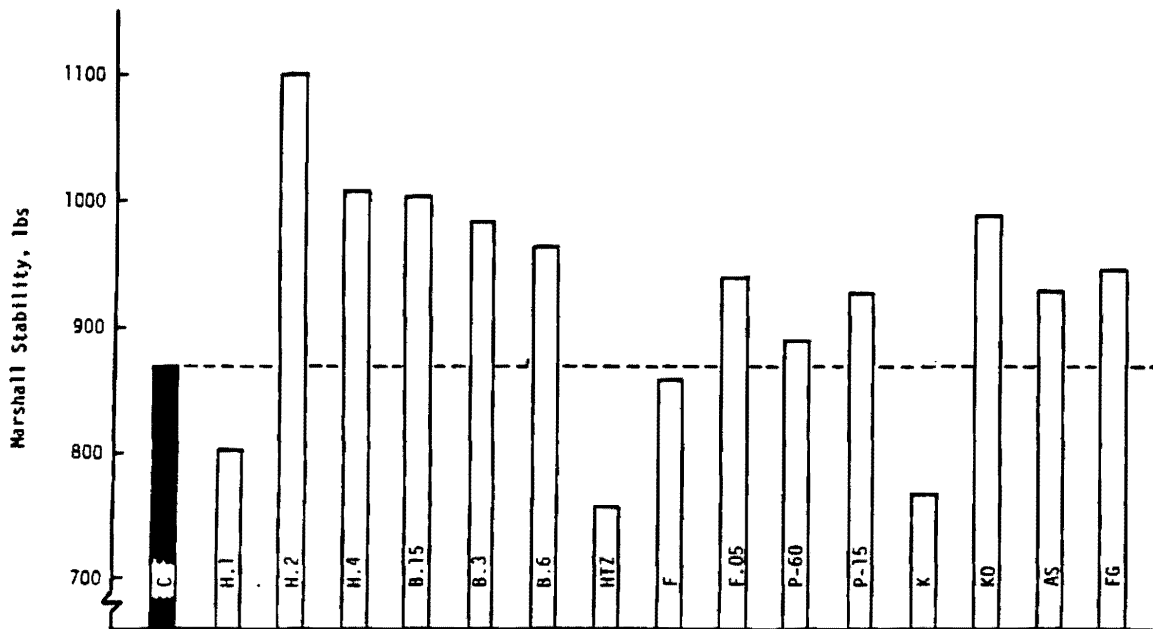


Figure 14. Marshall Stability at Optimum Asphalt Content for Gyratory Compacted Specimens.

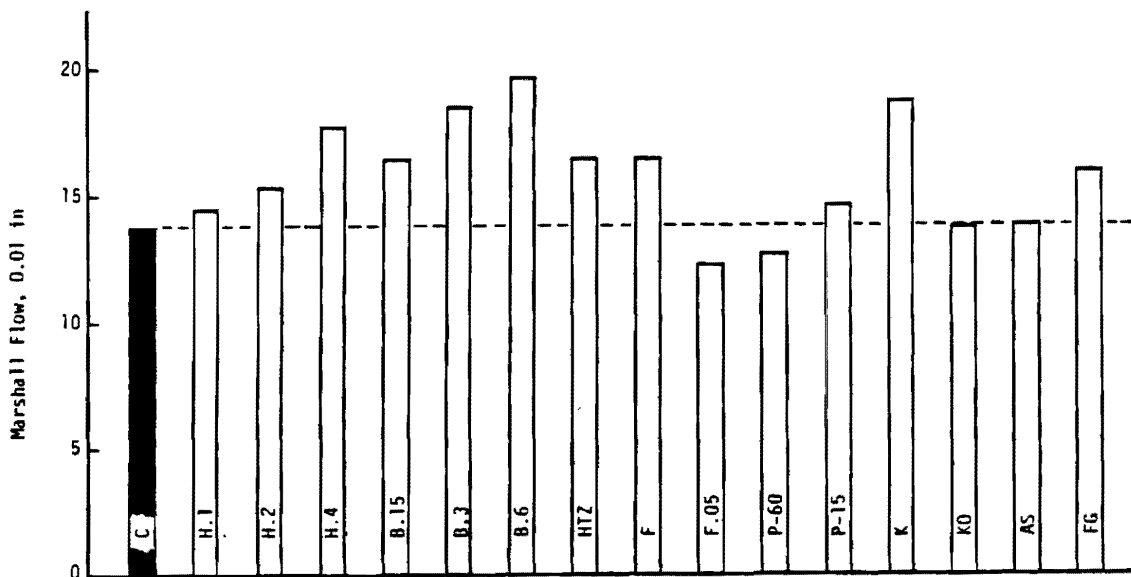


Figure 15. Marshall Flow at Optimum Asphalt Content for Gyratory Compacted Specimens.

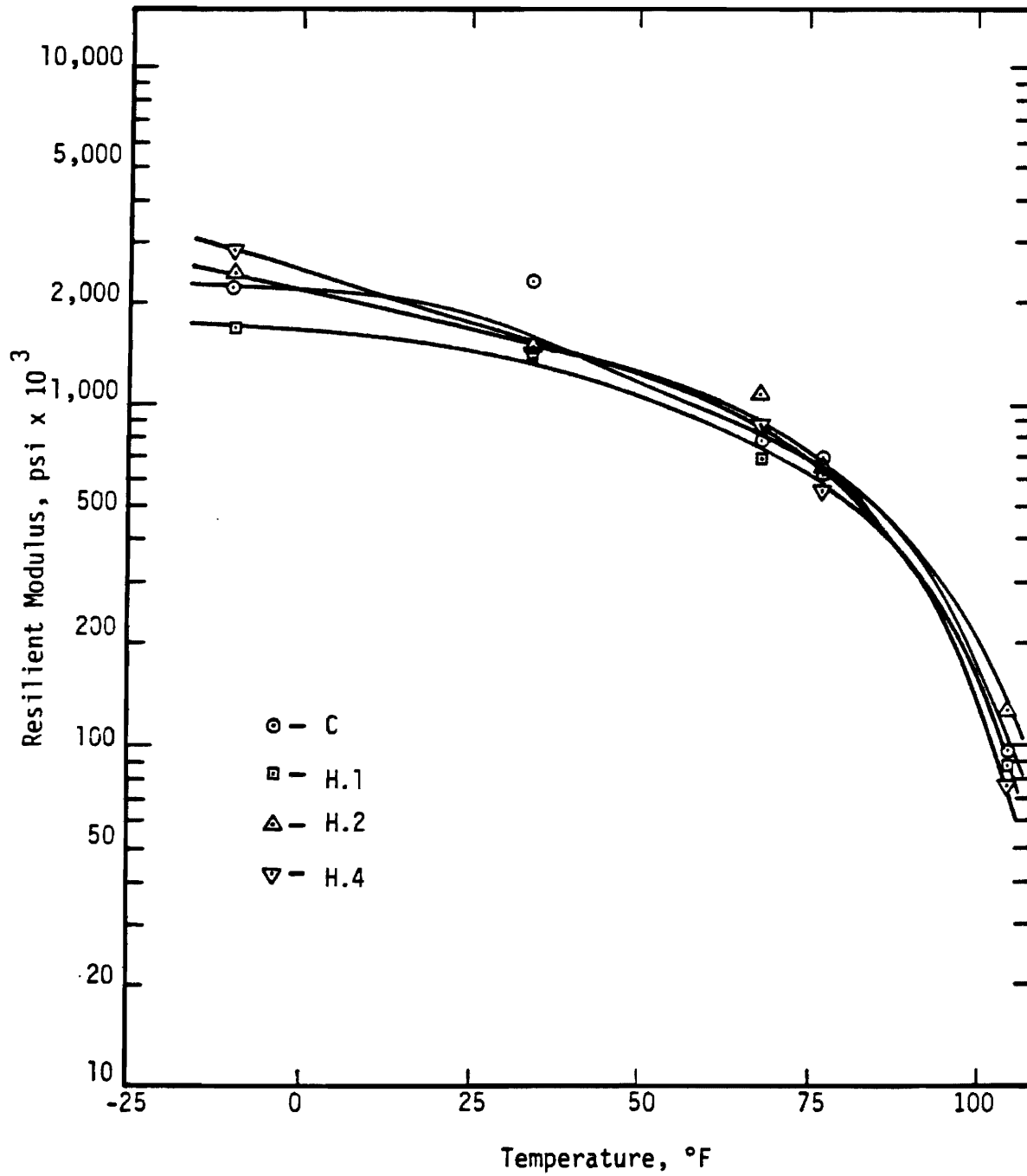


Figure 16. Resilient Modulus as a Function of Temperature for Control and Hercules Specimens.

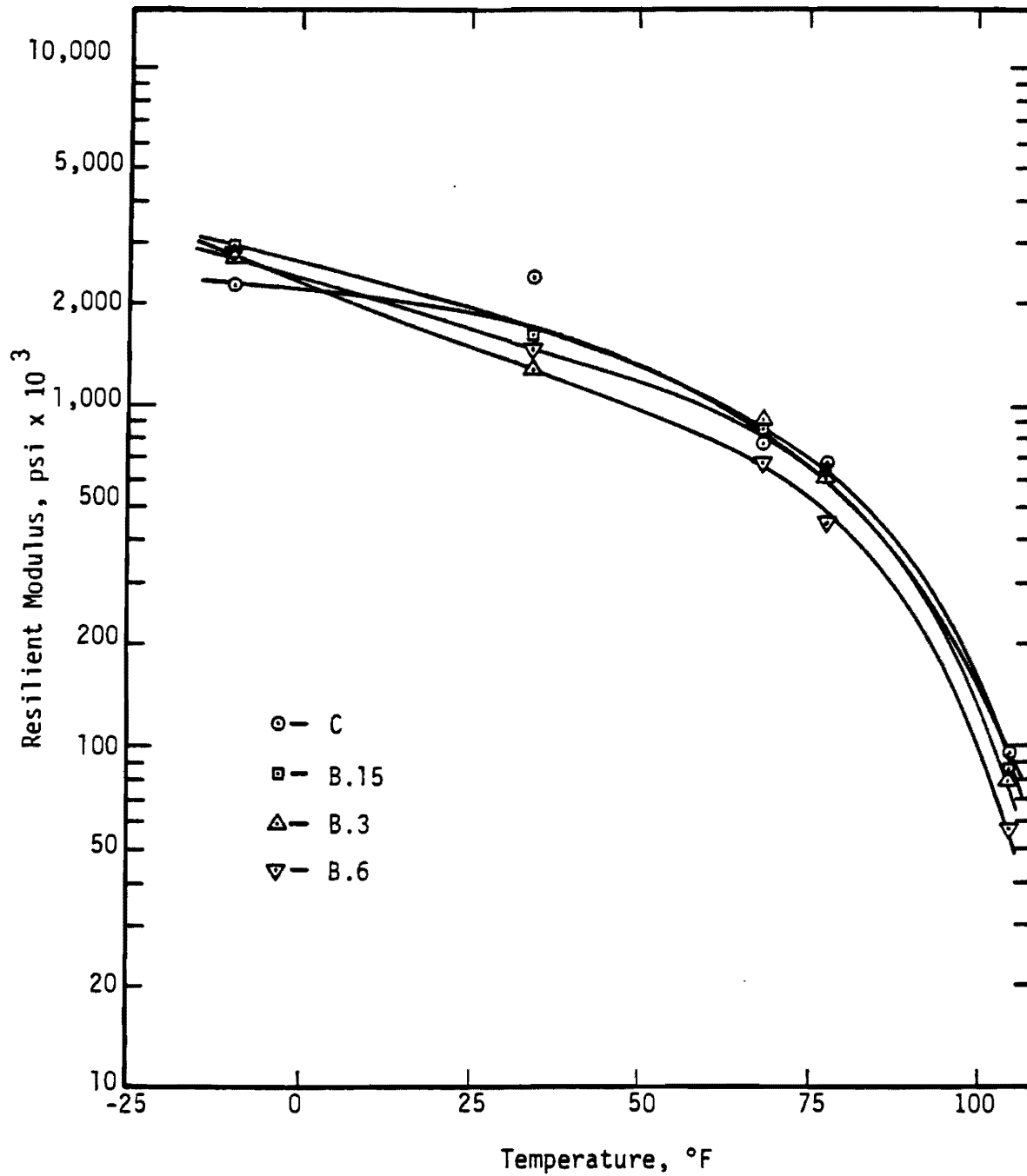


Figure 17. Resilient Modulus as a Function of Temperature for Control and BoniFiber Specimens.

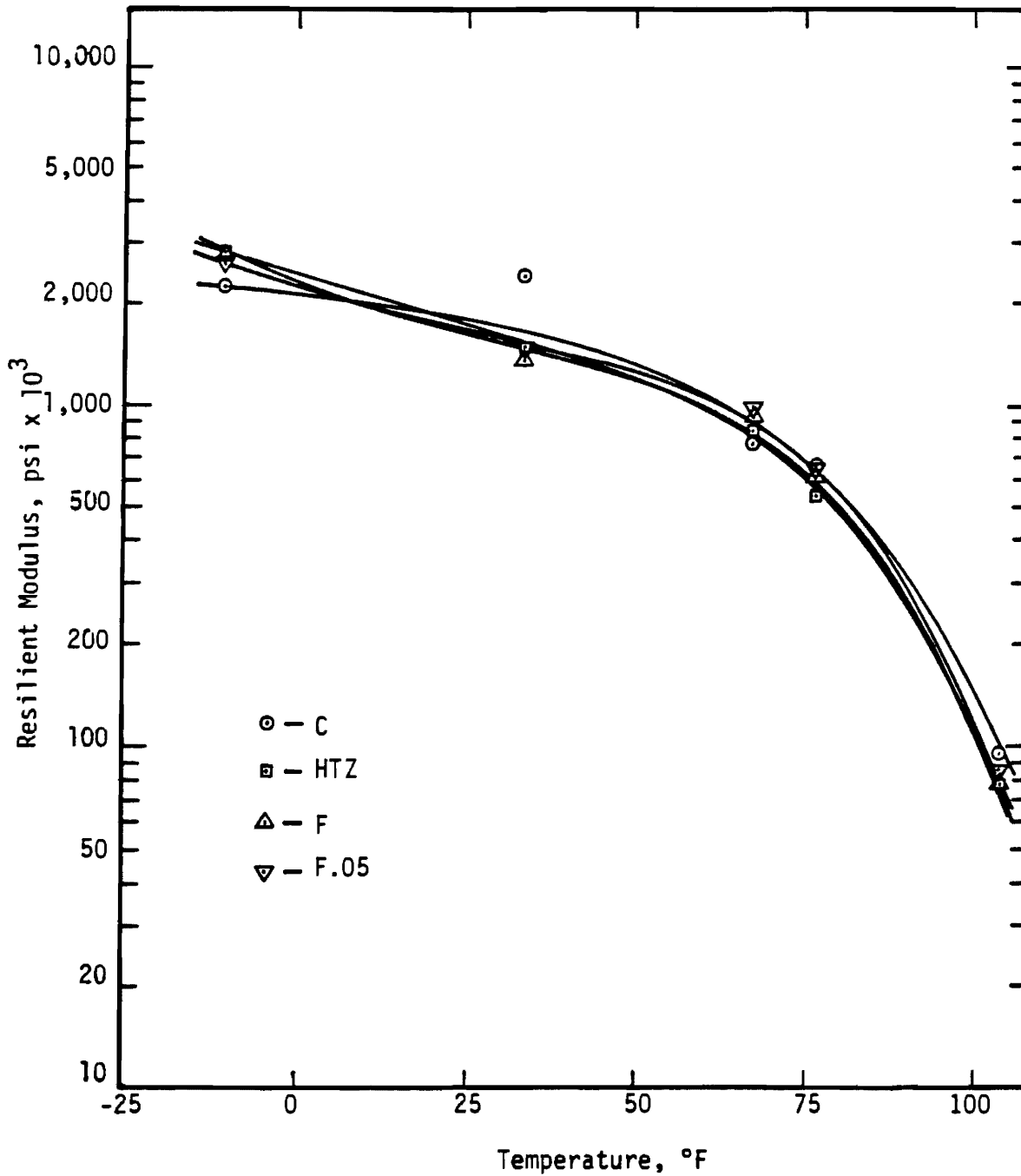


Figure 18. Resilient Modulus as a Function of Temperature for Control, Hoechst, and Forta-Fibre Specimens.

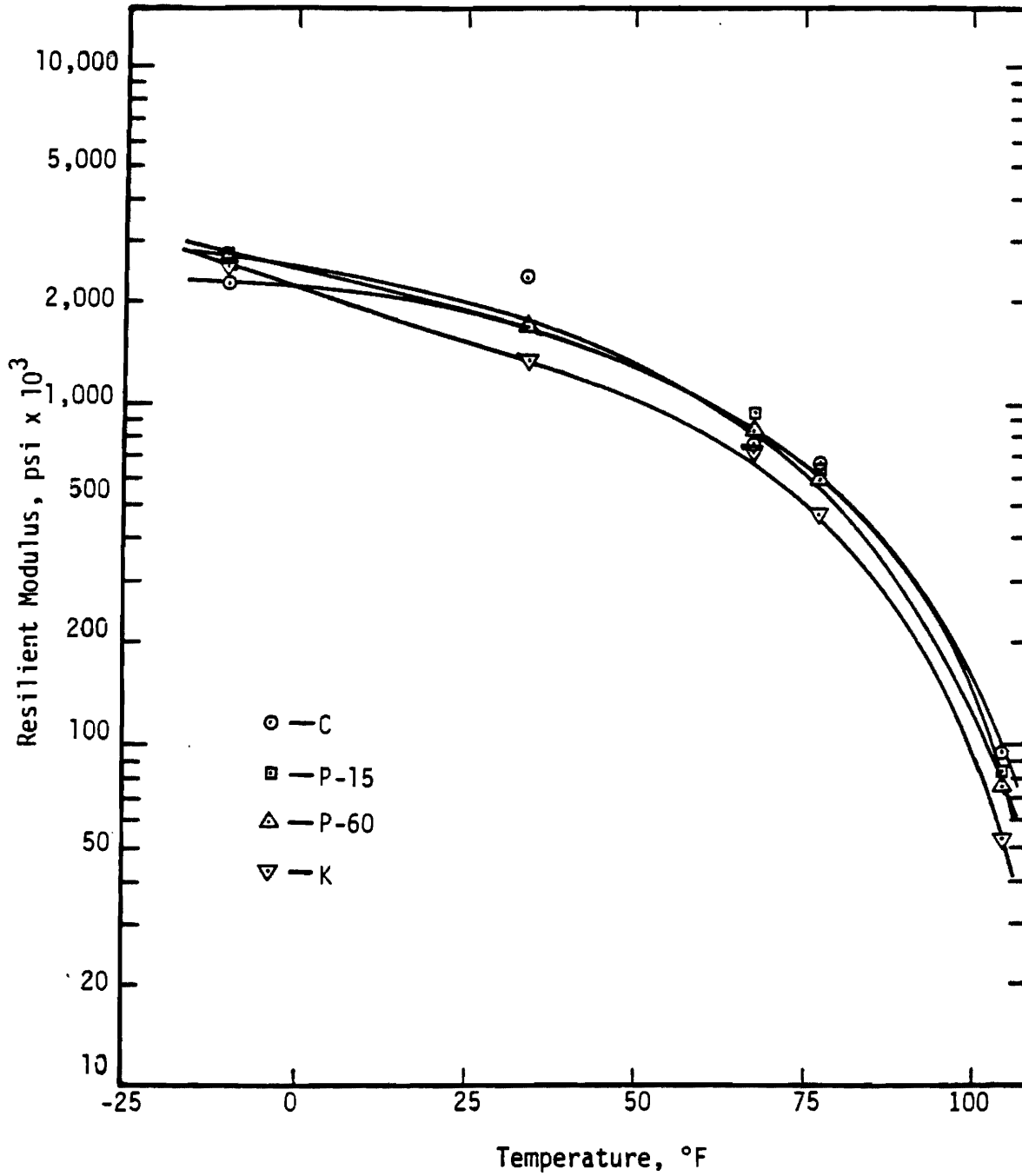


Figure 19. Resilient Modulus as a Function of Temperature for Control, Phillips, and Kevlar Specimens.

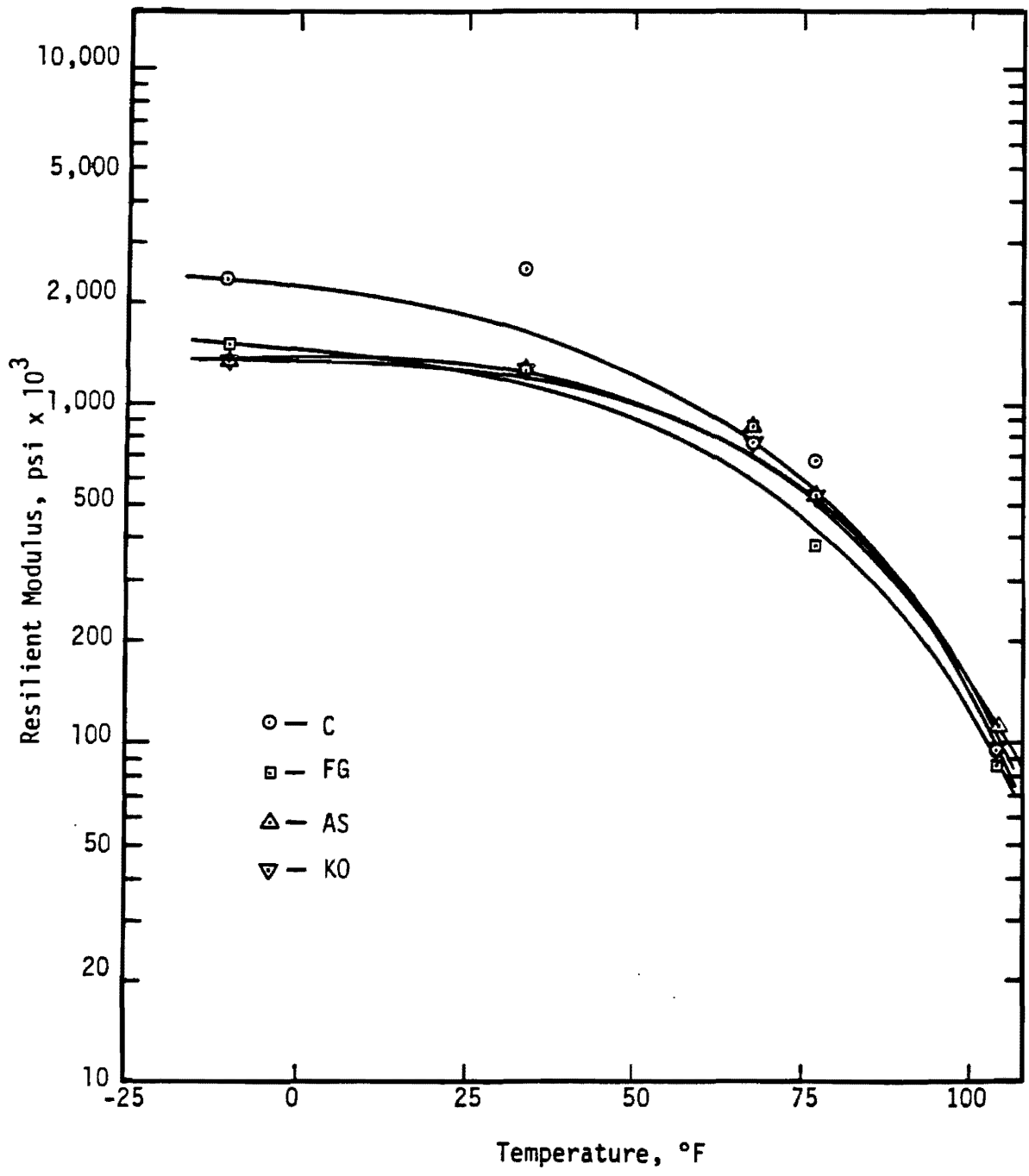


Figure 20. Resilient Modulus as a Function of Temperature for Control, Fiberglass, Asbestos, and Kayocel Specimens.

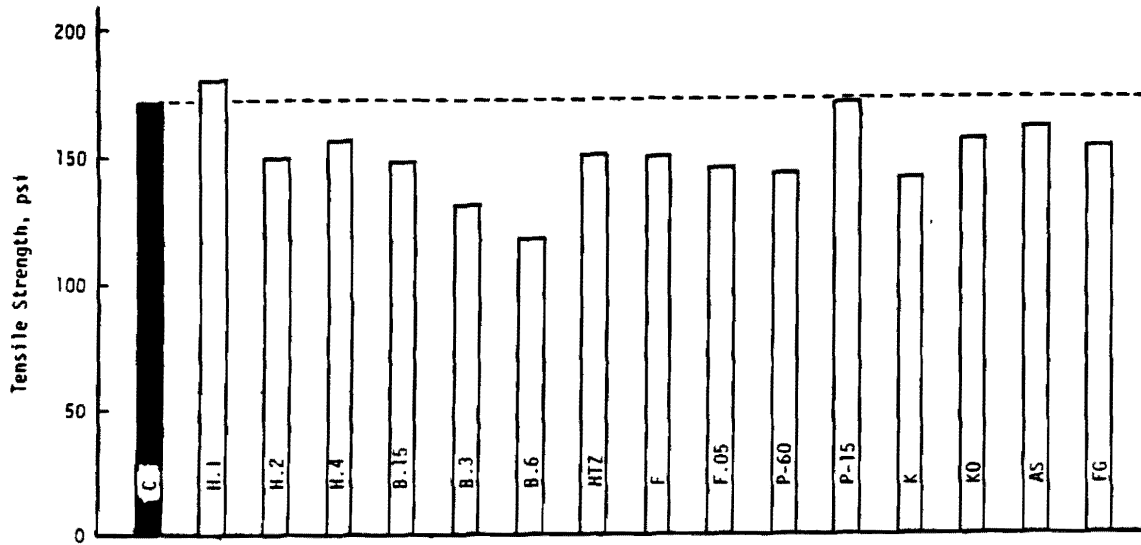


Figure 21. Tensile Strength of Gyratory Compacted Specimens Tested at 2 in/min and 77°F.

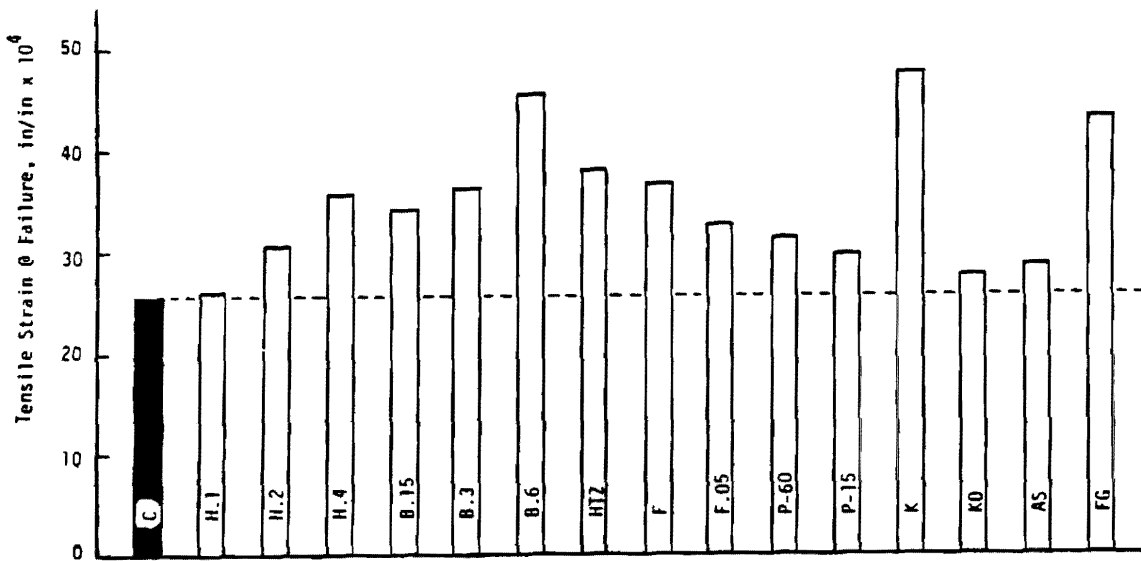


Figure 22. Tensile Strain at Failure of Gyratory Compacted Specimens Tested at 2 in/min and 77°F.

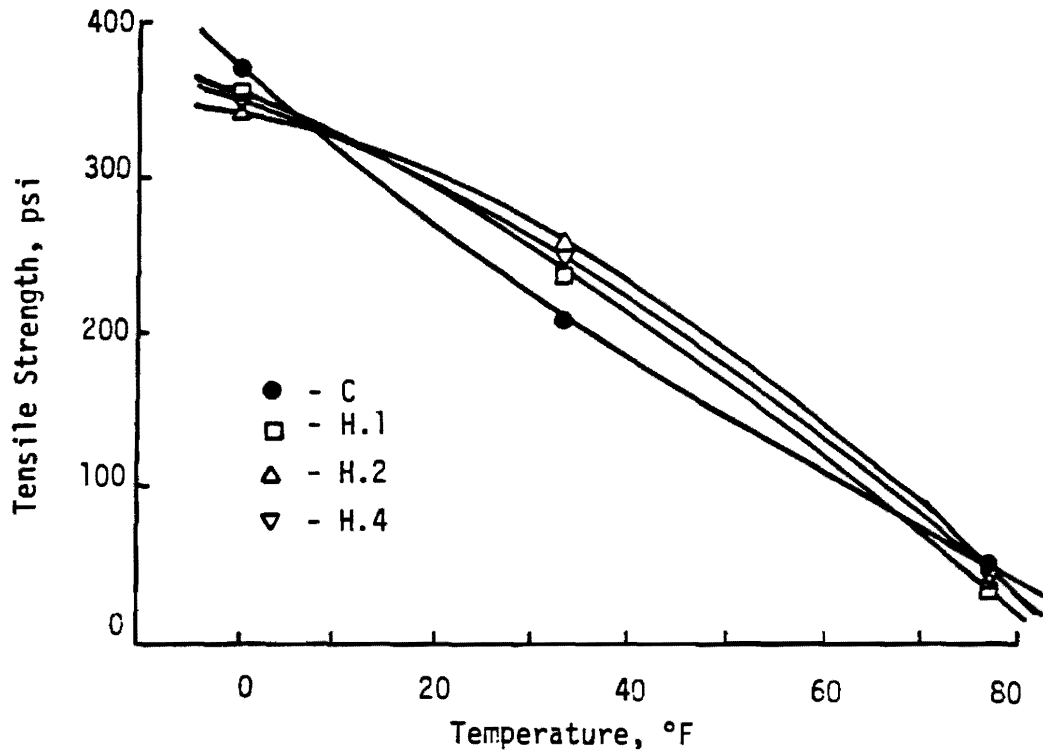


Figure 23. Tensile Strength for Control and Hercules Specimens as a Function of Temperature for a Displacement Rate of 0.02 in/min.

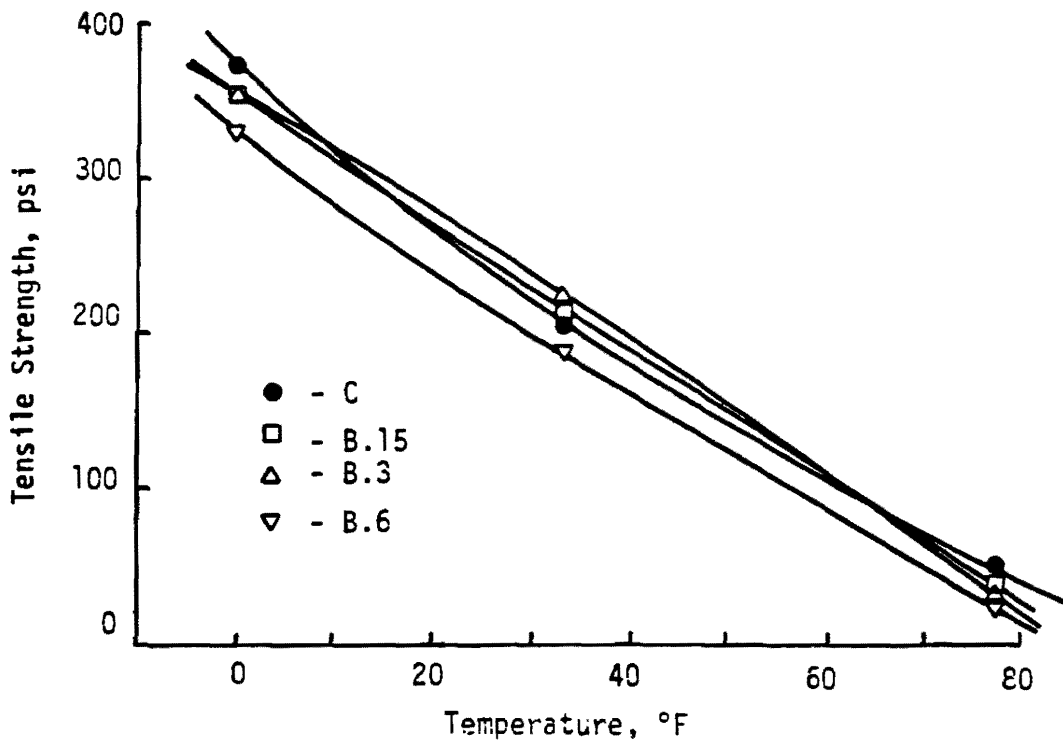


Figure 24. Tensile Strength for Control and Bonifiber Specimens as a Function of Temperature for a Displacement Rate of 0.02 in/min.

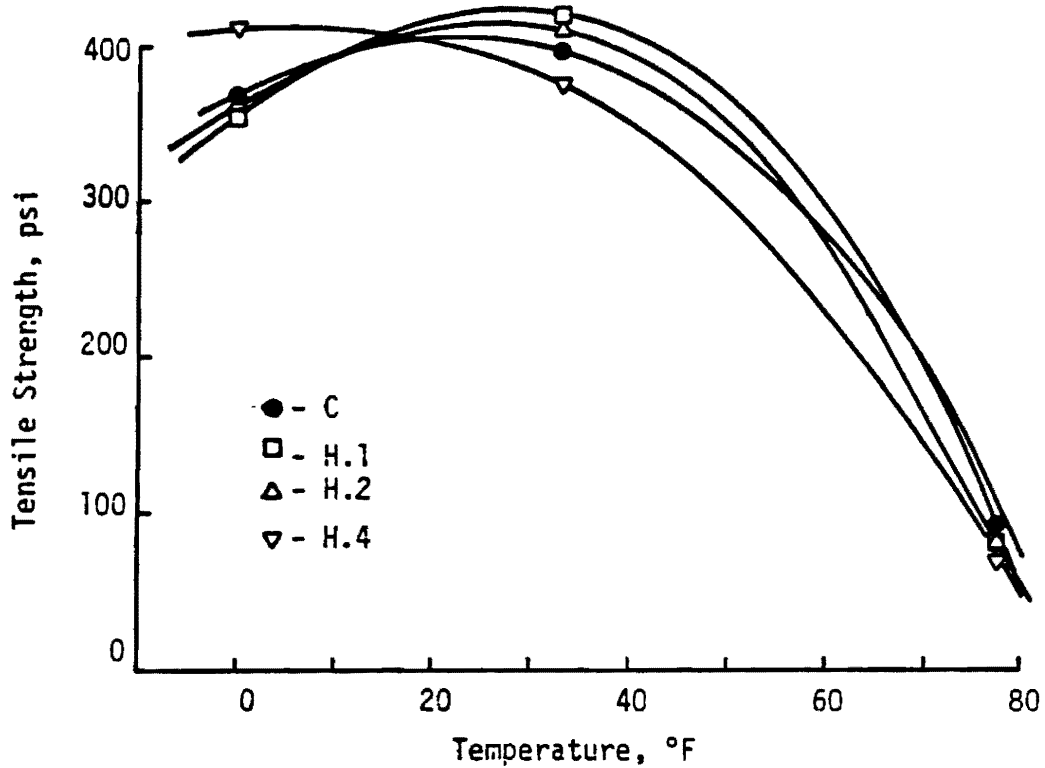


Figure 25. Tensile Strength for Control and Hercules Specimens as a Function of Temperature for a Displacement Rate of 0.2 in/min.

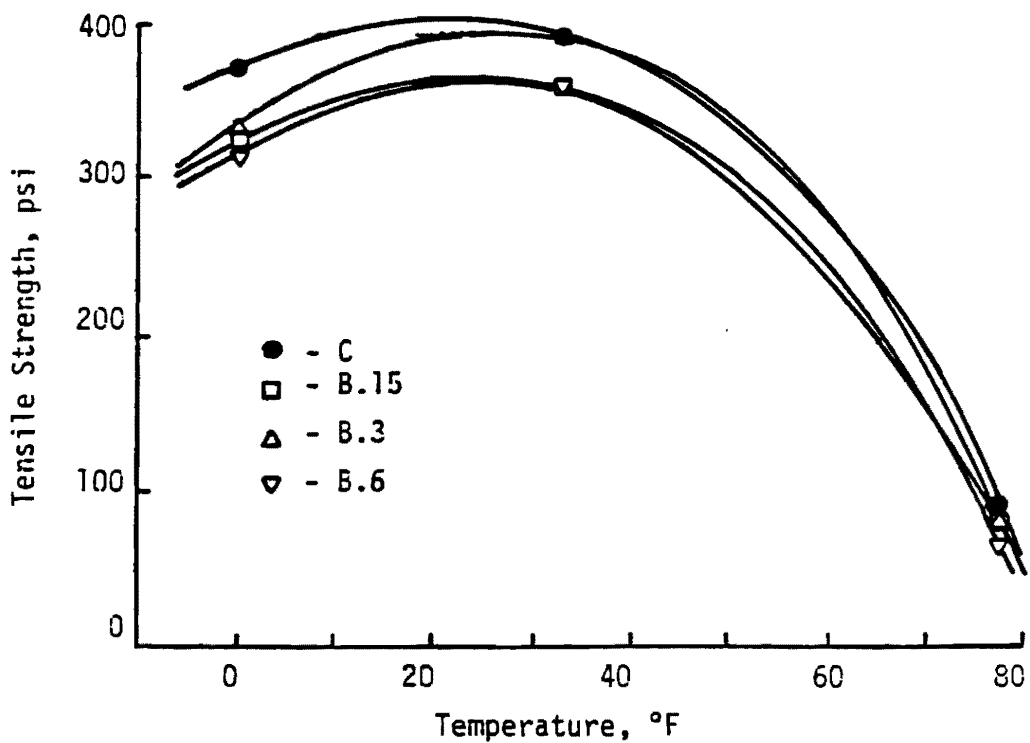


Figure 26. Tensile Strength for Control and Bonifiber Specimens as a Function of Temperature for a Displacement Rate of 0.2 in/min.

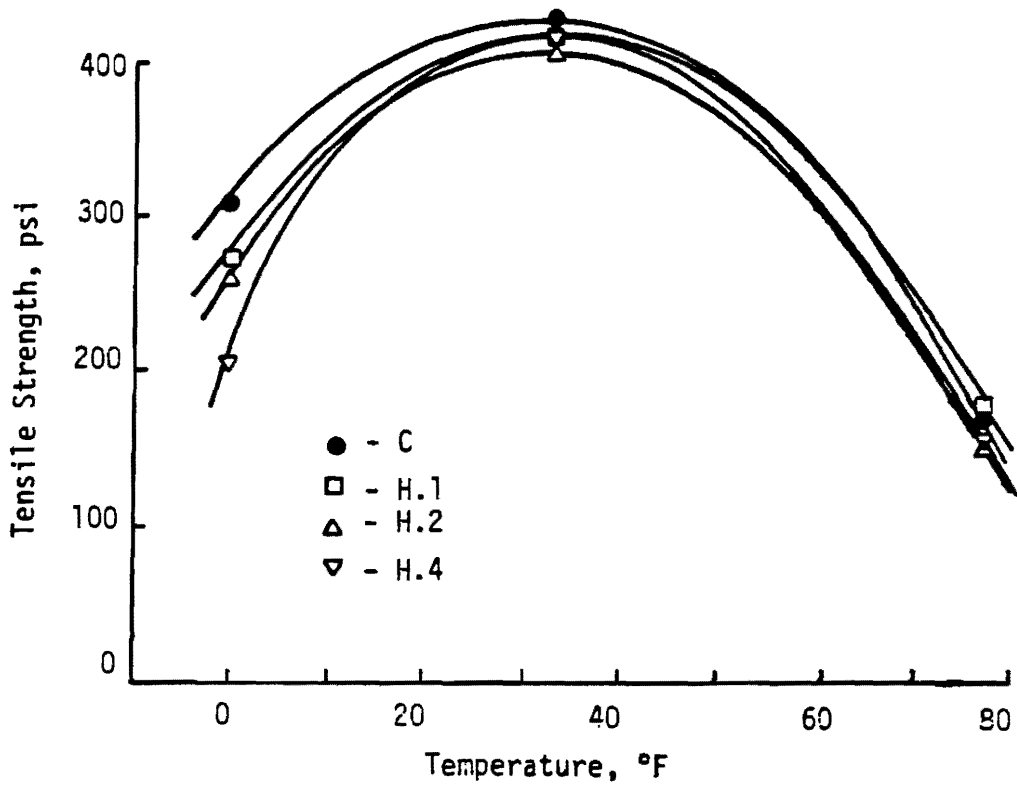


Figure 27. Tensile Strength for Control and Hercules Specimens as a Function of Temperature for a Displacement Rate of 2.0 in/min.

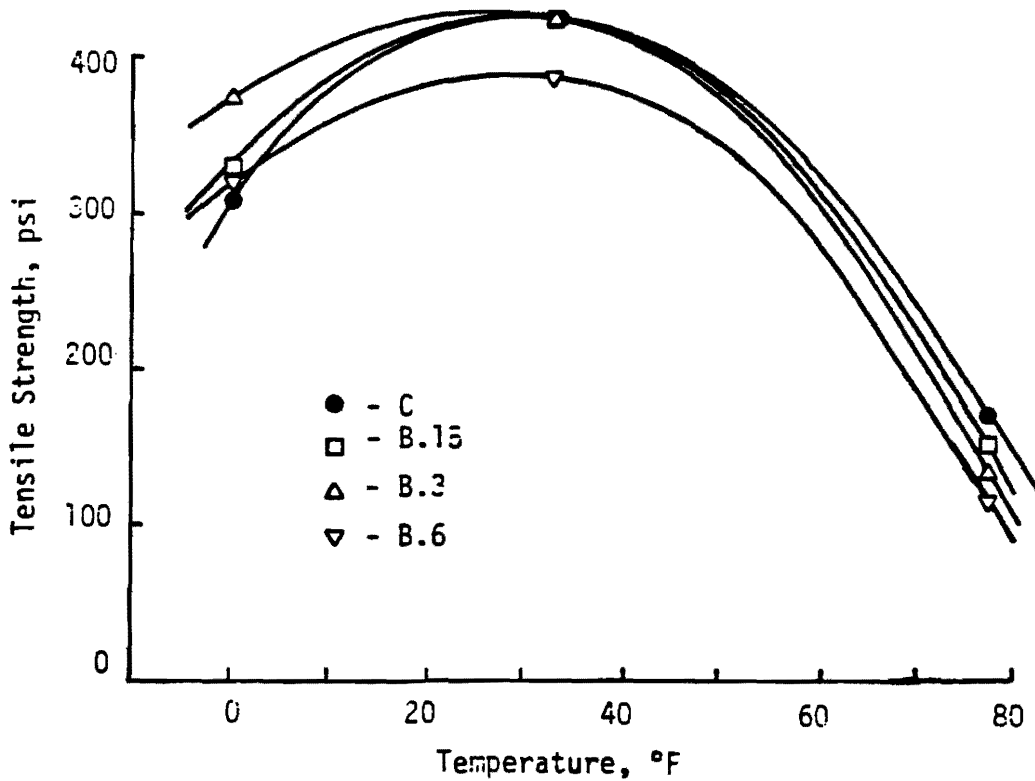


Figure 28. Tensile Strength for Control and Bonifiber Specimens as a Function of Temperature for a Displacement Rate of 2.0 in/min.

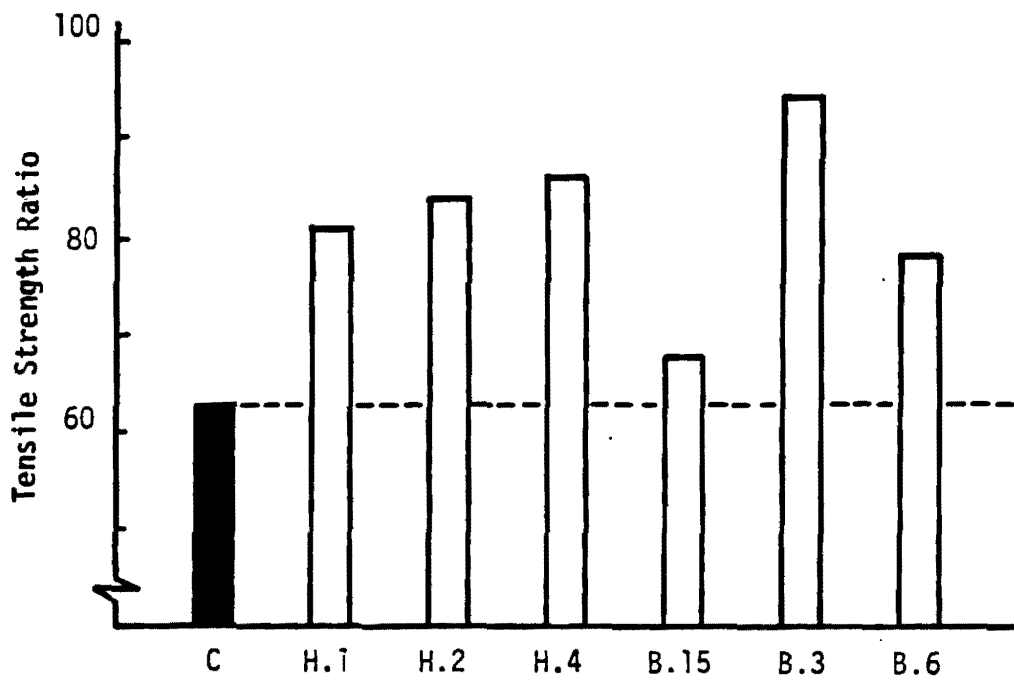


Figure 29. Tensile Strength Ratios after Accelerated Lottman Freeze - Thaw Procedure. (Each value represents an average of three.)

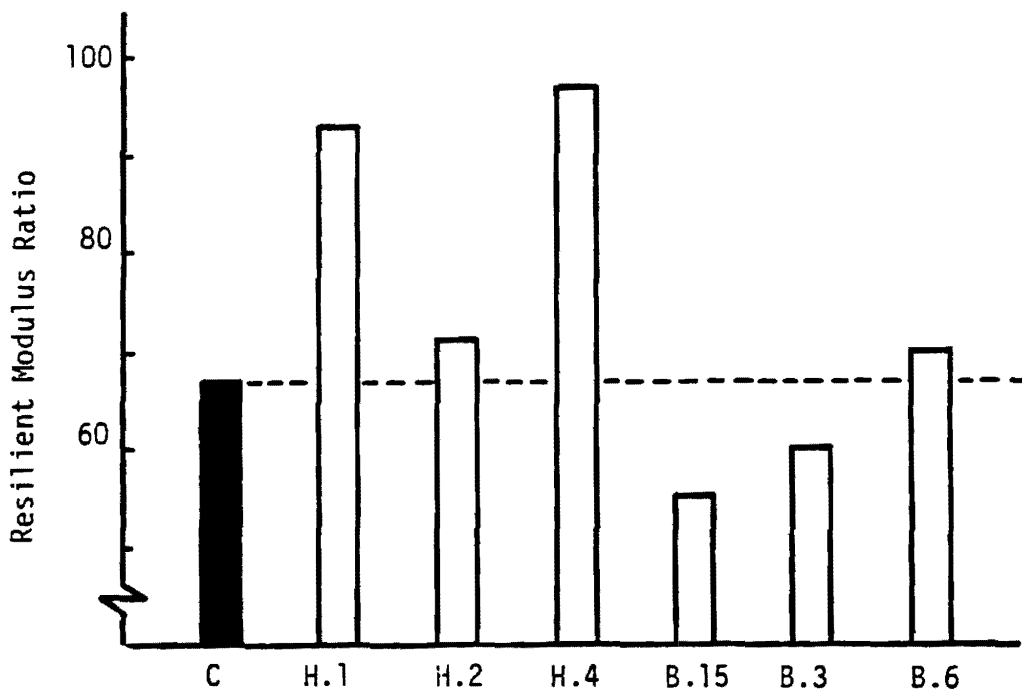


Figure 30. Resilient Modulus Ratios after Accelerated Lottman Freeze - Thaw Procedure. (Each value represents an average of three.)

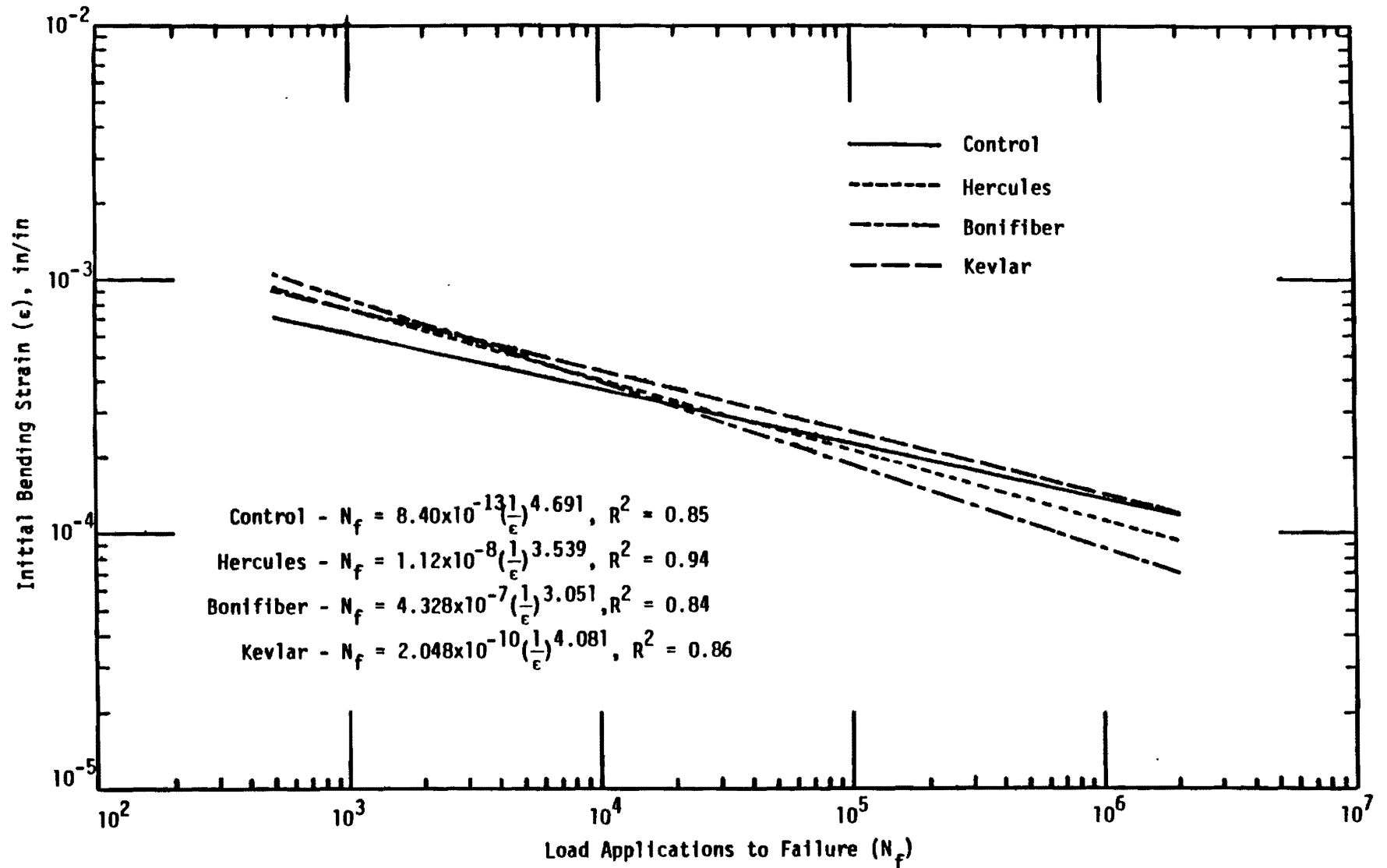


Figure 31. Strain as a Function of Load Applications to Failure.

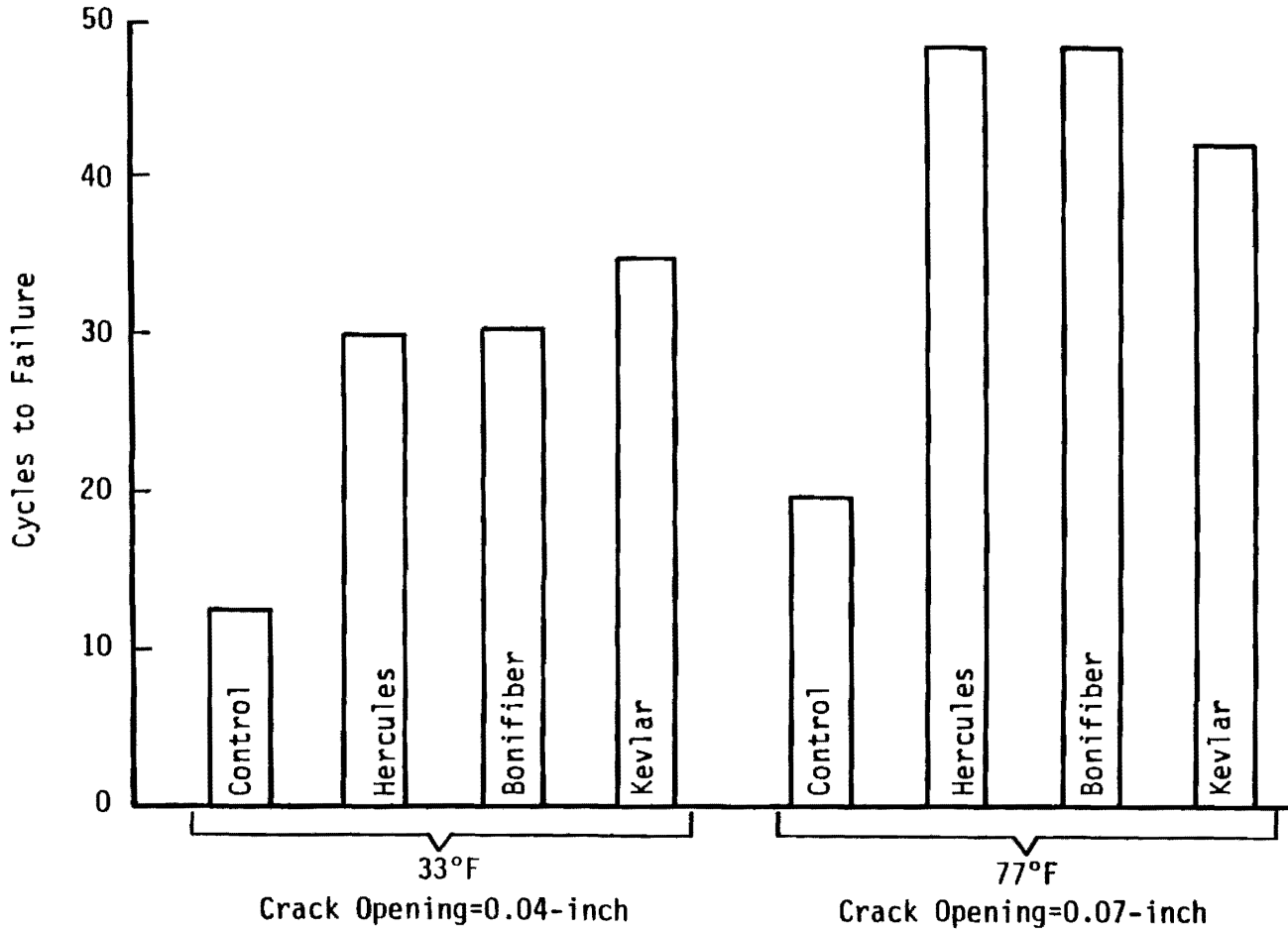


Figure 32. Number of Cycles at Failure for Overlay Specimens Tested.
(Each bar represents an average of 3 tests).

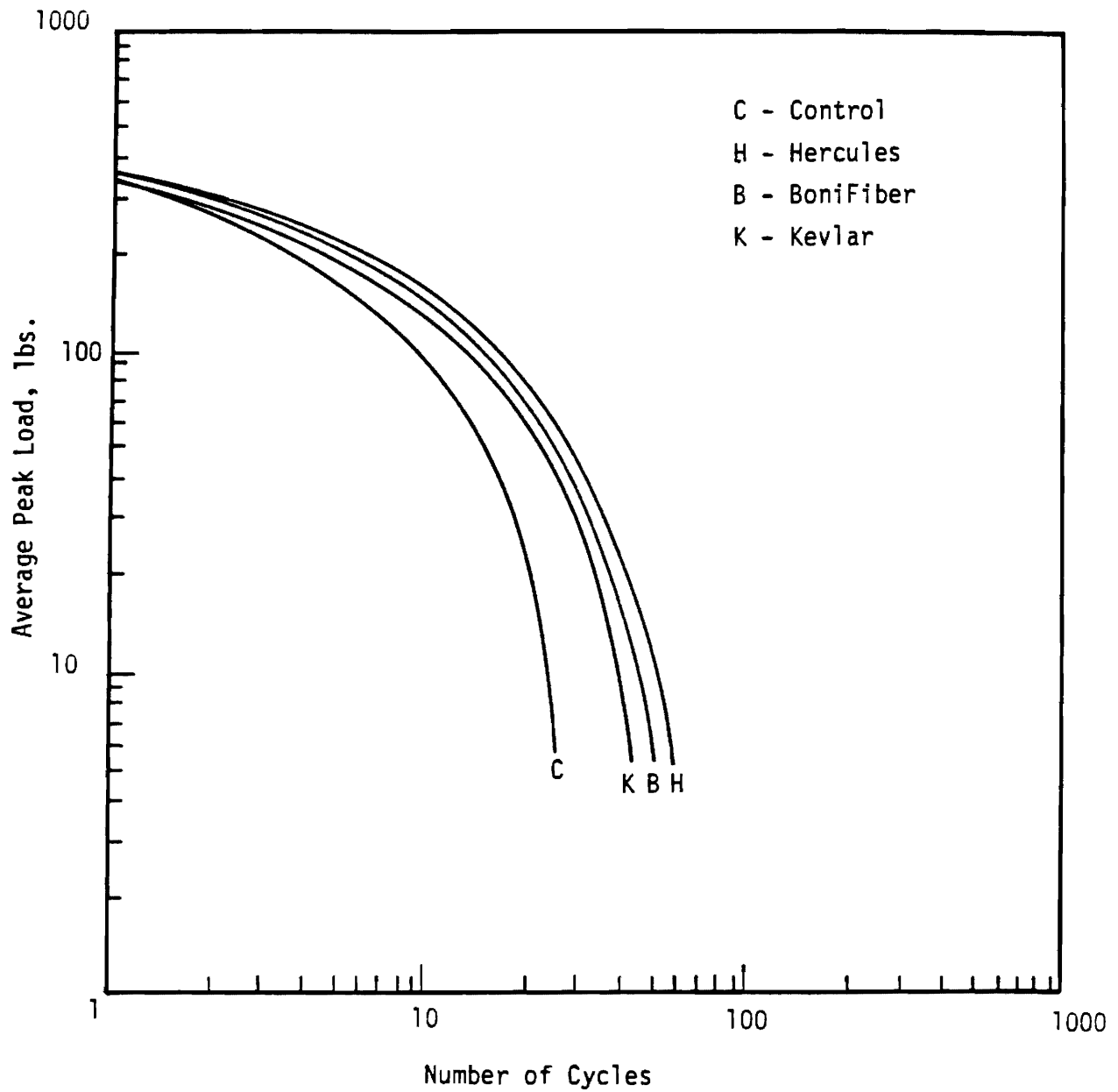


Figure 33. Average Peak Load Supported by Samples During the Overlay Test at 77°F.

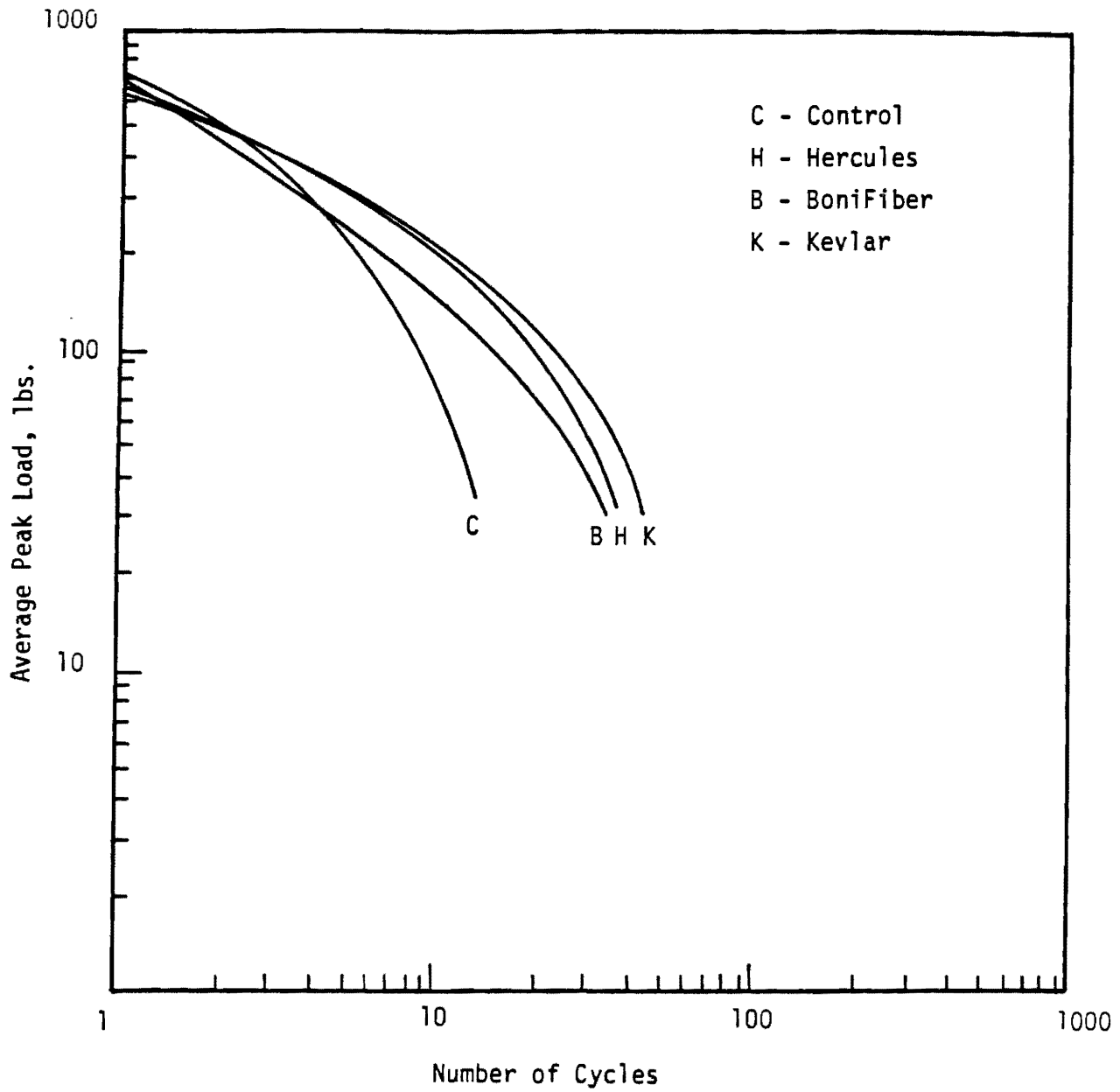


Figure 34. Average Peak Load Supported by Samples During the Overlay Test at 33°F.

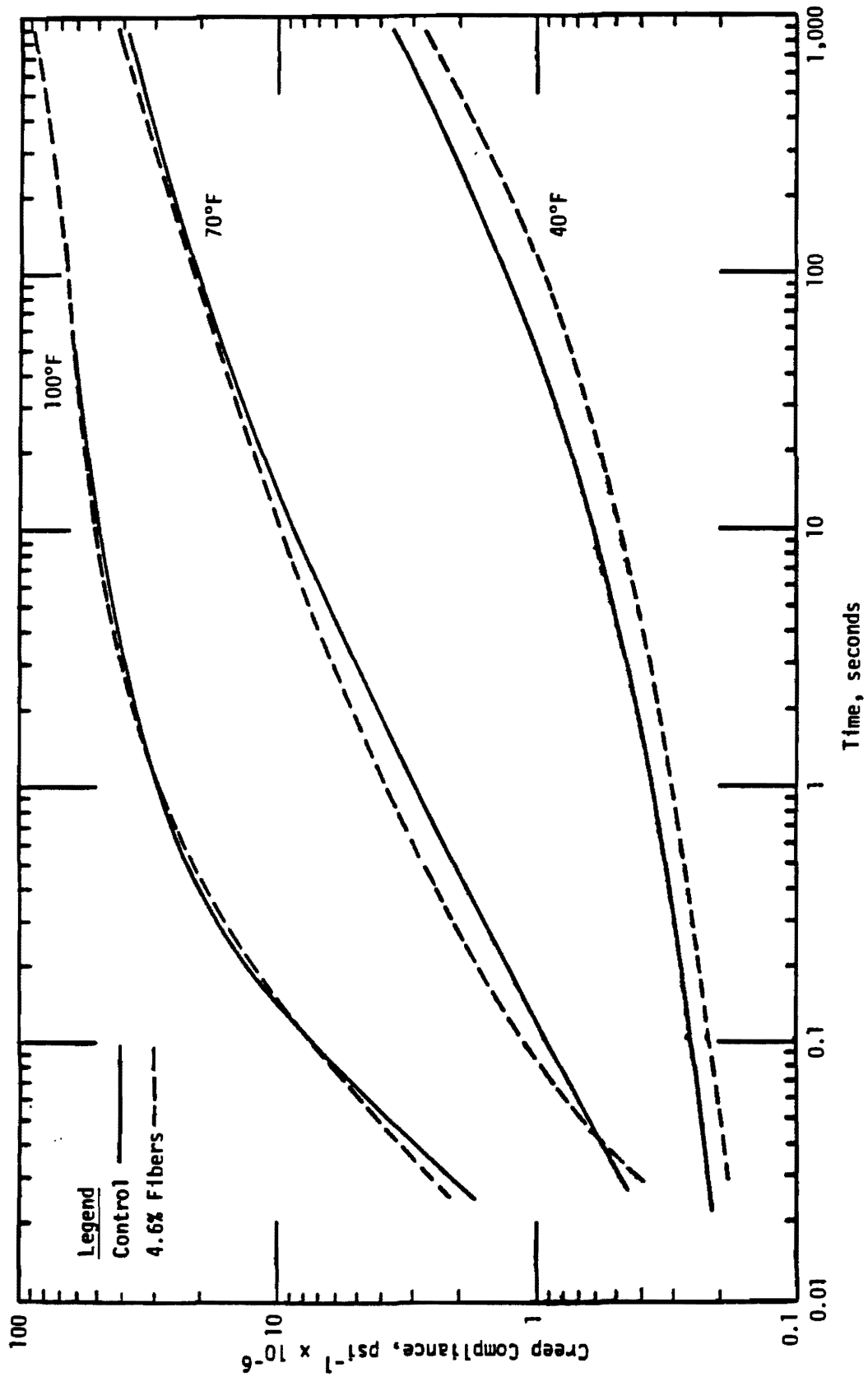


Figure 35. Creep Compliance Curves for Specimens Containing 4.6 percent Asphalt and Control Specimens.

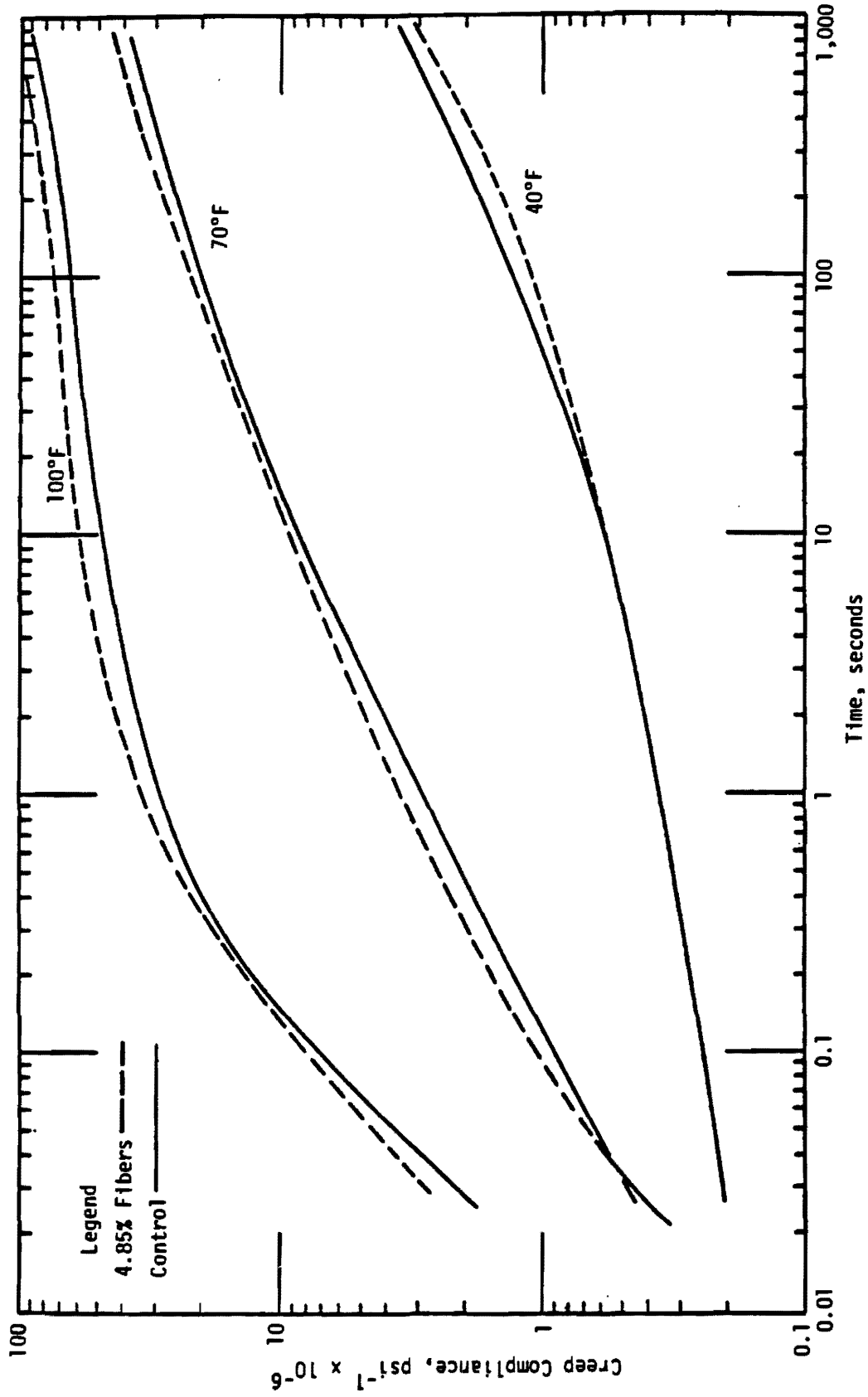


Figure 36. Creep Compliance Curves for Specimens Containing 4.85 percent Asphalt and Control Specimens.

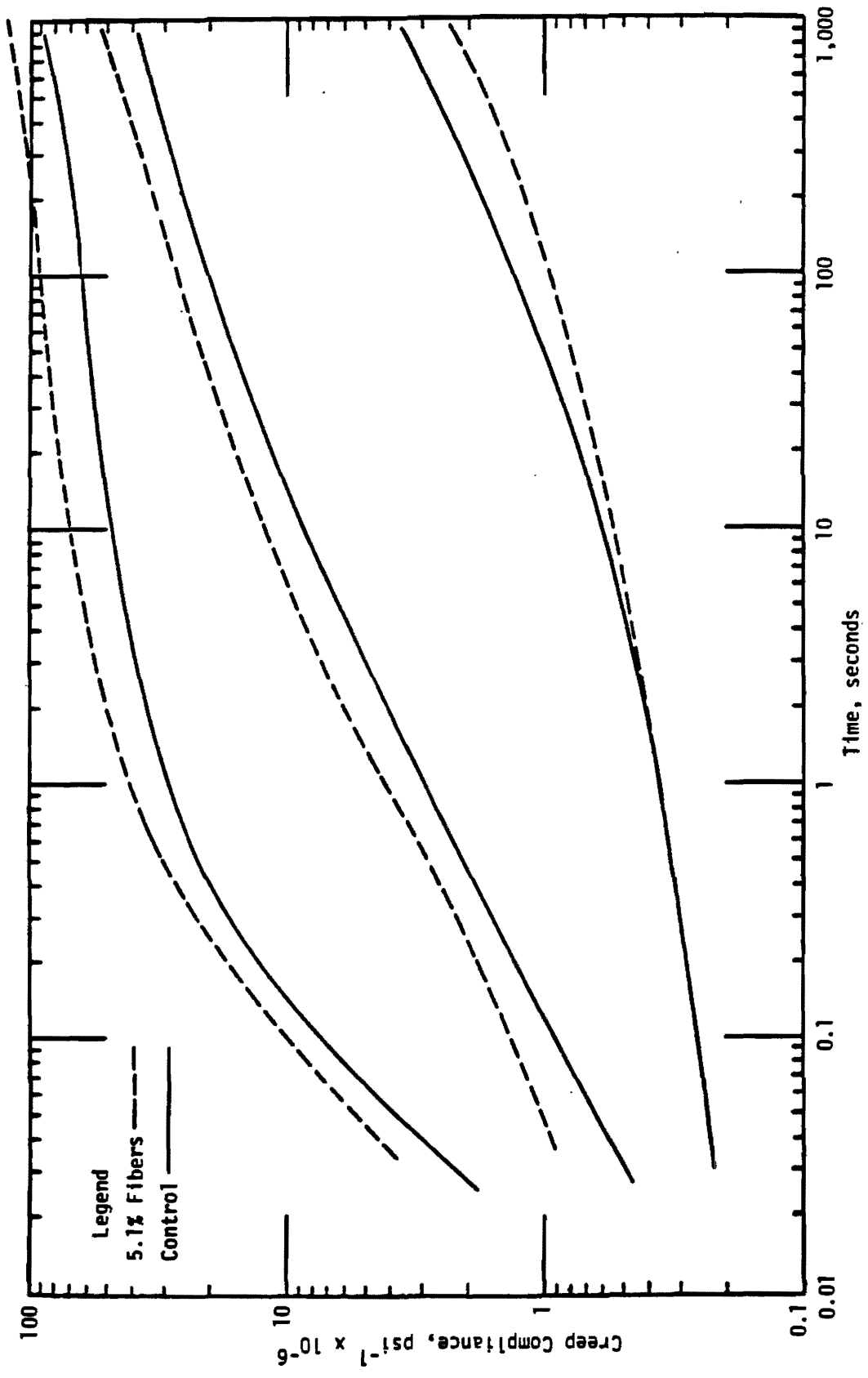


Figure 37. Creep Compliance for Specimens Containing 5.1 percent Asphalt and Control Specimens.

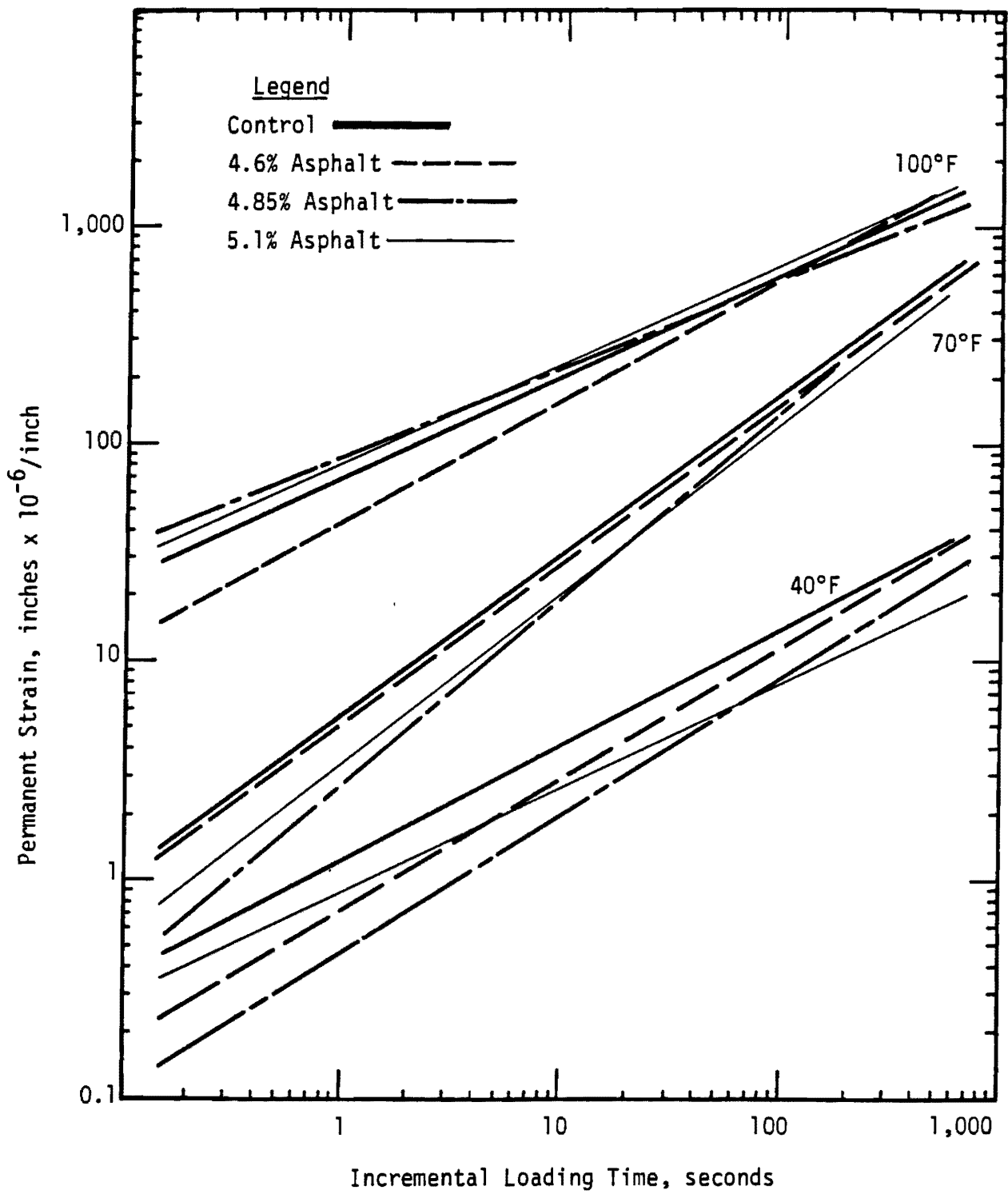


Figure 38. Permanent Strain from Incremental Static Loading Tests at 40, 70 and 100°F.

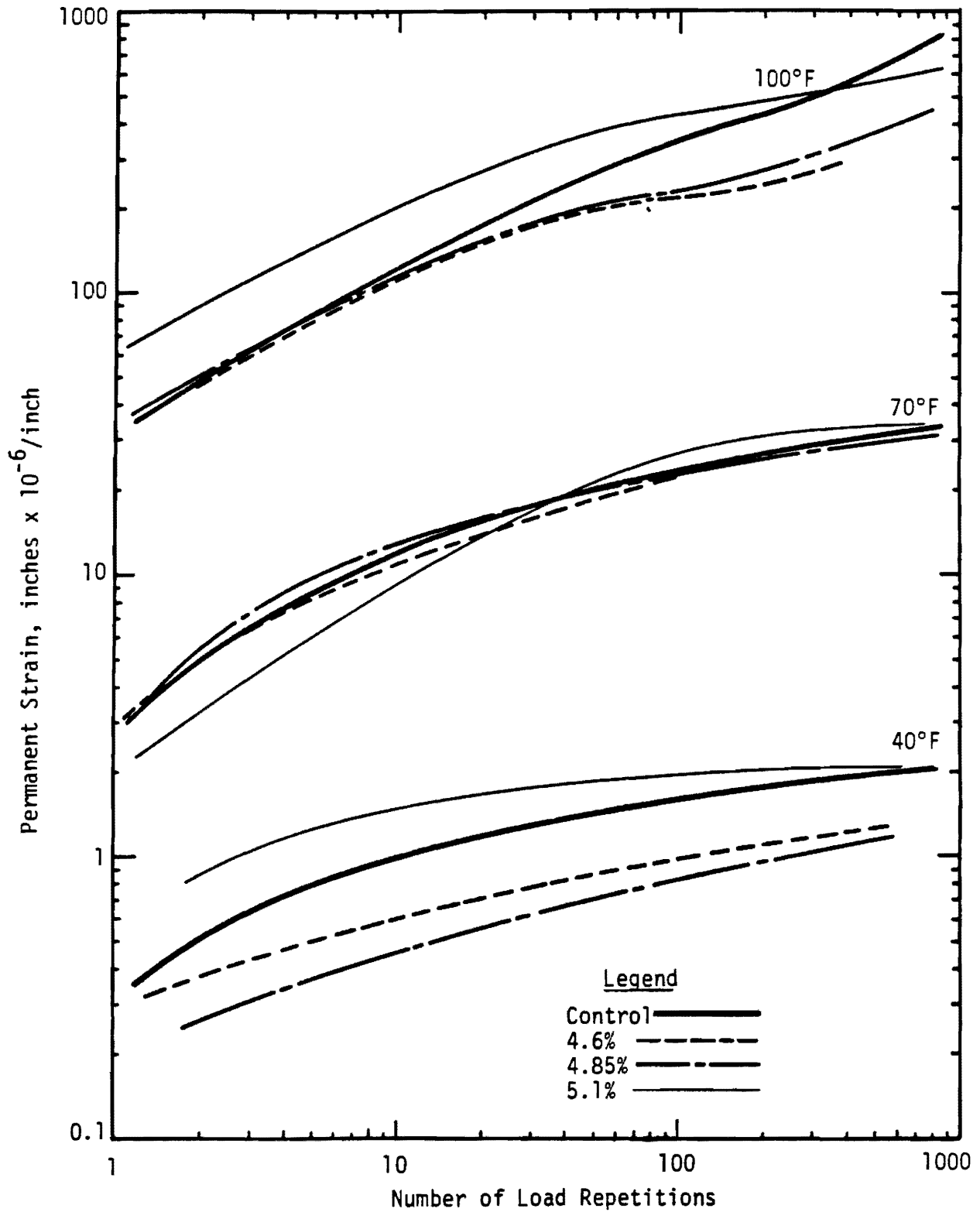


Figure 39. Results from Dynamic Direct Compression Loading Tests at 40, 70 and 100°F.

Subgrade	Climate	Type of Surface	Surface Thickness	Thick				Thin			
				Control	4.6% Asphalt	4.85% Asphalt	5.1% Asphalt	Control	4.6% Asphalt	4.85% Asphalt	5.1% Asphalt
				Hard Clay	Cool	3*	1	2	4	3	1
Mod.	3	1	2		4	3	1	2	4		
Warm	3	1	2		4	3	1	2	4		

Figure 40. Results from Factorial Predictive Performance Analysis Based on Present Serviceability Index (PSI).

*Numbers indicate ranking of mixtures by order of increasing PSI for thick and thin pavements. Lower numbers indicate better performance.

Surface Thickness Type of Surface Climate Subgrade		Thick				Thin			
		Control	4.6% Asphalt	4.85% Asphalt	5.1% Asphalt	Control	4.6% Asphalt	4.85% Asphalt	5.1% Asphalt
		Hard Clay	Cool	3*	1	2	4	3	1
Mod.	3		1	2	4	3	1	2	4
Warm	3		1	2	4	3	1	2	4

Figure 41. Results of Factorial Predictive Performance Analysis Based on Rut Depth.

* Numbers indicate ranking of mixtures by order of increasing rut depth for thick and thin pavements. Lower numbers indicate better performance.

Subgrade	Climate	Type of Surface	Surface Thickness	Thick				Thin			
				Control	4.6% Asphalt	4.85% Asphalt	5.1% Asphalt	Control	4.6% Asphalt	4.85% Asphalt	5.1% Asphalt
				Hard Clay	Cool	3*	1	2	4	3	1
Mod.	3	1	2		4	3	1	2	4		
Warm	3	1	2		4	3	1	2	4		

Figure 42. Results of Factorial Predictive Performance Analysis Based on Slope Variance.

* Numbers indicate ranking of mixtures by order of increasing slope variance for thick and thin pavements. Lower numbers indicate better performance.

Subgrade	Climate	Type of Surface	Surface Thickness	Thick				Thin			
				Control	4.6% Asphalt	4.85% Asphalt	5.1% Asphalt	Control	4.6% Asphalt	4.85% Asphalt	5.1% Asphalt
				Hard Clay	Cool	2*	1	3	4	1	2
Mod.	1	2	3		4	1	2	3	4		
Warm	1	2	3		4	1	2	3	4		

Figure 43. Results from Factorial Predictive Performance Analysis Based on Cracking.

* Numbers indicate ranking of mixtures by order of increasing cracking for thick and thin pavements. Lower numbers indicate better performance.

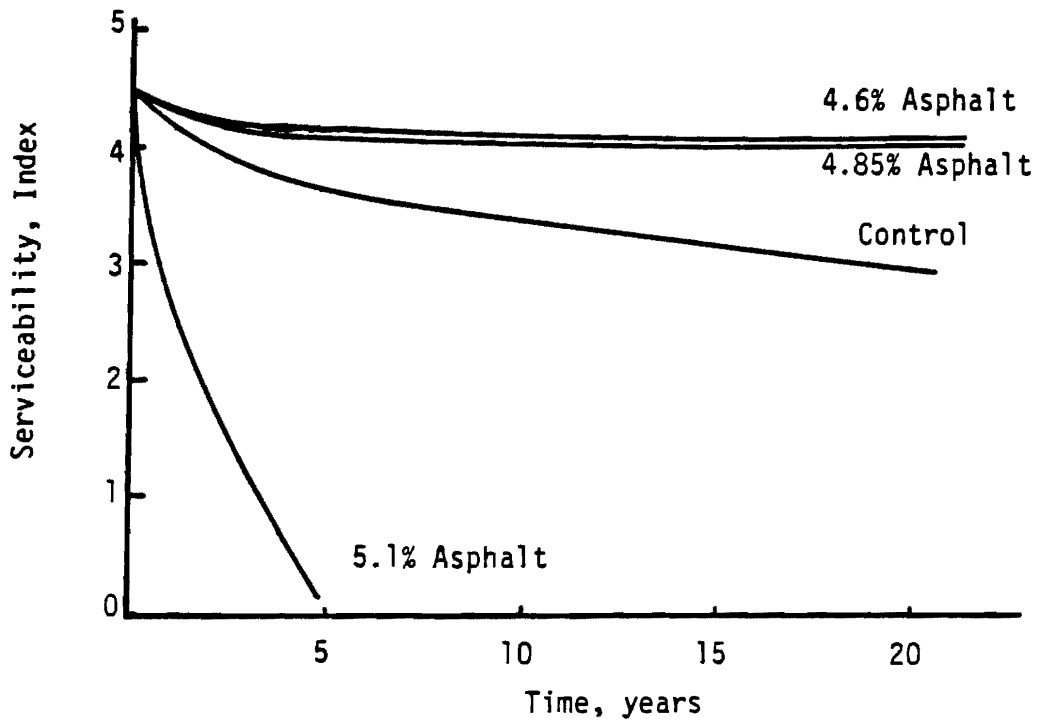


Figure 44. Serviceability Index versus Time for Thick Surface and Hard Subgrade at Moderate Temperature

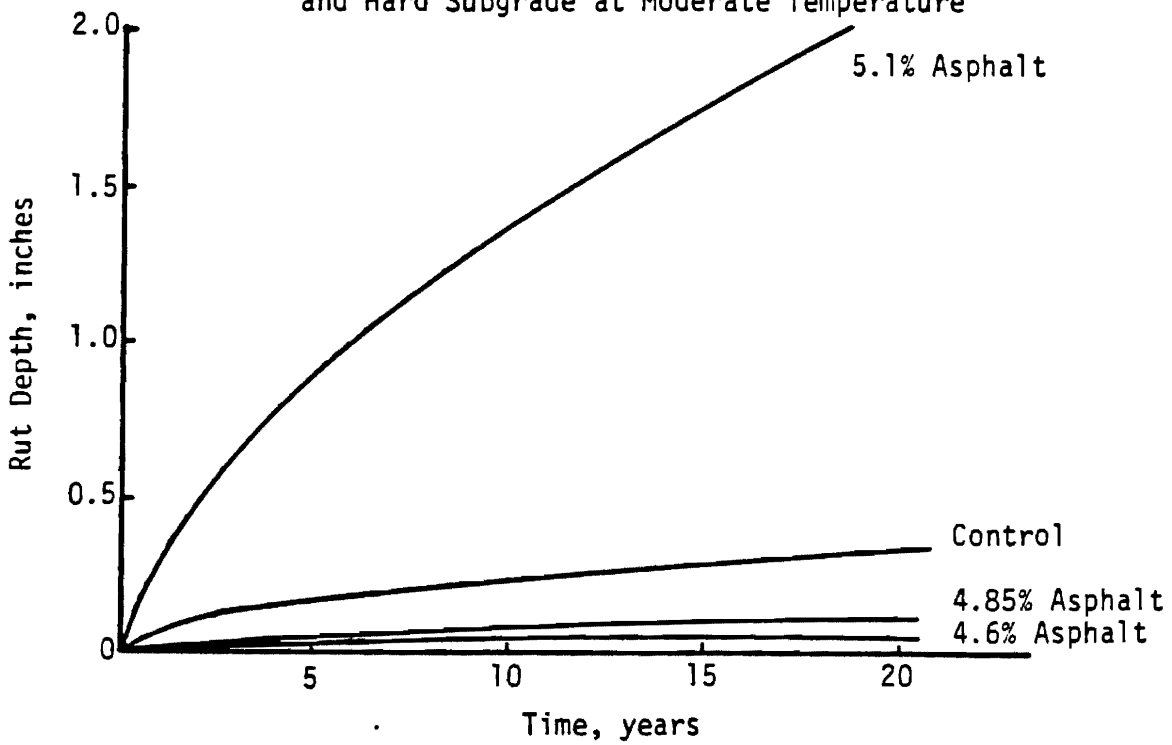


Figure 45. Rut Depth versus Time for Thick Surface and Hard Subgrade at Moderate Temperature.

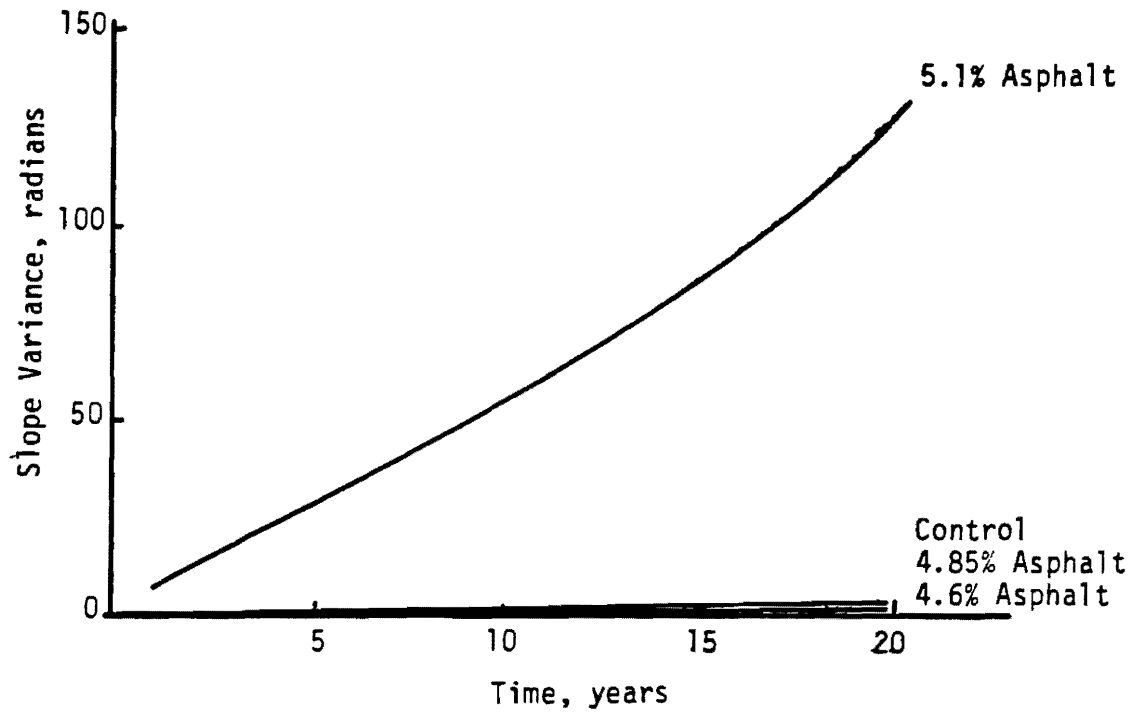


Figure 46. Slope Variance versus Time for Thick Surface and Hard Subgrade at Moderate Temperature.

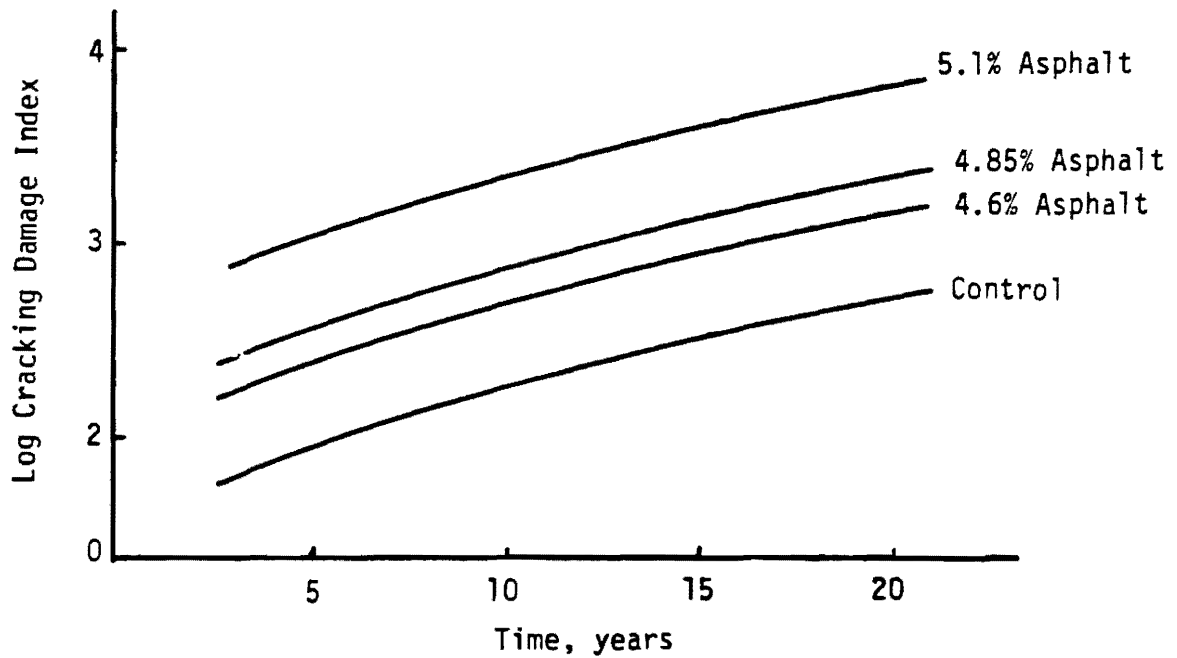


Figure 47. Cracking Damage Index versus Time for Thick Surface and Hard Subgrade at Moderate Temperature.

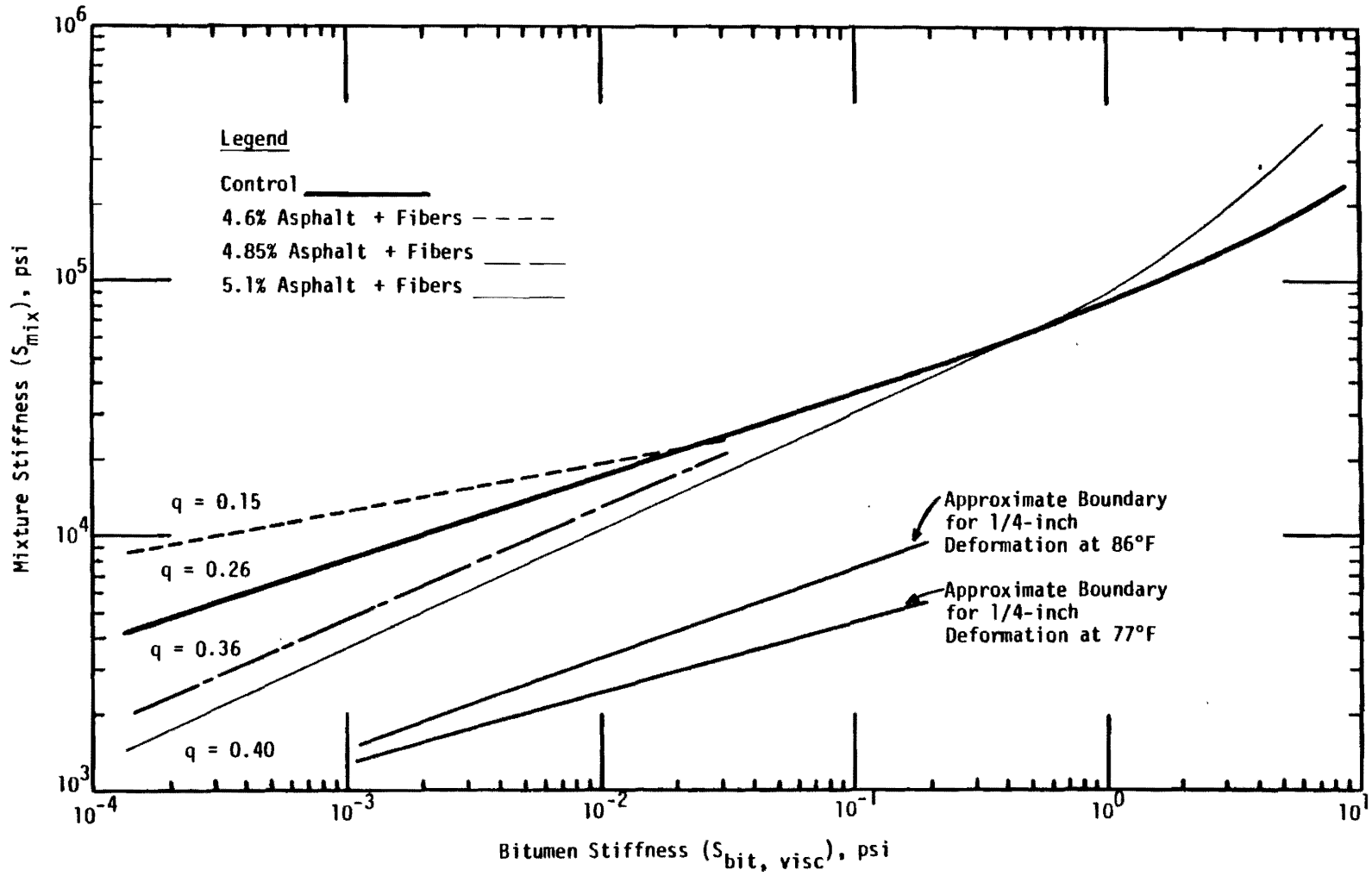


Figure 48. Relationship Between S_{bit} and S_{mix} .

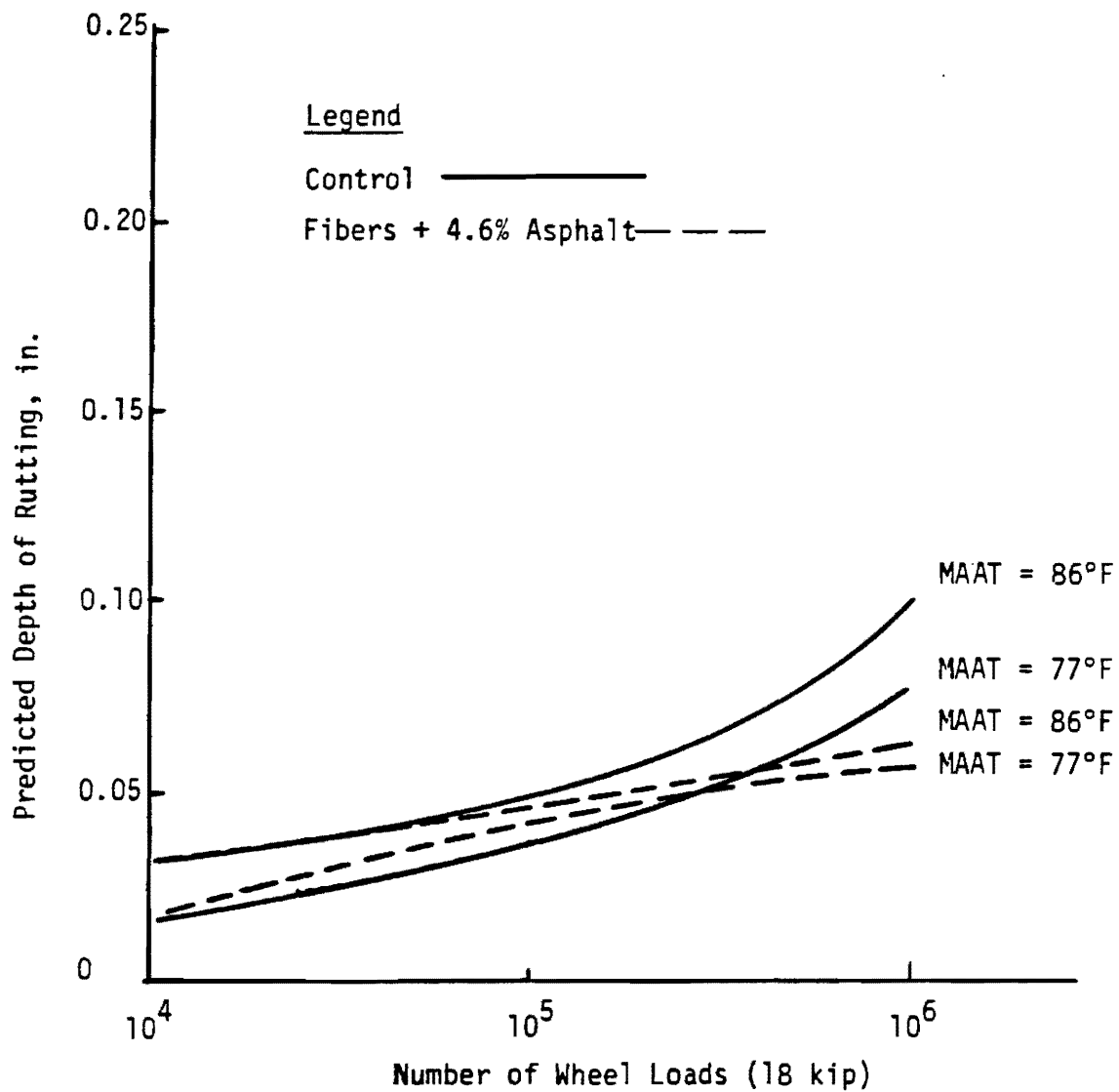


Figure 49. Predicted Depth of Rutting by Shell Method - Control Mix Versus Hercules Fiber Mix with 4.6 Percent Binder. (MAAT = mean annual air temperature)

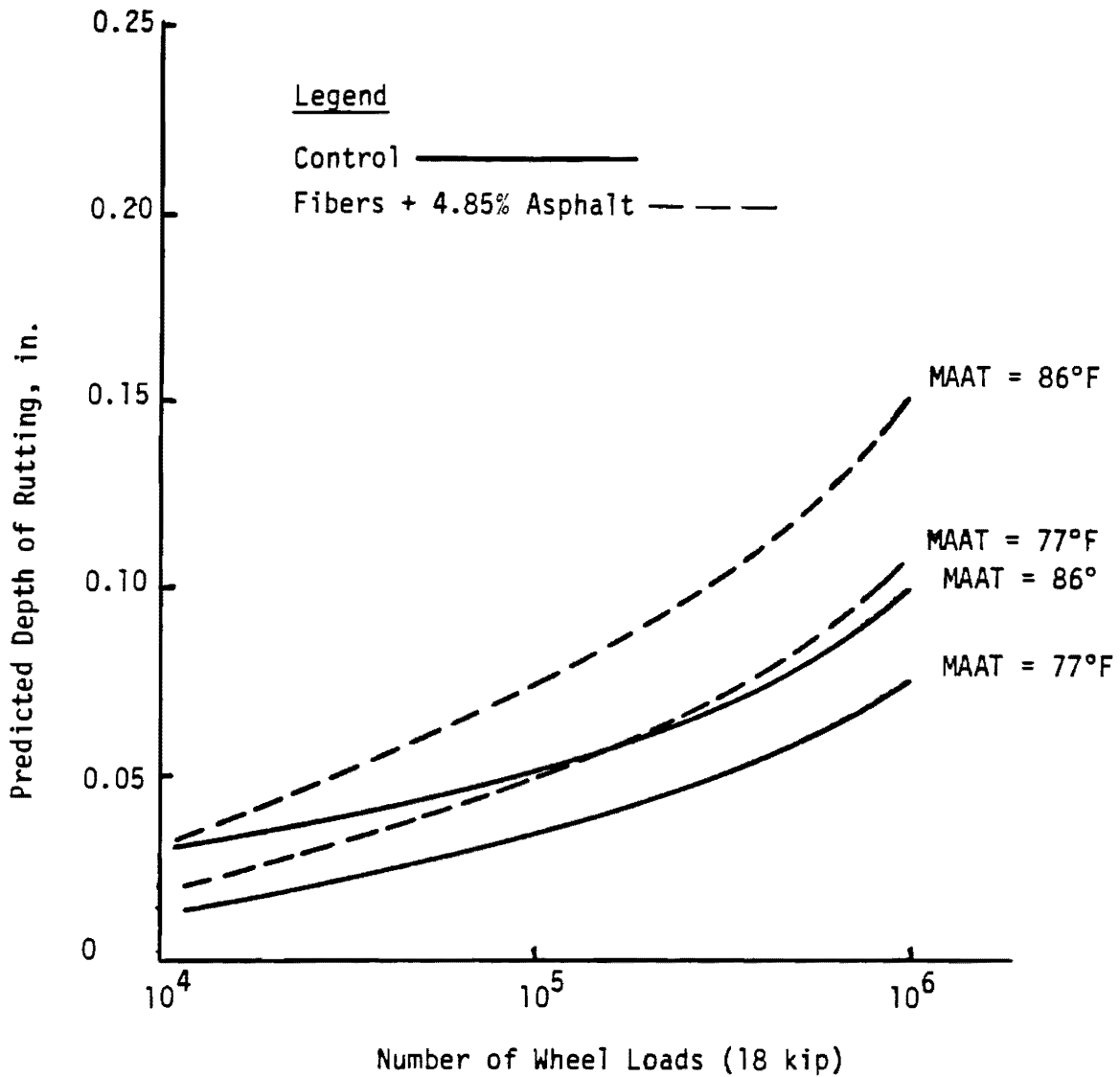


Figure 50. Predicted Depth of Rutting by Shell Method - Control Mix Versus Hercules Fiber Mix with 4.85 Percent Binder. (MAAT = mean annual air temperature)

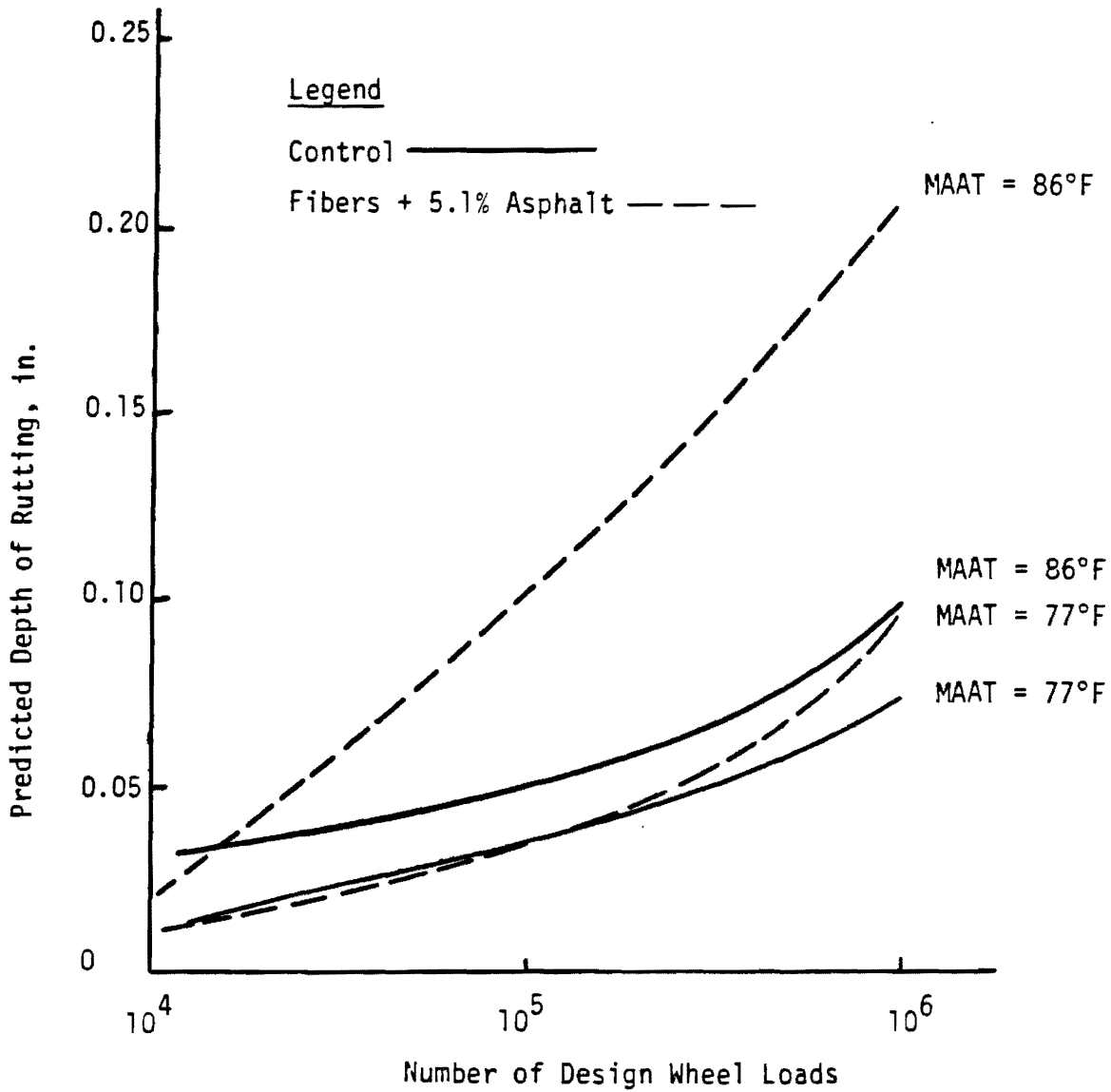


Figure 51. Predicted Depth of Rutting by Shell Method - Control Mix Versus Hercules Fiber Mix with 5.1 Percent Binder. (MAAT = mean annual air temperature)

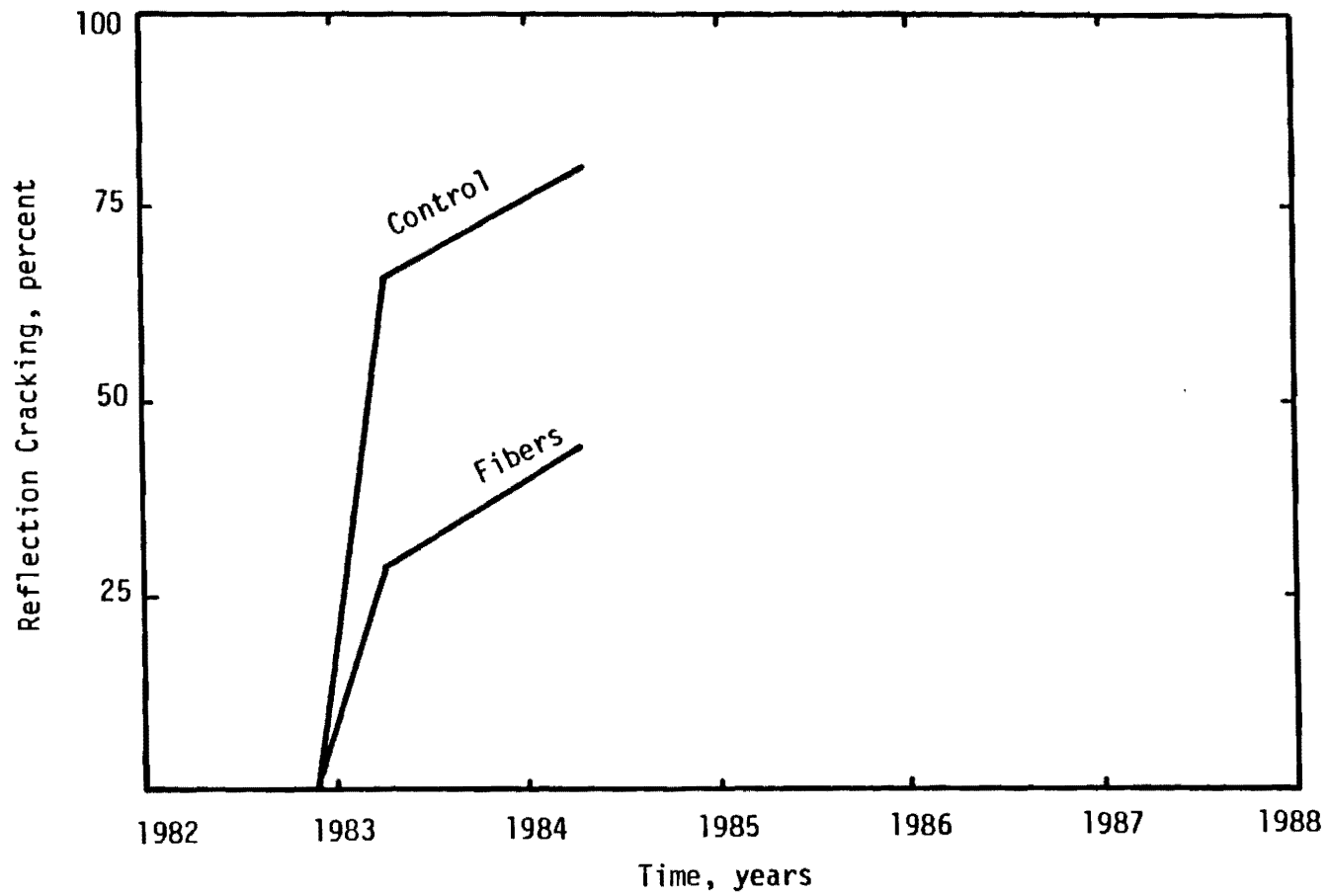


Figure 52. Reflection Cracking on US 83 in District 8.

REFERENCES

1. Moses, Exodus 5:7, The Holy Bible.
2. Busching, H. W., Elliott, E. H., and Reyneveld, N. G., "A State-of-the-Art Survey of Reinforced Asphalt Paving", Proceedings of the Association of Asphalt Paving Technologists, Volume 39, 1970, pp. 766-798.
3. Puzinauskas, V. P., "Filler in Asphalt Mixtures", Research Report 69-2, The Asphalt Institute, February, 1969.
4. "Asbestos Admixture in Asphalt Concrete", New York State Department of Public Works, Bureau of Physical Research, Physical Research Project, Engineering Research Series, Research Report RR60-5, December, 1960.
5. Hansen, R., et.al., "Effects of Asbestos Fibers in Asphaltic Concrete Paving Mixtures", Waterways Experiment Station, Miscellaneous Papers 4-344, Vicksburg, Mississippi, April, 1959.
6. Kallas, B. F. and Krueger, H. C., "Effects of Consistency of Asphalt Cements and Types of Mineral Filler on the Compaction of Asphalt Concrete", Proceedings, Association of Asphalt Paving Technologists, Vol. 29, 1960, pp. 152-171.
7. Kietzman, J. H., "Effect of Short Asbestos Fibers on Basic Physical Properties of Asphalt Pavement Mixes", Highway Research Board Bulletin 270, Washington, D.C., 1962, pp. 64-82.
8. Speer, T. L. and Kietzman, J. H., "Control of Asphalt Pavement Rutting With Asbestos Fiber", Highway Research Board Bulletin 329, Washington, D.C., 1962, pp. 64-82.
9. Tamburro, D. A., Blekicki, H. T. and Kietzman, J. H., "The Effects of Short Chrysolite Asbestos Fiber on the Structural Properties of Asphalt Pavements", Proceedings, Association of Asphalt Paving Technologists, Vol. 21, 1962, pp. 151-175.
10. Busching, H. W. and Antrim, J. W., "Fiber Reinforcement of Bituminous Mixtures", Proceedings, Association of Asphalt Paving Technologists, Vol. 37, 1968, pp. 629-659.
11. Brown, B. C. and Zearley, L. J., "Investigation of Synthetic Fiber as a Replacement for Asbestos in Asphalt Curb Mixes", (summary of laboratory test results), Iowa Department of Transportation, Ames, Iowa, December, 1977.

12. Scrimsher, T., "Report on BoniFiber B Polyester Fibers in Asphalt Concrete Pavements", (summary of laboratory test results), California Department of Transportation, Sacramento, California, April, 1980.
13. Epps, J. A., Holmgreen, R. J. and Button, J. W., "Mechanical Properties of Fiber-Reinforced Asphalt Concrete", Texas A&M Research Foundation, Report RF 3835-1, College Station, Texas, September, 1980.
14. Button, J. W. and Epps, J. A., "Mechanical Characterization of Fiber-Reinforced Bituminous Concrete", Texas A&M Research Foundation, Report 4061-1, College Station, Texas, February, 1981.
15. Busching, H. W., Achara, O. E. and Gaj, S. E., "Use of Short Polypropylene Fibers in Hot-Mix Asphalt Concrete - A Characterization Study", Department of Civil Engineering, Clemson University, Clemson, South Carolina, November, 1980.
16. "Fibrous Reinforced Slurry Seal Tensile Properties", Submitted to Slurry Seal of Arizona, Phoenix, Arizona, by Engineers Testing Laboratories, Inc., Phoenix, Arizona, February, 1981.
17. Busching, H. W. and Porcher, J. P., "Results of Flexure of Fiber-Reinforced Asphaltic Concrete Beams-Test Results from Brambles Specimens", Department of Civil Engineering, Clemson University, Clemson, South Carolina, March, 1982.
18. "Results of Marshall and Indirect Tensile Tests on BoniFiber Specimens", New Jersey Department of Transportation, Trenton, New Jersey, June, 1982.
19. "Fiber Asphalt Concrete and Extrudamat/SAMI Fatigue Testing", Resource International, Inc., Report RII 82-1170, Worthington, Ohio, July, 1982.
20. Button, J. W., Little, D. N., and Epps, J.A., "Predicted Performance of Asphalt Paving Mixtures Containing Hercules Fibers", sponsored by Hercules, Inc., College Station, Texas/Reno, Nevada, August, 1984.
21. Finemore, G. L., "Synthetic Fiber Applications", Tri-Regional Quality Assurance Workshop, Federal Highway Administration, Harrisburg, Pennsylvania, 1979.
22. Brunner, R. J., "Polyester Fibers for Asphaltic Pavement Reinforcements", Pennsylvania Department of Transportation, Research Project No. 77-18, Harrisburg, Pennsylvania, April, 1978.

23. Mellott, D. B., "Fiber Modified Cold Patch", Pennsylvania Department of Transportation, Research Project No. 78-12, Harrisburg, Pennsylvania, May, 1980.
24. Norton, R., "Asphalt Cement With Polyester Fibers as a Bridge Deck Waterproof Membrane", Maine Department of Transportation, Experimental Project 79002, Bangor, Maine, April, 1982.
25. Jacobs, K., "Construction Report for Polyester Fibers", Maine Department of Transportation, Experimental Project 81002, Bangor, Maine, November, 1981.
26. Mellot, D.B., "Use of DuPont Fibers in FJ-4", Pennsylvania Department of Transportation, Research Project No. 77-18, Harrisburg, Pennsylvania, June, 1978.
27. Martinez, B. P., Mills, D. R. and Steining, B., "Synthetic Fibers Reduce Reflection Cracking", Public Works, April, 1979, pp. 55-57.
28. Knight, N. E. and Casner, D., "Sealing Cracks in Bituminous Overlays of Rigid Bases", Pennsylvania Department of Transportation, Research Project 80-24, Harrisburg, Pennsylvania, August, 1982.
29. Smith, R. D. and Forsyth, R. A., "Experimental AC Overlays of PCC Pavement", California Department of Transportation, Contract No. 03-217334, Sacramento, California, April, 1983.
30. Mills, D. R. and Keller, T., "The Effectiveness of Synthetic Fiber-Reinforced Asphaltic Concrete Overlays in Delaware", Delaware Department of Transportation, Dover, Delaware, November, 1982.
31. Brewer, W. B., "Fiber Slurry Seal", Oklahoma Department of Transportation, Project No. 2668, Oklahoma City, Oklahoma, March, 1983.
32. Branciforte, S., "Synthetic Fiber in Asphalt Paving Materials - Reflective Cracking Study", Connecticut Department of Transportation, Wethersfield, Connecticut, March, 1982.
33. Frascoia, R. I., "Experimental Use of Polyester Fiber Modified Bituminous Pavement on Vermont Route 12A", Vermont Agency of Transportation, Report 82-7, Montpelier, Vermont, June, 1983.
34. Whiteley, D. C., "The Experimental Use of Fibrous Reinforced Bituminous Concrete", New York State Department of Transportation, Technical Report 83-2, Albany, N.Y., February, 1983.

35. "Fiberized Slurry Seal: An Old Contender Gets Tough", Roads, November, 1983, pp. 24-26.
36. Martinez, B. P. and Bamberger, J. W., "Polyester Fibers Replace Asbestos in Asphalt Curb Mix", Public Works, January, 1979, pp. 73-74.
37. Martinez, B. P. and Wilson, J. E., "Polyester Fibers Replace Asbestos in Bridge Deck Membranes", Public Works, August, 1979, pp. 100-137.
38. Robson, J. and Cohen, M., "City Investigates Different Roadway Repair Methods", Public Works, April, 1984, pp. 70-71.
39. "Roadway Designed to Resist Cracking", Public Works, April, 1984, pp. 106.
40. Schmidt, R. J., "A Practical Method for Measuring the Resilient Modulus of Asphalt-Treated Mixes", Highway Research Record No. 404, Highway Research Board, 1972.
41. Button, J. W., Epps, J. A., Little, D. N. and Gallaway, B. M., "Influence of Asphalt Temperature Susceptibility on Pavement Construction and Performance", National Cooperative Highway Research Program, Report 268, December, 1983.
42. Button, J. W., Epps, J. A. and Gallaway, B. M., "Laboratory Evaluation of Selected Shale Oil Asphalts in Paving Mixtures", Report No. LERC-3635-1, U. S. Department of Energy, January, 1978.
43. Robertson, R. E., Ensley, E. K. and Peterson, J. C., "Physiochemical Studies of Tender-Mix and Nontender-Mix Asphalts", Federal Highway Administration Report No. FHWA/RD-80/130, December, 1980.
44. Schmidt, R. J. and Graf, P. E., "The Effect of Water on the Resilient Modulus of Asphalt-Treated Mixes", Proceedings, Association of Asphalt Paving Technologists, Vol. 41, 1971, pp. 118-162.
45. Button, J. W., Valdez, R. R., Epps, J. A. and Little, D. N. "Development Work on a Test Procedure to Identify Water Susceptible Asphalt Mixtures", Research Report 287-1, Texas Transportation Institute, Texas A&M University, June, 1982.
46. Lottman, R. P., "Predicting Moisture-Induced Damage of Asphalt Concrete", National Cooperative Highway Research Program, Report No. 192, Transportation Research Board, 1978.
47. Lottman, R. P., "Predicting Moisture-Induced Damage to Asphaltic concrete", Progress Report on Field Evaluation Phase of NCHRP Project 4-8(3)/1, November, 1980.

48. Kenis, W. J., "Predictive Design Procedures, VESYS Users Manual - An Interim Design Procedure for Flexible Pavements Using the VESYS Structural Subsystem", U.S. Department of Transportation, Federal Highway Administration, Report No. FHWA-RD-77-154, 1978.
49. Deacon, J. A., "Fatigue of Asphalt Concrete", Graduate Report, The Institute of Transportation and Traffic Engineering, University of California, Berkeley, 1965.
50. Germann, F. P. and Lytton, R. L., "Methodology for Predicting the Reflection Cracking Life of Asphalt Concrete Overlays", Research Report 207-5, Texas Transportation Institute, Texas A&M University, March, 1979.
51. Rauhut, J. B., O'Quin, J. C. and Hudson, W. R., "Sensitivity Analysis of FHWA Structural Model VESYS II", FHWA Report RD-76-23, Federal Highway Administration, Washington, D.C., March, 1978.
52. Pickett, D. E., Saylak, D., Lytton, R. L., Conger, W. E., Newcomb, D., and Schapery, R. A., "Extension and Replacement of Asphalt Cement with Sulfur", FHWA Report RD-78-95, Federal Highway Administration, Washington, D.C., March, 1978.
53. Sharma, M. G. and Kim, K. S., "Non-Linear Visoelastic Properties of Bituminous Concrete", Journal of Testing and Evaluation, Volume 3, No. 3, May, 1975.
54. Claessen, A.I.M., Edwards, J. M., Sommer, P. and Uge', P., "Asphalt Pavement Design - The Shell Method", Proceedings, Fourth International Conference Structural Design of Asphalt Pavements, Volume 1, University of Michigan, August, 1977, pp. 39-74.

APPENDIX A
Data From Tests Performed to
Determine Optimum Asphalt Content

Table A1 . Optimum Mixture Properties of Gytratory Compacted Specimens.

Property	Control	H.10	H.20	H.40	B.15	B.30	B.60	HTZ	F	F.05	P60	P15	K	K0	AS	FG
Design Asphalt Content percent by wt. of total mix	4.6	4.75	5.0	5.2	4.8	5.2	5.35	5.2	5.1	4.6	4.7	4.9	5.3	4.9	5.0	4.8
Bulk Specific Gravity of Compacted Mixture	2.38	2.35	2.35	2.33	2.36	2.34	2.30	2.33	2.34	2.37	2.35	2.35	2.30	2.35	2.36	2.32
Maximum Specific Gravity of Mixture	2.47	2.47	2.45	2.44	2.47	2.45	2.45	2.45	2.44	2.48	2.47	2.45	2.45	2.45	2.46	2.45
Effective Specific Gravity of Aggregate*	2.65	2.65	2.63	2.63	2.65	2.65	2.65	2.65	2.63	2.65	2.65	2.64	2.65	2.64	2.65	2.63
Asphalt Absorption, percent by wt. by aggregate	0.21	0.36	0.36	0.52	0.40	0.62	0.85	0.66	0.36	0.34	0.42	0.33	0.62	0.32	0.39	0.09
Effective Asphalt Content, percent by wt. of total mix	4.4	4.4	4.7	4.7	4.4	4.6	4.5	4.6	4.8	4.3	4.3	4.6	4.7	4.6	4.6	4.7
Voids in Mineral Aggregate, percent bulk volume	13.8	14.8	14.5	14.9	14.5	14.8	16.2	15.3	15.0	14.0	14.3	14.5	16.3	14.6	14.6	15.8
Voids Filled with Asphalt, percent of total voids	73	67	72	71	69	70	62	67	71	69	68	71	64	71	72	67
Air Void Content, percent total volume	3.8	4.8	4.0	4.4	4.9	4.4	6.2	5.1	4.3	4.5	4.5	4.2	5.9	4.2	4.1	5.2
Fiber Content, percent by wt. of total mix	0.0	0.10	0.20	0.40	0.15	0.30	0.60	0.30	0.22	0.05	0.20	0.20	0.31	0.30	0.55	0.55
Specific Gravity of Fiber	-	0.91	0.91	0.91	1.38	1.38	1.38	1.38	1.00	1.00	0.91	0.91	1.44	1.37	2.50	2.50

*Fibers are considered part of the aggregate.

Table A2. Data Summary of Optimum Mixture Design of Control Specimens.

Asphalt Content, percent by total weight of mixture	3.4	3.9	4.3	4.8	5.2
Bulk Specific Gravity of Compacted Mixture.	2.311	2.364	2.372	2.397	2.403
Maximum Specific Gravity of Mixture.	2.516	2.499	2.481	2.464	2.447
Voids in Mineral Aggregate, percent bulk volume.	15.1	13.7	13.7	13.3	13.4
Effective Asphalt Content, percent by total weight of mixture.	3.2	3.7	4.1	4.6	5.0
Voids Filled with Asphalt, percent total voids.	47	61	68	80	86
Air Void Content, percent total volume.	8.1	5.4	4.4	2.1	1.1
Hveem Stability.	29	33	32	28	28
Marshall Stability*, lbs.	790	950	940	1080	1020
Marshall Flow*, 0.01 inch.	13	13	15	17	17

*These values were obtained from the averages of two tests. All other values are averages of three tests.

Table A3. Data Summary of Optimum Mixture Design of Hercules Fibers, 0.1 percent fibers by total weight of mixture.

Asphalt Content, percent by total weight of mixture.	3.8	4.3	4.8	5.2	5.7
Bulk Specific Gravity of Compacted Mixture.	2.335	2.356	2.380	2.388	2.387
Maximum Specific Gravity of Mixture.	2.500	2.483	2.466	2.448	2.431
Voids in Mineral Aggregate, percent bulk volume.	14	14	14	14	14
Effective Asphalt Content, percent by total weight of mixture.	3.5	4.0	4.5	4.9	5.4
Voids Filled with Asphalt, percent total voids.	56	65	73	80	88
Air Void Content, percent total volume.	6.6	5.2	3.5	2.4	1.8
Hveem Stability.	29	30	30	26	19
Marshall Stability*, lbs.	770	960	1050	1030	1030
Marshall Flow*, 0.01 inch.	13	15	16	16	18

*These values were obtained from the average of two tests. All other values are averages of three tests.

Table A4. Data Summary of Optimum Mixture Design of Hercules Fibers, 0.2 percent fibers by total weight of mixture.

Asphalt Content, percent by total weight of mixture	3.8	4.3	4.8	5.2	5.7
Bulk Specific Gravity of Compacted Mixture.	2.332	2.340	2.350	2.368	2.369
Maximum Specific Gravity of Mixture.	2.492	2.474	2.456	2.439	2.421
Voids in Mineral Aggregate, percent bulk volume.	14.0	14.2	14.3	14.0	14.4
Effective Asphalt Content, percent by total weight of mixture.	3.5	4.0	4.5	4.9	5.4
Voids Filled with Asphalt, percent total voids.	56	63	71	80	85
Air Void Content, percent total volume.	6.4	5.4	4.3	2.9	2.2
Hveem Stability.	30	30	27	28	21
Marshall Stability*, lbs.	920	940	930	1090	1080
Marshall Flow*, 0.01 inch.	14	16	19	16	17

*These values were obtained from the average of two tests. All other values are averages of three tests.

Table A5. Data Summary of Optimum Mixture Design of Hercules Fibers, 0.4 percent fibers by total weight of mixture.

Asphalt Content, percent by total weight of mixture.	3.8	4.3	4.7	5.2	5.6
Bulk Specific Gravity of Compacted Mixture.	2.232	2.278	2.284	2.315	2.327
Maximum Specific Gravity of Mixture.	2.485	2.468	2.452	2.435	2.419
Voids in Mineral Aggregate, percent bulk volume.	17.2	16.0	16.1	15.4	15.3
Effective Asphalt Content, percent by total weight of mixture.	3.3	3.8	4.2	4.7	5.1
Voids Filled with Asphalt, percent total voids.	41	52	57	68	75
Air Void Content, percent total volume.	10.2	7.7	6.9	4.9	3.8
Hveem Stability.	27	28	28	28	22
Marshall Stability*, lbs.	790	940	870	860	860
Marshall Flow*, 0.01 inch.	16	17	19	18	19

*These values were obtained from the averages of two tests. All other values are averages of three tests.

Table A6. Data Summary of Optimum Mixture Design of BoniFibers, 0.15 percent fibers by total weight of mixture.

Asphalt Content, percent by total weight of mixture.	3.8	4.3	4.8	5.2	5.7
Bulk Specific Gravity of Compacted Mixture.	2.322	2.351	2.376	2.379	2.392
Maximum Specific Gravity of Mixture.	2.495	2.481	2.467	2.453	2.439
Voids in Mineral Aggregate, percent bulk volume.	14.8	14.2	13.7	14.0	14.0
Effective Asphalt Content, percent by total weight of mixture.	3.4	3.9	4.4	4.8	5.3
Voids Filled with Asphalt, percent total voids.	51	62	73	78	87
Air Void Content, percent total volume.	6.9	5.2	3.7	3.0	1.9
Hveem Stability.	34	33	30	28	20
Marshall Stability*, lbs.	900	1070	1110	1130	1150
Marshall Flow*, 0.01 inch.	16	16	16	15	15

*These values were obtained from the averages of two tests. All other values are averages of three tests.

Table A7. Data Summary of Optimum Mixture Design of BoniFibers, 0.30 percent fibers by total weight of mixture.

Asphalt Content, percent by total weight of mixture.	3.8	4.3	4.8	5.2	5.6
Bulk Specific Gravity of Compacted Mixture.	2.299	2.327	2.346	2.353	2.363
Maximum Specific Gravity of Mixture.	2.500	2.484	2.467	2.451	2.434
Voids in Mineral Aggregate, percent bulk volume.	15.2	14.6	14.3	14.4	14.4
Effective Asphalt Content, percent by total weight of mixture.	3.2	3.7	4.2	4.6	5.0
Voids Filled with Asphalt, percent total voids.	46	57	66	72	79
Air Void Content, percent total volume.	8.0	6.3	4.9	4.0	2.9
Hveem Stability.	31	30	28	28	26
Marshall Stability*, lbs.	1000	1070	1120	1120	1130
Marshall Flow*, 0.01 inch.	18	18	18	20	19

*These values were obtained from the averages of two tests. All other values are averages of three tests.

Table A8. Data Summary of Optimum Mixture Design of BoniFibers, 0.60 percent fibers by total weight of mixture.

Asphalt Content, percent by total weight of mixture.	3.8	4.3	4.7	5.2	5.6
Bulk Specific Gravity of Compacted Mixture.	2.225	2.273	2.304	2.314	2.325
Maximum Specific Gravity of Mixture.	2.487	2.476	2.465	2.453	2.442
Voids in Mineral Aggregate, percent bulk volume.	17.5	16.2	15.4	15.5	15.5
Effective Asphalt Content, percent by total weight of mixture.	3.0	3.5	3.9	4.4	4.8
Voids Filled with Asphalt, percent total voids.	37	47	56	63	69
Air Void Content, percent total volume.	10.5	8.2	6.5	5.7	4.8
Hveem Stability.	31	31	31	35	26
Marshall Stability*, lbs.	800	870	920	960	920
Marshall Flow*, 0.01 inch.	18	19	18	20	17

*These values were obtained from the averages of two tests. All other values are averages of three tests.

Table A9. Data Summary of Optimum Mixture Design of Hoechst Fibers, 0.30 percent fibers by total weight of mixture.

Asphalt Content, percent by total weight of mixture.	3.8	4.3	4.8	5.2	5.6
Bulk Specific Gravity of Compacted Mixture.*	2.261	2.267	2.297	2.312	2.314
Maximum Specific Gravity of Mixture.	2.504	2.487	2.471	2.454	2.438
Voids in Mineral Aggregate, percent bulk volume.	16.6	16.8	16.1	15.9	16.2
Effective Asphalt Content, percent by total weight of mixture.	3.2	3.7	4.2	4.6	5.0
Voids Filled with Asphalt, percent total voids.	42	48	58	64	69
Air Void Content, percent total volume.	9.7	8.8	7.0	5.8	5.1
Hveem Stability.	27	24	23	22	18
Marshall Stability, lbs.	790	880	880	870	880
Marshall Flow, 0.01 inch.	16	17	17	16	19

*Values are averages of three tests.

Table A10. Data Summary of Optimum Mixture Design of Forta Fibre, 0.22 percent fibers by total weight of mixture.

Asphalt Content, percent by total weight of mixture.	3.8	4.3	4.8	5.2	5.7
Bulk Specific Gravity of Compacted Mixture.*	2.235	2.259	2.332	2.347	2.350
Maximum Specific Gravity of Mixture.	2.515	2.489	2.464	2.439	2.413
Voids in Mineral Aggregate, percent bulk volume.	17.6	17.1	14.9	14.7	15.0
Effective Asphalt Content, percent by total weight of mixture.	3.5	4.0	4.5	4.9	5.4
Voids Filled with Asphalt, percent total voids.	43	51	68	75	81
Air Void Content, percent total volume.	11.1	9.3	5.3	3.8	2.6
Hveem Stability.	24	22	23	22	19
Marshall Stability, lbs.	800	850	1020	990	970
Marshall Flow, 0.01 inch.	15	16	17	15	17

*Values are averages of three tests.

Table All. Data Summary of Optimum Mixture Design of Phillips-60, 0.20 percent fibers by total weight of mixture.

Asphalt Content, percent by total weight of mixture.	3.8	4.3	4.8	5.2	5.7
Bulk Specific Gravity of Compacted Mixture.*	2.340	2.358	2.371	2.389	2.391
Maximum Specific Gravity of Mixture.	2.505	2.485	2.465	2.445	2.426
Voids in Mineral Aggregate, percent bulk volume.	14.0	13.8	13.8	13.5	13.9
Effective Asphalt Content, percent by total weight of mixture.	3.4	3.9	4.4	4.8	5.3
Voids Filled with Asphalt, percent total voids.	55	64	73	82	88
Air Void Content, percent total volume.	6.6	5.1	3.8	2.3	1.5
Hveem Stability.	28	28	24	21	19
Marshall Stability, lbs.	1030	1000	1150	1120	1500
Marshall Flow, 0.01 inch.	13	15	16	17	17

*Values are averages of three tests.

Table A12. Data Summary of Optimum Mixture Design of Phillips-15, 0.20 percent fibers by total weight of mixture.

Asphalt Content, percent by total weight of mixture.	3.8	4.3	4.8	5.2	5.7
Bulk Specific Gravity of Compacted Mixture.*	2.285	2.355	2.347	2.372	2.361
Maximum Specific Gravity of Mixture.	2.481	2.468	2.455	2.442	2.429
Voids in Mineral Aggregate, percent bulk volume.	15.9	13.7	14.5	13.9	14.8
Effective Asphalt Content, percent by total weight of mixture.	3.5	4.0	4.5	4.9	5.4
Voids Filled with Asphalt, percent total voids.	48	66	70	80	83
Air Void Content, percent total volume.	7.9	4.6	4.4	2.9	2.8
Hveem Stability.	27	24	25	22	19
Marshall Stability, lbs.	1140	1420	1340	1160	1060
Marshall Flow, 0.01	15	16	16	17	18

*Values are averages of three tests.

Table A13. Data Summary of Optimum Mixture Design of Kevlar, 0.31 percent fibers by total weight of mixture.

Asphalt Content, percent by total weight of mixture.	3.8	4.3	4.8	5.2	5.6
Bulk Specific Gravity of Compacted Mixture.*	2.212	2.294	2.280	2.310	2.322
Maximum Specific Gravity of Mixture.	2.510	2.490	2.471	2.451	2.432
Voids in Mineral Aggregate, percent bulk volume.	18.3	15.7	16.7	15.9	15.9
Effective Asphalt Content, percent by total weight of mixture.	3.2	3.7	4.2	4.6	5.0
Voids Filled with Asphalt, percent total voids.	37	52	55	64	70
Air Void Content, percent total volume.	11.9	7.9	7.7	5.8	4.5
Hveem Stability.	25	26	24	22	19
Marshall Stability, lbs.	920	1390	1140	910	1000
Marshall Flow, 0.01 inch.	18	18	21	16	19

*Values are averages of three tests.

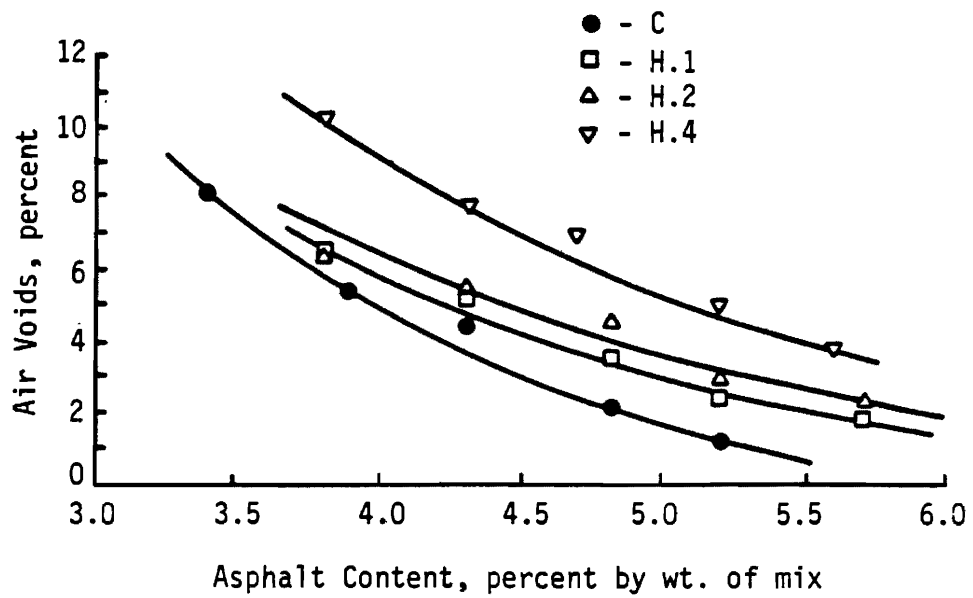


Figure A1. Air Void Content as a Function of Asphalt Content for Control and Hercules Specimens.

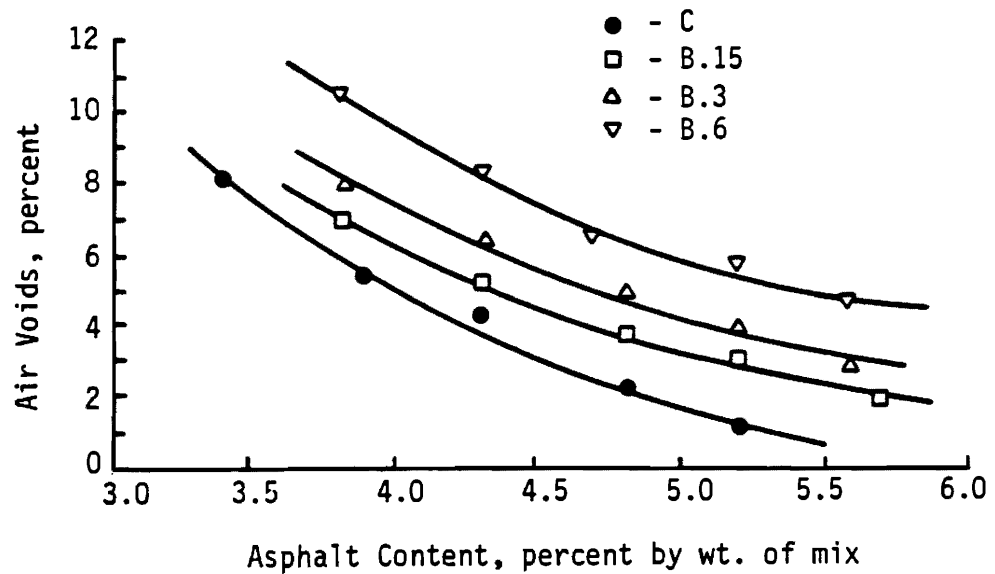


Figure A2. Air Void Content as a Function of Asphalt Content for Control and BoniFiber Specimens.

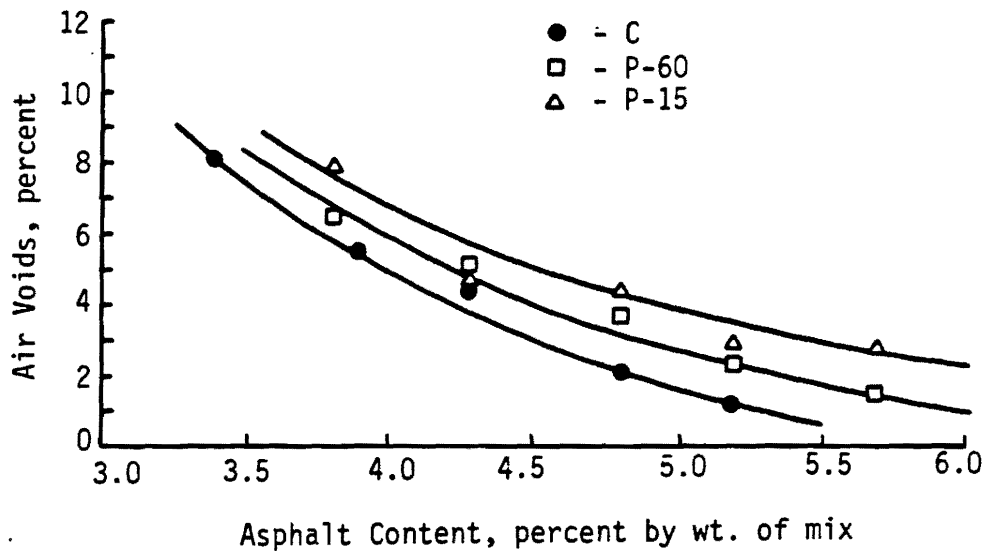


Figure A3. Air Void Content as a Function of Asphalt Content for Control and Phillips Specimens.

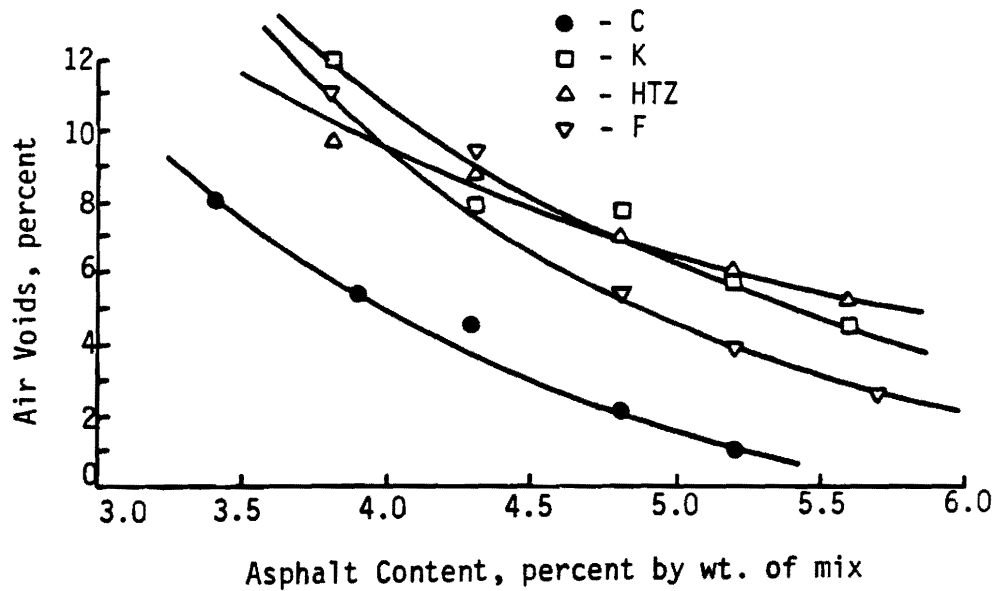


Figure A4. Air Void Content as a Function of Asphalt Content for Control, Kevlar, Hoechst, and Forta Fibre Specimens.

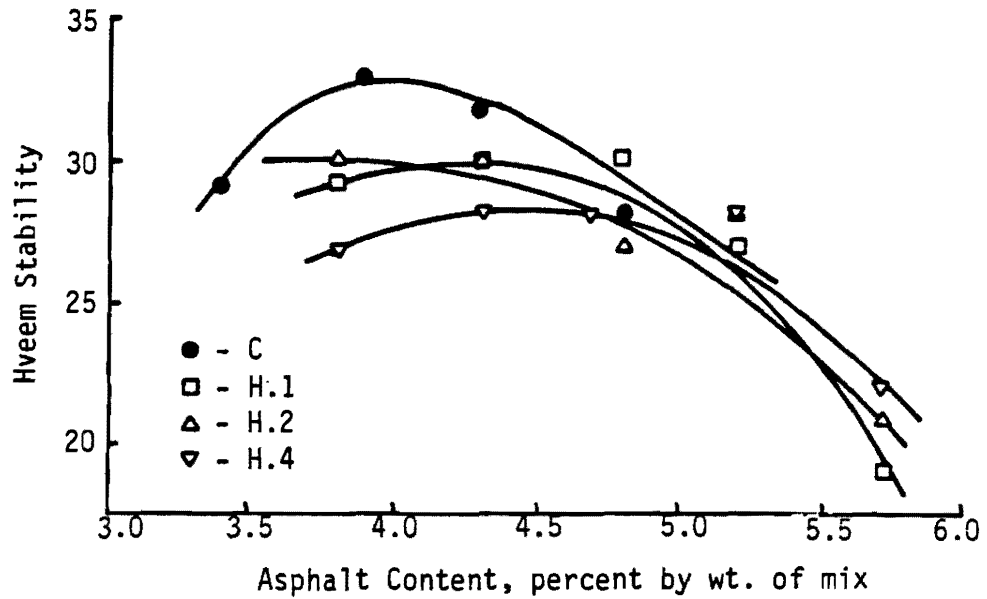


Figure A5. Hveem Stability as a Function of Asphalt Content for Control and Hercules Specimens.

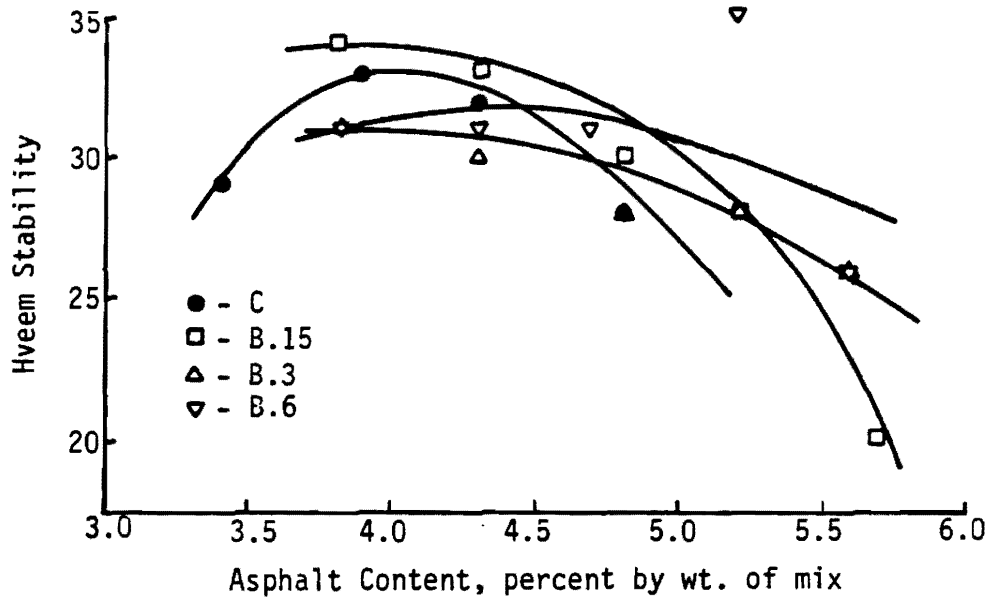


Figure A6. Hveem Stability as a Function of Asphalt Content for Control and BoniFiber Specimens.

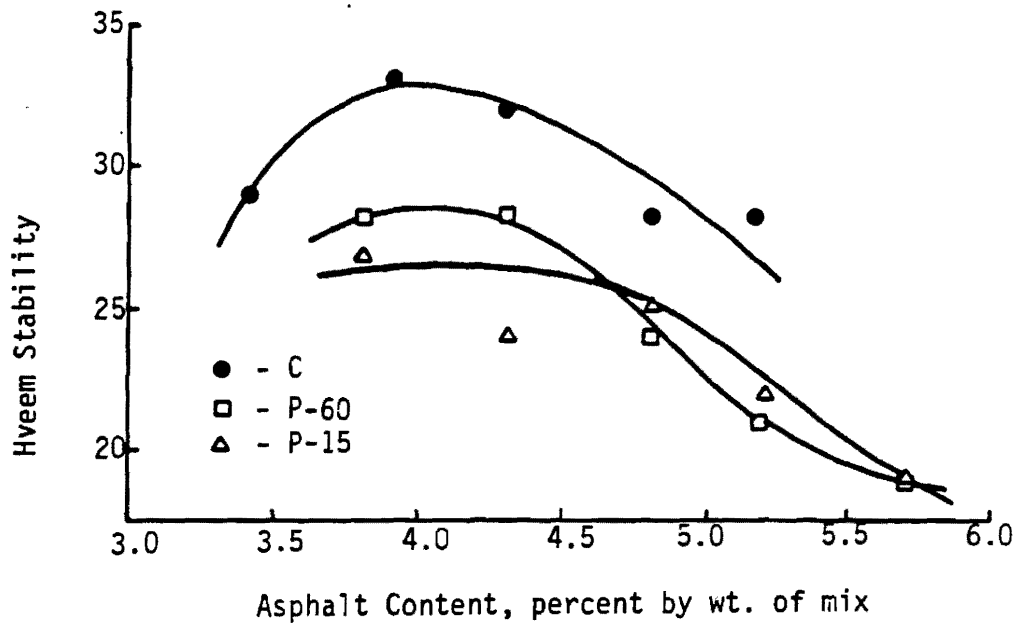


Figure A7. Hveem Stability as a Function of Asphalt Content for Control and Phillips Specimens.

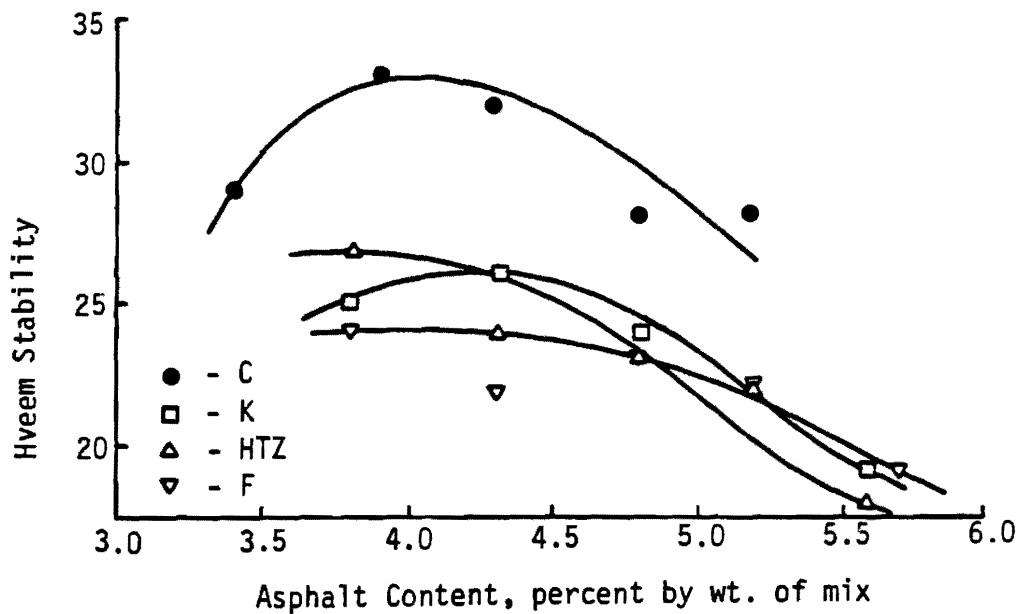


Figure A8. Hveem Stability as a Function of Asphalt Content for Control, Kevlar, Hoechst, and Forta Fibre Specimens.

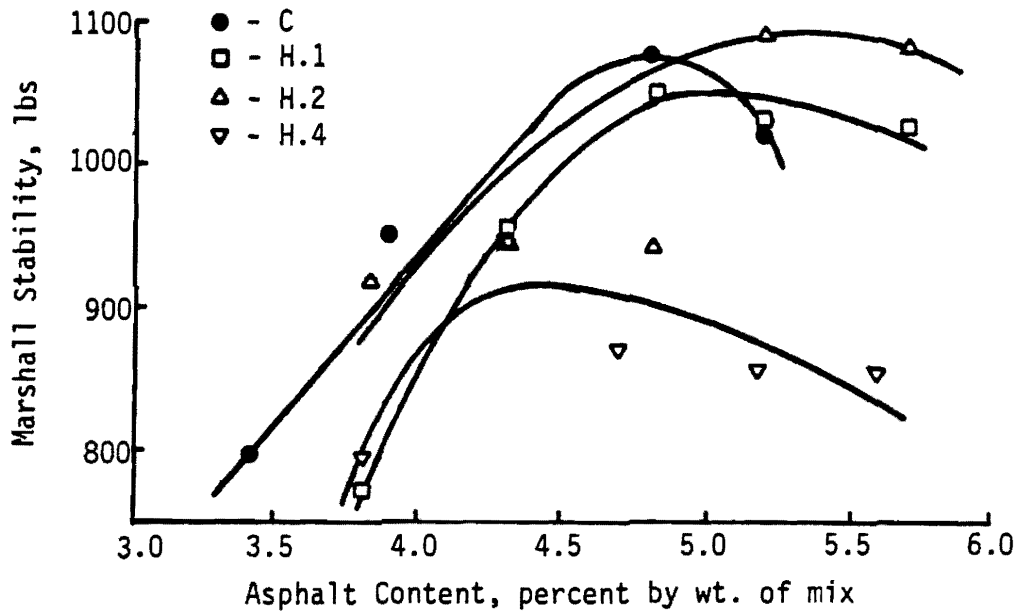


Figure A9. Marshall Stability as a Function of Asphalt Content for Control and Hercules Specimens.

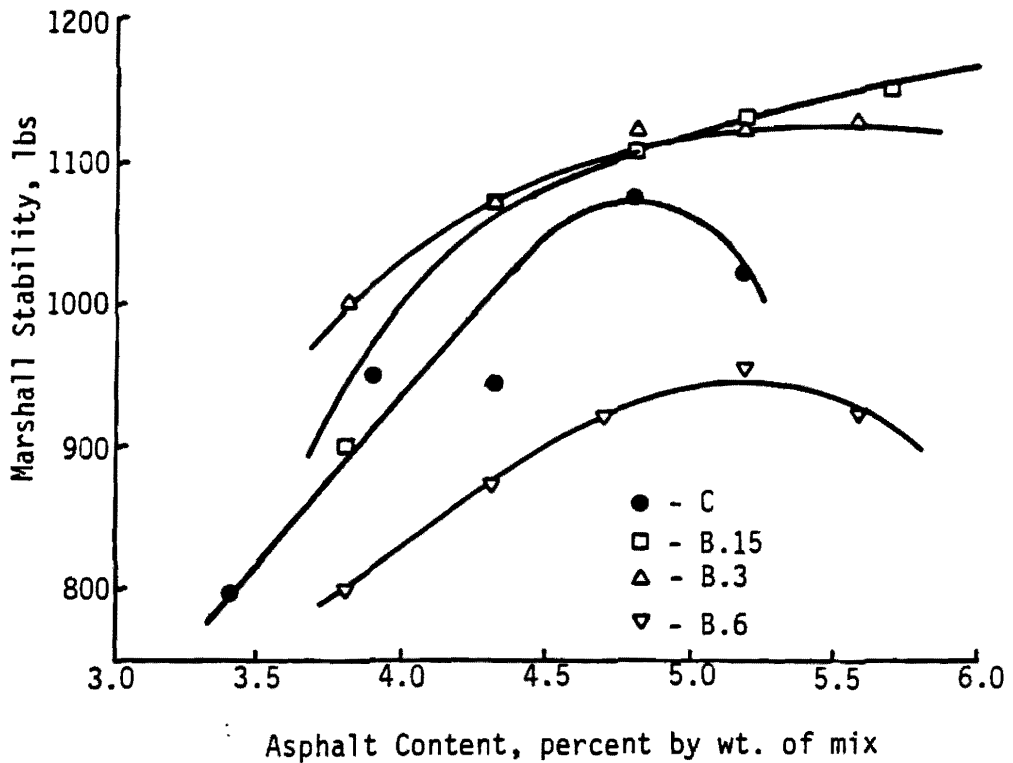


Figure A10. Marshall Stability as a Function of Asphalt Content for Control and BoniFiber Specimens.

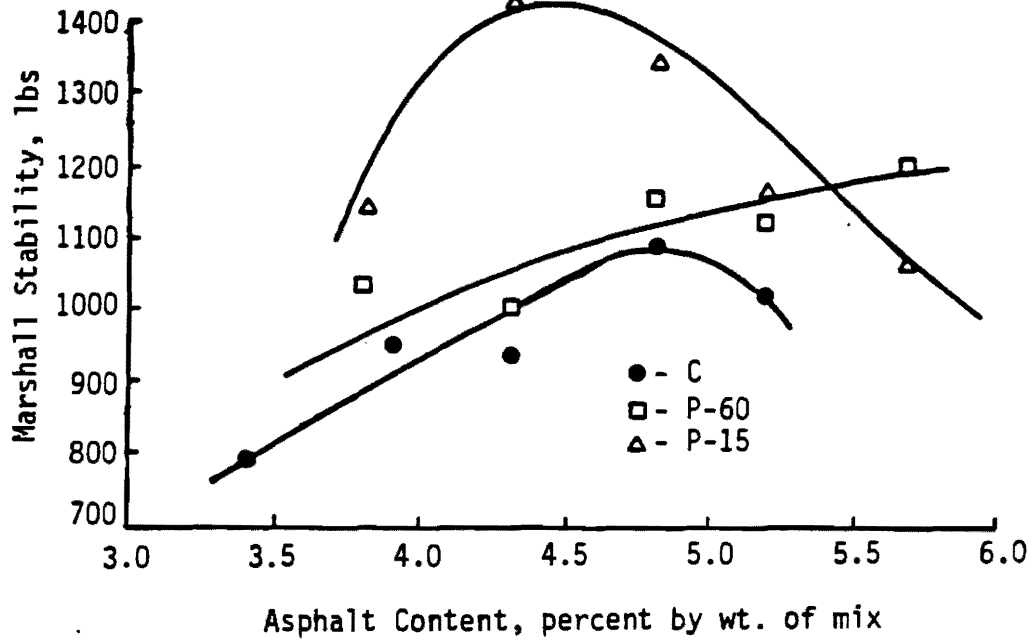


Figure A11. Marshall Stability as a Function of Asphalt Content for Control and Phillips Specimens.

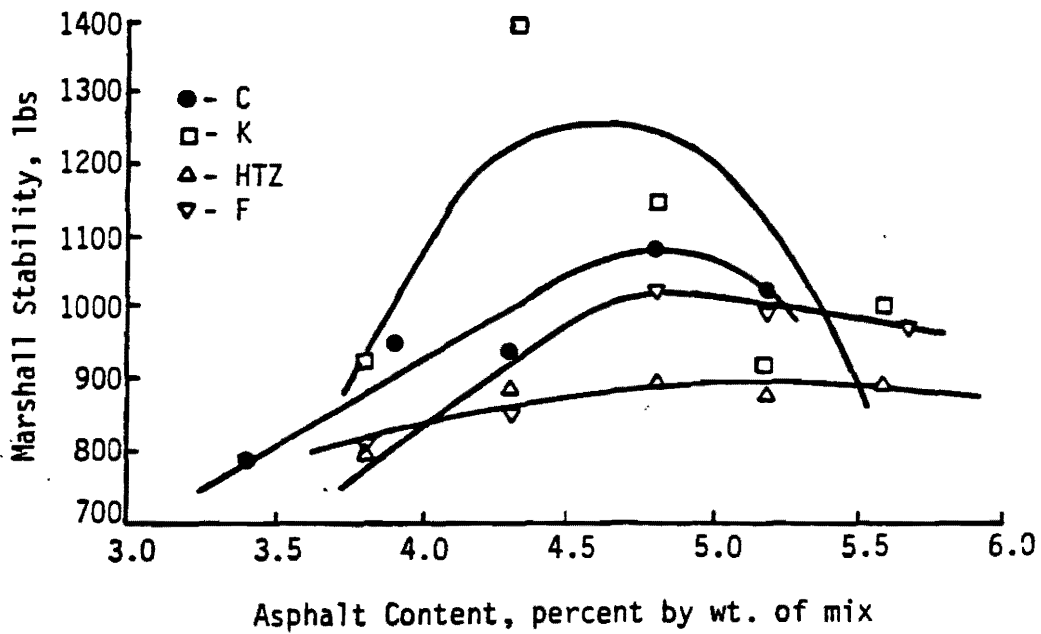


Figure A12. Marshall Stability as a Function of Asphalt Content for Control, Kevlar, Hoechst, and Forta Fibre Specimens.

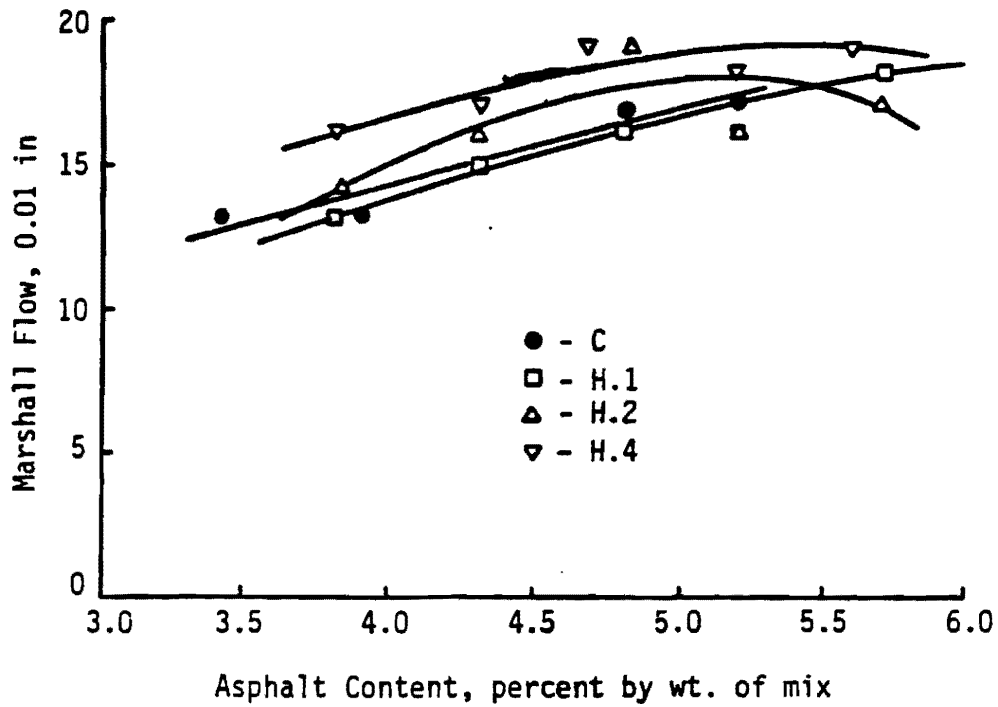


Figure A13. Marshall Flow as a Function of Asphalt Content for Control and Hercules Specimens.

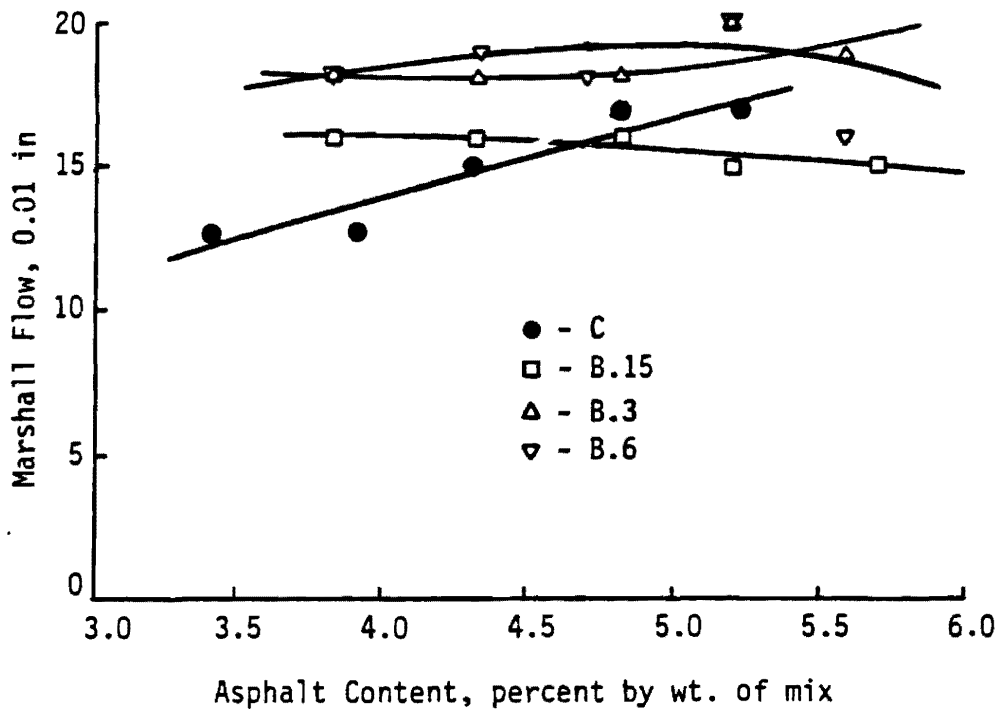


Figure A14. Marshall Flow as a Function of Asphalt Content for Control and Bonifiber Specimens.

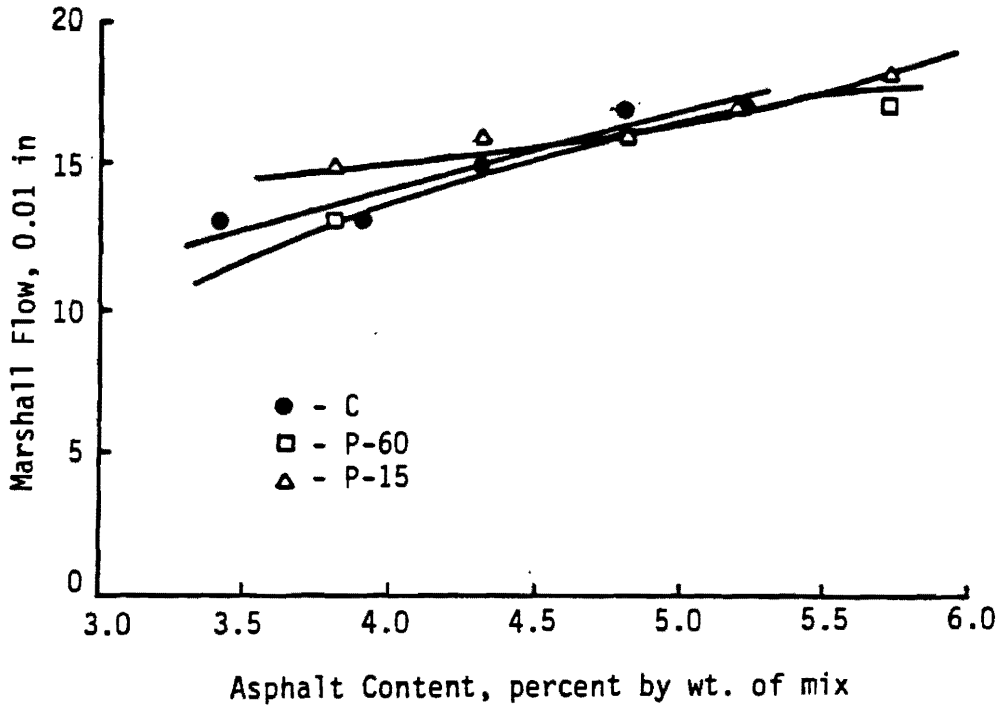


Figure A15. Marshall Flow as a Function of Asphalt Content for Control and Phillips Specimens.

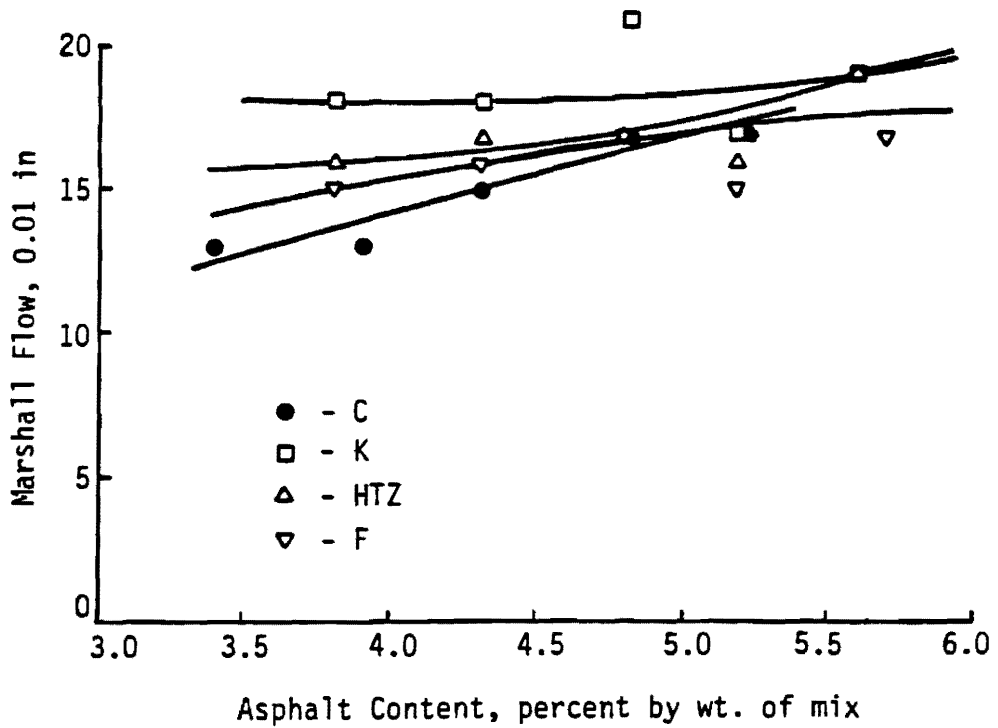


Figure A16. Marshall Flow as a Function of Asphalt Content for Control, Kevlar, Hoechst, and Forta Fiber Specimens.

APPENDIX B

Results of Tests on Gyrotory and Marshall
Compacted Specimens

Table B1. Properties of Mixtures With and Without Fibers.

Mixture Type	Asphalt Content, percent by wt. mix	Bulk Specific Gravity	Rice Specific Gravity	Air Void Content, percent	Hveem Stability	Marshall Test		Resilient Modulus, psi x 10 ³					Tensile Properties **	
						Stability, lbs.	Flow, 0.01 in.	-10°F	33°F	68°F	77°F	104°F	Tensile Strength, psi	Strain @ Failure, in/in
Control	4.6	2.377	2.470	3.8	27	870	14	2,200	2,290	770	680	96	170	0.0026
0.10% Hercules*	4.8	2.346	2.465	4.8	25	800	15	1,860	1,520	690	610	86	180	0.0027
0.20% Hercules	5.0	2.348	2.447	4.0	28	1,080	16	2,630	1,620	1,130	660	130	150	0.0031
0.40% Hercules	5.2	2.328	2.435	4.4	25	1,010	18	2,800	1,580	890	570	76	160	0.0036
0.15% BoniFibers	4.8	2.355	2.466	6.2	26	970	20	2,990	1,670	850	650	85	150	0.0034
0.30% BoniFibers	5.2	2.342	2.451	4.4	29	990	19	2,820	1,320	900	610	79	130	0.0037
0.60% BoniFibers	5.4	2.298	2.449	6.2	26	970	20	2,860	1,450	680	440	56	120	0.0046
0.30% Hoechst	5.2	2.329	2.454	5.1	24	760	17	2,780	1,630	850	570	78	150	0.0038
0.22% Forta-Fibre	5.1	2.336	2.442	4.3	22	880	17	2,750	1,550	920	630	79	150	0.0037
0.05% Forta-Fibre	4.6	2.369	2.476	4.5	29	940	12	2,700	1,640	940	660	83	150	0.0033
0.20% Phillips-15	4.9	2.349	2.451	4.2	28	930	15	2,780	1,700	960	660	88	170	0.0030
0.20% Phillips-60	4.7	2.353	2.467	4.5	27	890	13	2,700	1,710	850	600	76	140	0.0032
0.31% Kevlar	5.3	2.303	2.446	5.9	24	770	19	2,640	1,430	750	480	52	140	0.0048
0.55% Fiberglass	4.8	2.323	2.451	5.2	26	940	16	1,530	1,220	860	380	84	150	0.0043
0.55% Asbestos	5.0	2.355	2.456	4.1	29	930	14	1,440	1,250	870	530	110	160	0.0029
0.30% Kayocel	4.9	2.348	2.452	4.2	30	990	14	1,400	1,280	790	540	98	160	0.0028

*Percent fibers by weight of mix.

**Tensile test performed at 77°F and 2 in/min.

Table B2. Tensile Properties of Gyrotory Compacted Specimens at 0°F.

Type Mixture	Tensile Properties @ 0.02 in/min			Tensile Properties @ 0.2 in/min			Tensile Properties @ 2.0 in/min		
	Tensile Strength, psi	Strain @ Failure, in/in	Secant Modulus, psi	Tensile Strength, psi	Strain @ Failure, in/in	Secant Modulus, psi	Tensile Strength, psi	Strain @ Failure, in/in	Secant Modulus, psi
C	370	0.00013	2,100,000	370	-*	-	310	-*	-
H.1	360	0.00014	1,900,000	360	-	-	270	-	-
H.2	340	0.00017	2,200,000	360	-	-	260	-	-
H.4	350	0.00012	3,000,000	410	-	-	210	-	-
B.15	360	0.00014	2,700,000	320	-	-	330	-	-
B.3	350	0.00015	2,500,000	330	-	-	370	-	-
B.6	330	0.00019	1,700,000	310	-	-	320	-	-

* Strains very small and difficult to accurately measure.

Table B3. Tensile Properties of Gyratory Compacted Specimens at 33⁰F.

Type Mixture	Tensile Properties @ 0.02 in/min			Tensile Properties @ 0.2 in/min			Tensile Properties @ 2.0 in/min		
	Tensile Strength, psi	Strain @ Failure, in/in	Secant Modulus, psi	Tensile Strength, psi	Strain @ Failure, in/in	Secant Modulus, psi	Tensile Strength, psi	Strain @ Failure, in/in	Secant Modulus, psi
C	210	0.00064	320,000	390	0.00045	990,000	430	0.00026	1,300,000
H.1	240	0.00096	250,000	420	0.00032	1,900,000	420	0.00038	1,100,000
H.2	250	0.00051	520,000	410	0.00027	1,500,000	410	0.00060	700,000
H.4	250	0.00094	270,000	370	0.00037	1,000,000	420	0.00049	920,000
B.15	210	0.00081	260,000	360	0.00053	760,000	430	0.00060	720,000
B.3	220	0.00083	270,000	390	0.00036	1,100,000	430	0.00075	600,000
B.6	190	0.00106	180,000	360	0.00042	880,000	380	0.00102	380,000

Table B4. Tensile Properties of Gyrotory Compacted Specimens at 77⁰F.

Type Mixture	Tensile Properties @ 0.02 in/min			Tensile Properties @ 0.2 in/min			Tensile Properties @ 2.0 in/min		
	Tensile Strength, psi	Strain @ Failure, in/in	Secant Modulus, psi	Tensile Strength, psi	Strain @ Failure, in/in	Secant Modulus, psi	Tensile Strength, psi	Strain @ Failure, in/in	Secant Modulus, psi
C	49	0.0019	16,000	87	0.0036	30,000	170	0.0026	67,000
H.1	31	0.0044	7,000	81	0.0032	25,000	180	0.0027	72,000
H.2	37	0.0037	11,000	80	0.0033	25,000	150	0.0031	49,000
H.4	36	0.0047	8,000	70	0.0042	17,000	160	0.0036	44,000
B.15	34	0.0040	9,000	77	0.0040	19,000	150	0.0034	48,000
B.3	30	0.0048	6,000	77	0.0040	19,000	130	0.0037	37,000
B.6	24	0.0059	4,000	67	0.0047	14,000	120	0.0046	26,000

Table B5. Properties of Gyrotory Compacted Specimens Before and After Accelerated Lottman Procedure.

Type Mixture	Before Treatment				After Treatment				Resilient Modulus Ratio	Tensile Strength Ratio
	Resilient Modulus @ 77°F, ³ psi x 10 ³	Tensile Properties*			Resilient Modulus @ 77°F, ³ psi x 10 ³	Tensile Properties*				
		Tensile Strength, psi	Strain @ Failure, in/in	Secant Modulus, psi		Tensile Strength, psi	Strain @ Failure, in/in	Secant Modulus, psi		
C	680	170	0.0026	67,400	450	110	0.0036	30,900	0.67	0.63
H.1	610	180	0.0027	71,900	570	150	0.0029	50,900	0.93	0.81
H.2	660	150	0.0031	49,000	470	130	0.0035	36,700	0.71	0.84
H.4	570	160	0.0036	44,000	550	130	0.0044	30,400	0.97	0.86
B.15	650	150	0.0034	47,800	340	100	0.0045	22,600	0.55	0.68
B.3	610	130	0.0037	36,900	360	120	0.0040	33,600	0.60	0.94
B.6	440	120	0.0046	26,400	310	90	0.0058	15,800	0.70	0.78

*Tensile tests at 2 in/min and 77°F.

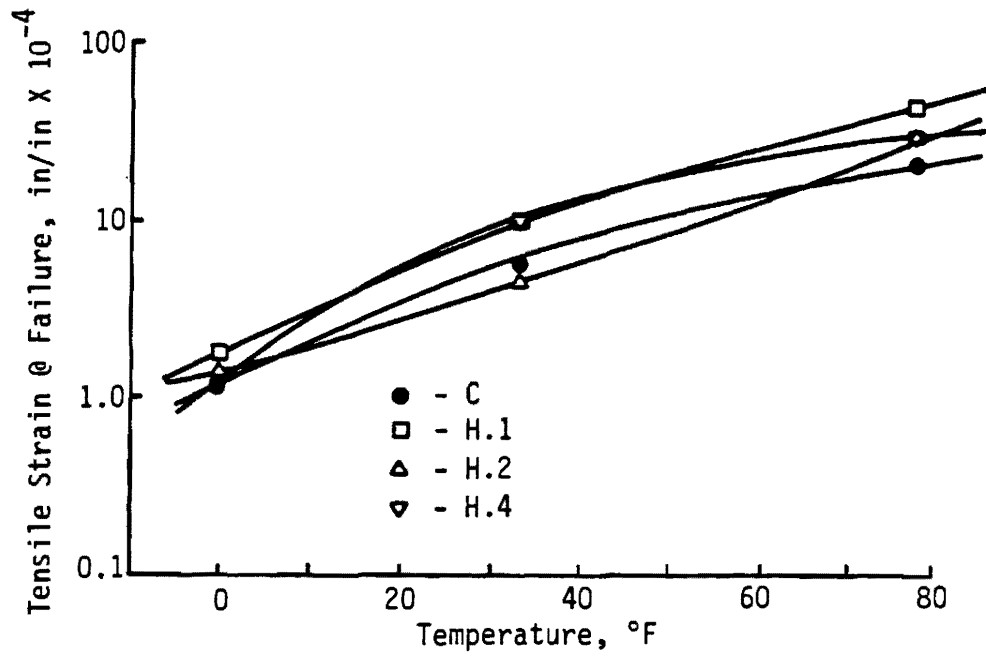


Figure B1. Tensile Strain at Failure for Control and Hercules Specimens as a Function of Temperature for a Displacement Rate of 0.02 in/min.

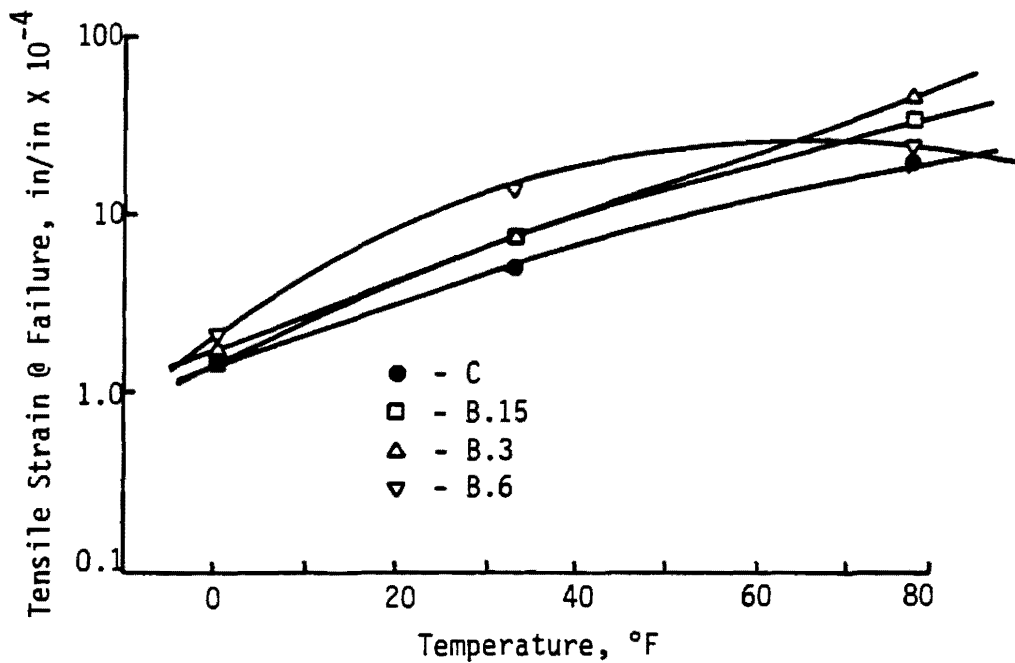


Figure B2. Tensile Strain at Failure for Control and BoniFiber Specimens as a Function of Temperature for a Displacement Rate of 0.02 in/min.

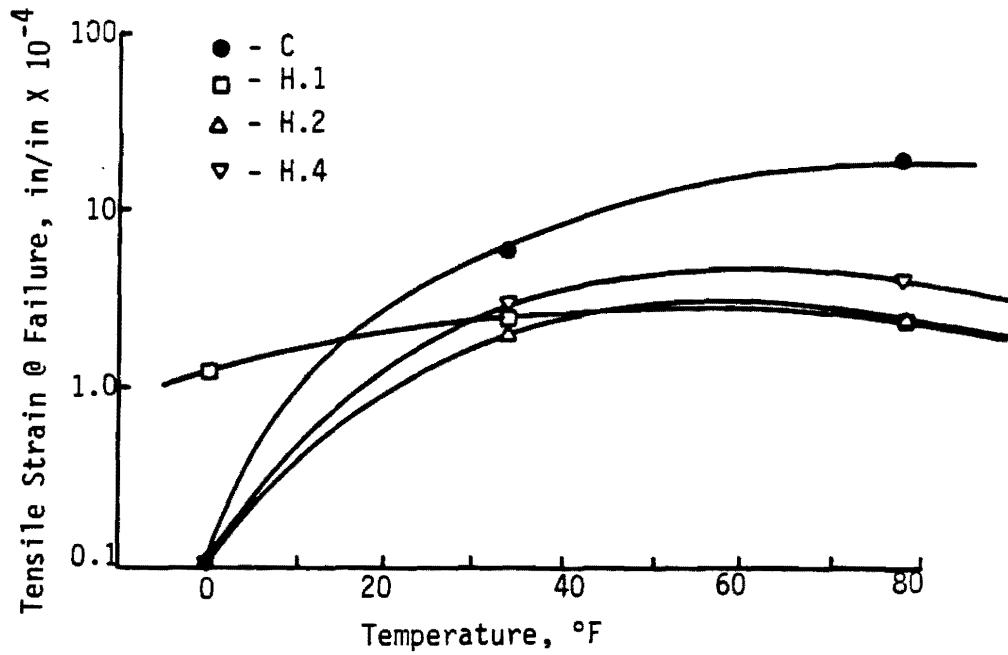


Figure B3. Tensile Strain at Failure for Control and Hercules Specimens as a Function of Temperature for a Displacement Rate of 0.2 in/min.

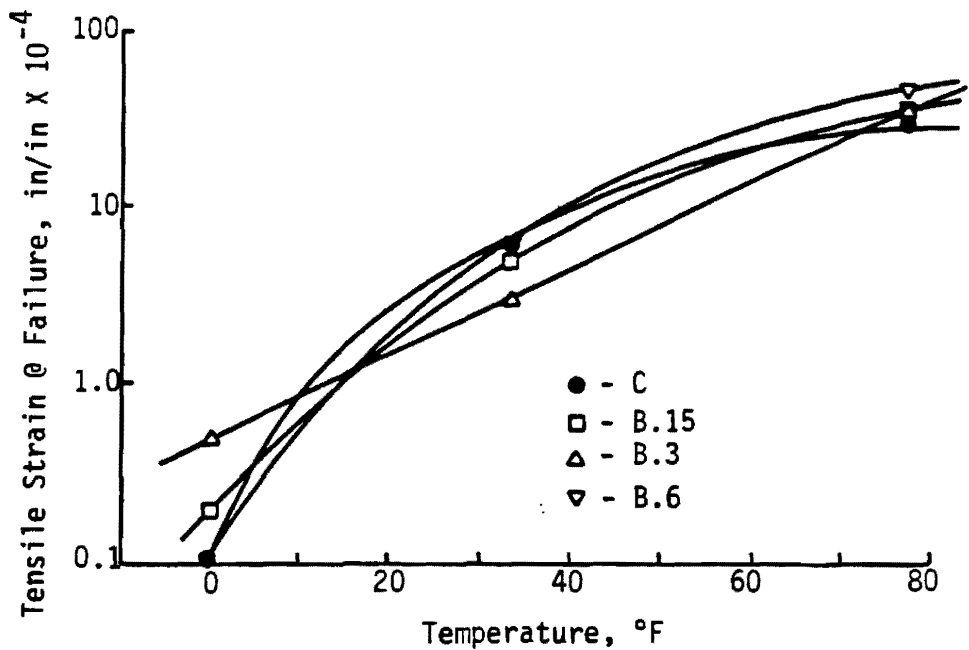


Figure B4. Tensile Strain at Failure for Control and BoniFiber Specimens as a Function of Temperature for a Displacement of 0.2 in/min.

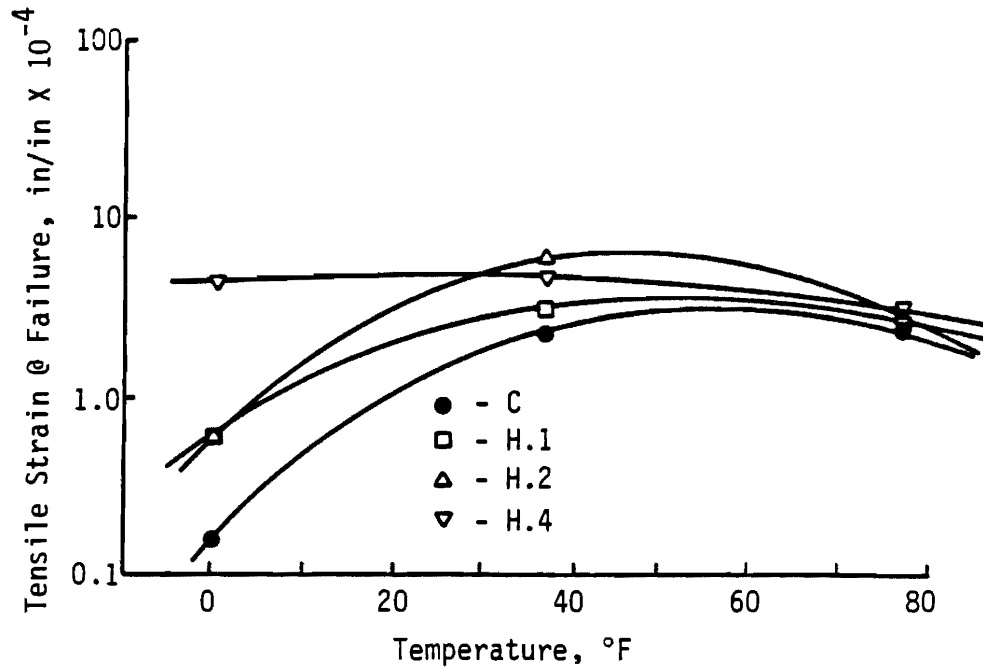


Figure B5. Tensile Strength at Failure for Control and Hercules Specimens as a Function of Temperature for a Displacement Rate of 2.0 in/min.

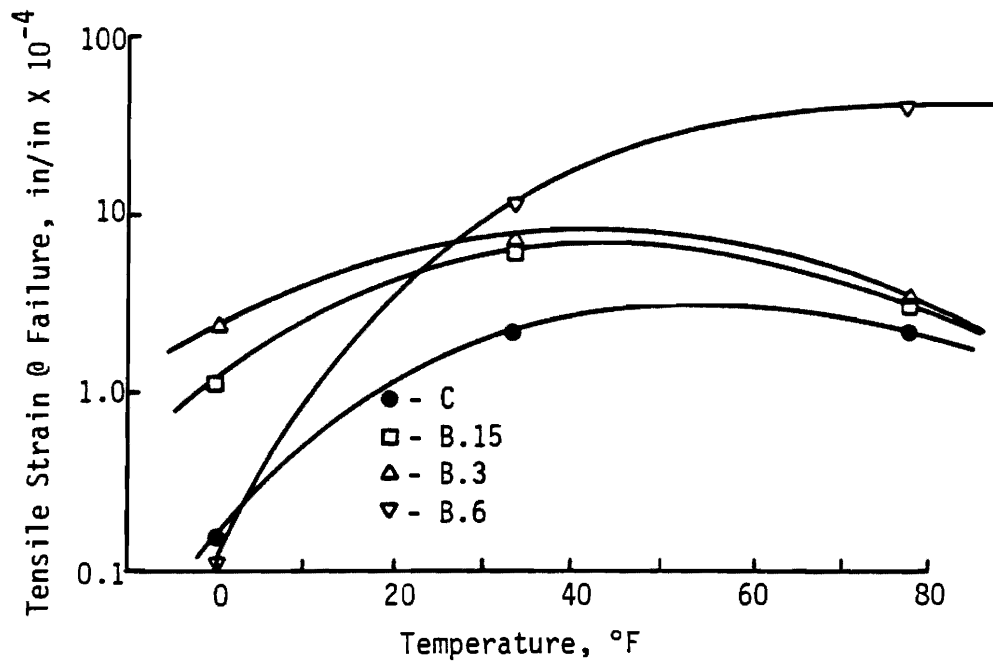
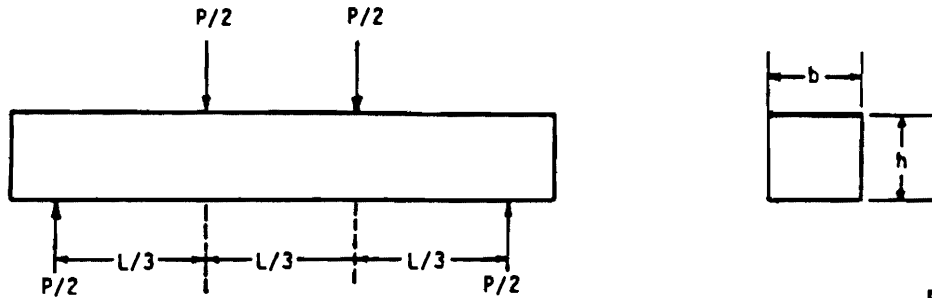


Figure B6. Tensile Strength at Failure for Control and BoniFiber Specimens as a Function of Temperature for a Displacement Rate of 2.0 in/min.

APPENDIX C

Data From Flexural Fatigue Testing

Summary of Formulae
for
Third-Point Loaded Beam



Equation No.

Peak stress in extreme fiber = $\sigma_{\max} = \frac{PL}{bh^2}$, psi (C1)

Initial stiffness modulus = $E = \frac{0.213 PL^3}{W_0 bh^3} + \frac{0.400 PL(1+\mu)}{W_0 bh}$,
psi (C2)

Initial bending strain in extreme fiber = $\epsilon = \frac{\sigma}{E}$, in./in.
(Hooke's Law) (C3)

Total input energy = $U_f = \frac{10.2 P W_0 N_f}{23}$, in.-lb (C4)

- where
- P = applied load, lbs
 - L = test length of beam, in.
 - b = width of beam, in.
 - h = depth of beam, in.
 - W_0 = center deflection of beam at 200th cycle, in.
 - μ = Poisson's ratio (assumed 0.35)
 - N_f = number of cycles to failure

Table C1. Statistical Summary of Flexural Fatigue Results.

Sample Type	Stress Level	Statistic	Bulk Specific Gravity of Mixture	Air Voids, Percent	Input Stress, psi	Bending Strain at 200 Cycles, in/in x 10 ⁻⁴	Cycles to Failure	Initial Stiffness Modulus, psi	Total Energy Input, lb-in
Control Specimens	Low	Mean	2.341	5.2	99	1.9	281,000	543,000	59,000
		Std. Dev.*	0.002	0.1	1.7	0.3	157,000	100,000	33,000
		Coef. Var.**	0.1	1.5	1.7	16	56	18	55
Control Specimens	Medium	Mean	2.330	5.7	154	2.8	38,000	545,000	19,000
		Std. Dev.	0.01	0.4	2	0.3	9,000	27,000	4,000
		Coef. Var.	0.4	7	1.3	10	23	5	21
Control Specimens	High	Mean	2.337	5.4	183	3.2	27,000	597,000	19,000
		Std. Dev.	0.005	0.2	3	0.5	20,000	105,000	12,000
		Coef. Var.	0.2	4	1.7	15	73	18	63
Hercules Specimens	Low	Mean	2.282	6.8	75	1.6	356,000	481,000	49,000
		Std. Dev.	0.003	0.2	2	0.1	210,000	37,000	27,000
		Coef. Var.	0.1	2	3	6	59	8	55
Hercules Specimens	Medium	Mean	2.277	7.0	98	2.5	54,000	408,000	15,000
		Std. Dev.	0.008	0.3	0.9	0.2	33,000	33,000	8,000
		Coef. Var.	0.4	4	0.9	8	60	8	56
Hercules Specimens	High	Mean	2.287	6.5	147	4.5	11,000	331,000	8,000
		Std. Dev.	0.005	0.2	1.0	0.3	4,000	31,000	3,000
		Coef. Var.	0.2	3	0.7	6	38	9	34

Table C1. (Continued).

Sample Type	Stress Level	Statistic	Bulk Specific Gravity of Mixture	Air Voids, percent	Input Stress, psi	Bending Strain at 200 Cycles, in/in x 10 ⁻⁴	Cycles to Failure	Initial Stiffness Modulus, psi	Total Energy Input, lb-in
BoniFiber Specimens	Low	Mean	2.238	8.6	48	1.1	623,000	522,000	43,000
		Std. Dev.	0.006	0.3	1.4	0.5	336,000	292,000	36,000
		Coef. Var.	0.3	3	3	42	54	56	84
BoniFiber Specimens	Medium	Mean	2.219	9.5	101	4.0	10,000	255,000	5,000
		Std. Dev.	0.017	0.7	2	0.4	6,000	32,000	2,000
		Coef. Var.	0.8	7	2	10	62	13	53
BoniFiber Specimens	High	Mean	2.233	8.9	148	6.4	4,000	241,000	4,000
		Std. Dev.	0.015	0.6	4	1.7	2,000	61,000	1,000
		Coef. Var.	0.7	7	3	27	47	25	27
Kevlar Specimens	Low	Mean	2.211	9.6	51	2.2	145,000	231,000	18,000
		Std. Dev.	0.002	0.1	1.1	0.3	101,000	18,000	11,000
		Coef. Var.	0.1	1.0	2	16	70	8	60
Kevlar Specimens	Medium	Mean	2.210	9.6	102	4.4	18,000	240,000	10,000
		Std. Dev.	0.006	0.2	3	0.7	5,000	24,000	3,000
		Coef. Var.	0.2	2	2	16	27	10	34
Kevlar Specimens	High	Mean	2.218	9.3	154	7.1	1,400	221,000	2,000
		Std. Dev.	0.005	0.2	3	1.2	500	33,000	800
		Coef. Var.	0.2	2	1.8	16	39	15	44

* Standard Deviation

** Coefficient of Variation in percent

Table C2. Flexural Fatigue Results of Individual Control Specimens.

Specimen No.	Height, inches	Bulk Specific Gravity	Air Voids, percent	Input Stress, psi	Cycles to Failure	Bending Strain at 200 Cycles, in/in x 10 ⁻⁴	Initial Stiffness Modulus, psi	Total Energy Input, lb-in
1	3.0	2.339	5.3	96.7	169,126	2.2	435,253	40,961
2	3.0	2.343	5.1	99.0	459,470	1.8	561,327	96,805
3	3.0	2.341	5.2	99.9	213,116	1.6	633,369	39,766
4	3.0	2.331	5.6	152.1	46,528	2.9	524,071	23,608
5	2.9	2.339	5.3	156.0	28,962	3.0	536,250	16,063
6	3.1	2.320	6.1	153.6	38,919	2.5	575,178	17,700
7	3.0	2.332	5.6	179.2	13,599	3.8	476,184	11,344
8	3.0	2.336	5.4	183.7	18,062	3.0	656,125	12,301
9	3.0	2.342	5.2	185.2	50,390	2.9	659,941	32,196

Table C3. Flexural Fatigue Results of Individual Hercules Fiber Specimens*

Specimen No.	Height, inches	Bulk Specific Gravity	Air Voids, percent	Input Stress, psi	Cycles to Failure	Bending Strain at 200 Cycles, in/in x 10 ⁻⁴	Initial Stiffness Modulus, psi	Total Energy Input, lb-in
1	3.06	2.284	6.7	96.7	89,469	2.4	409,569	24,204
2	3.10	2.279	6.9	98.5	47,330	2.3	439,963	12,604
3	3.08	2.268	7.3	97.6	25,334	2.7	374,525	7,925
4	3.03	2.292	6.3	146.0	8,271	4.7	315,881	6,903
5	3.11	2.282	6.7	148.0	8,165	4.7	310,075	6,689
6	3.09	2.287	6.5	147.5	15,164	4.2	366,004	11,746
7	3.07	2.279	6.9	74.0	271,665	1.6	464,118	36,880
8	3.04	2.285	6.6	77.1	596,000	1.5	523,011	80,770
9	3.05	2.281	6.8	73.0	201,782	1.7	455,955	30,477

*Fiber content is 0.20% by weight of mixture.

Table C4. Flexural Fatigue Results of Individual BoniFiber Specimens*

Specimen No.	Height, inches	Bulk Specific Gravity	Air Voids, percent	Input Stress, psi	Cycles to Failure	Bending Strain at 200 Cycles, in/in x 10 ⁻⁴	Initial Stiffness Modulus, psi	Total Energy Input, lb-in
1	3.03	2.239	8.7	153.0	3,712	5.9	257,605	3,942
2	3.05	2.243	8.5	147.1	5,179	5.0	291,899	4,507
3	3.14	2.216	9.6	145.0	1,819	8.3	173,906	2,557
4	3.06	2.236	8.8	102.7	17,341	3.6	288,925	7,430
5	3.17	2.218	9.6	102.7	7,215	4.0	252,885	3,343
6	3.11	2.202	10.2	99.0	5,915	4.4	224,573	3,086
7	3.09	2.237	8.4	46.0	576,236	1.2	386,224	38,070
8	3.06	2.233	8.9	47.9	313,300	0.6	856,742	9,781
9	3.04	2.245	8.4	48.6	980,000	1.5	323,114	81,120

*Fiber content is 0.30% by weight of mixture.

Table C5. Flexural Fatigue Results of Individual Kevlar Fiber Specimens*

Specimen No.	Height, inches	Bulk Specific Gravity	Air Voids, percent	Input Stress, psi	Cycles to Failure	Bending Strain at 200 Cycles, in/in x 10 ⁻⁴	Initial Stiffness Modulus, psi	Total Energy Input, lb-in
1	3.13	2.223	9.1	151.1	1,800	6.0	253,253	1,906
2	3.11	2.214	9.5	156.0	795	7.1	220,832	1,029
3	3.15	2.216	9.4	156.0	1,736	8.3	187,461	2,647
4	3.12	2.213	9.5	102.0	12,300	4.3	244,466	6,491
5	3.14	2.204	9.9	105.0	18,978	5.2	214,218	13,072
6	3.11	2.214	9.5	100.0	21,344	3.8	262,534	9,534
7	3.11	2.211	9.6	50.9	42,587	2.2	229,384	5,782
8	3.09	2.213	9.5	49.4	244,643	1.9	249,158	26,506
9	3.14	2.209	9.7	51.5	147,410	2.5	213,243	23,038

*Fiber content is 0.31% by weight of mixture.

APPENDIX D

Data from Overlay Tester
(Resistance to Thermal Reflection Cracking)

Table D1. Summary of Overlay Test Results.

Type Mixture	Test Temperature, °F	Fiber Content, percent	Air Voids, Percent*	Number of Cycles at Failure*
Control	33**	0	7.0	12
Hercules	33	0.2	7.2	30
BoniFiber	33	0.3	7.9	30
Kevlar	33	0.31	9.5	35
Control	77***	0	7.3	20
Hercules	77	0.2	6.9	49
BoniFiber	77	0.3	8.2	49
Kevlar	77	0.31	9.5	43

* Average of three specimens.

** Crack opening was 0.04 inches.

*** Crack opening was 0.07 inches.

Table D2. Physical Properties of Individual Overlay Test Beams and Number of Cycles to Failure.

Type Mixture	Test Temperature, °F	Fiber Content, percent	Sample Number	Sample Height, inches	Bulk Specific Gravity	Air Voids, percent	Number of Cycles at Failure
Control	77 *	0	10	3.02	2.277	7.8	10
	77	0	11	3.03	2.296	7.0	31
	77	0	12	2.98	2.298	7.0	19
	33 **	0	13	3.01	2.295	7.1	12
	33	0	14	3.00	2.302	6.8	15
	33	0	15	3.01	2.298	7.0	10
Hercules	77	0.2	10	3.04	2.289	6.5	42
	77	0.2	11	3.07	2.274	7.1	55
	77	0.2	12	3.08	2.271	7.2	49
	33	0.2	13	3.03	2.271	7.2	33
	33	0.2	14	3.02	2.267	7.4	31
	33	0.2	15	3.04	2.273	7.1	26
Bonifiber	77	0.3	10	3.01	2.257	7.9	39
	77	0.3	11	3.08	2.252	8.1	47
	77	0.3	12	3.01	2.234	8.6	60
	33	0.3	13	3.02	2.250	8.2	29
	33	0.3	14	3.07	2.262	7.7	27
	33	0.3	15	3.02	2.260	7.8	35
Kevlar	77	0.31	10	3.11	2.213	9.5	40
	77	0.31	11	3.10	2.223	9.1	36
	77	0.31	12	3.09	2.204	9.9	52
	33	0.31	13	3.14	2.213	9.5	38
	33	0.31	14	3.13	2.210	9.6	31
	33	0.31	15	3.08	2.216	9.4	37

* Crack opening at 77°F was 0.07 inches.

** Crack opening at 33°F was 0.04 inches.

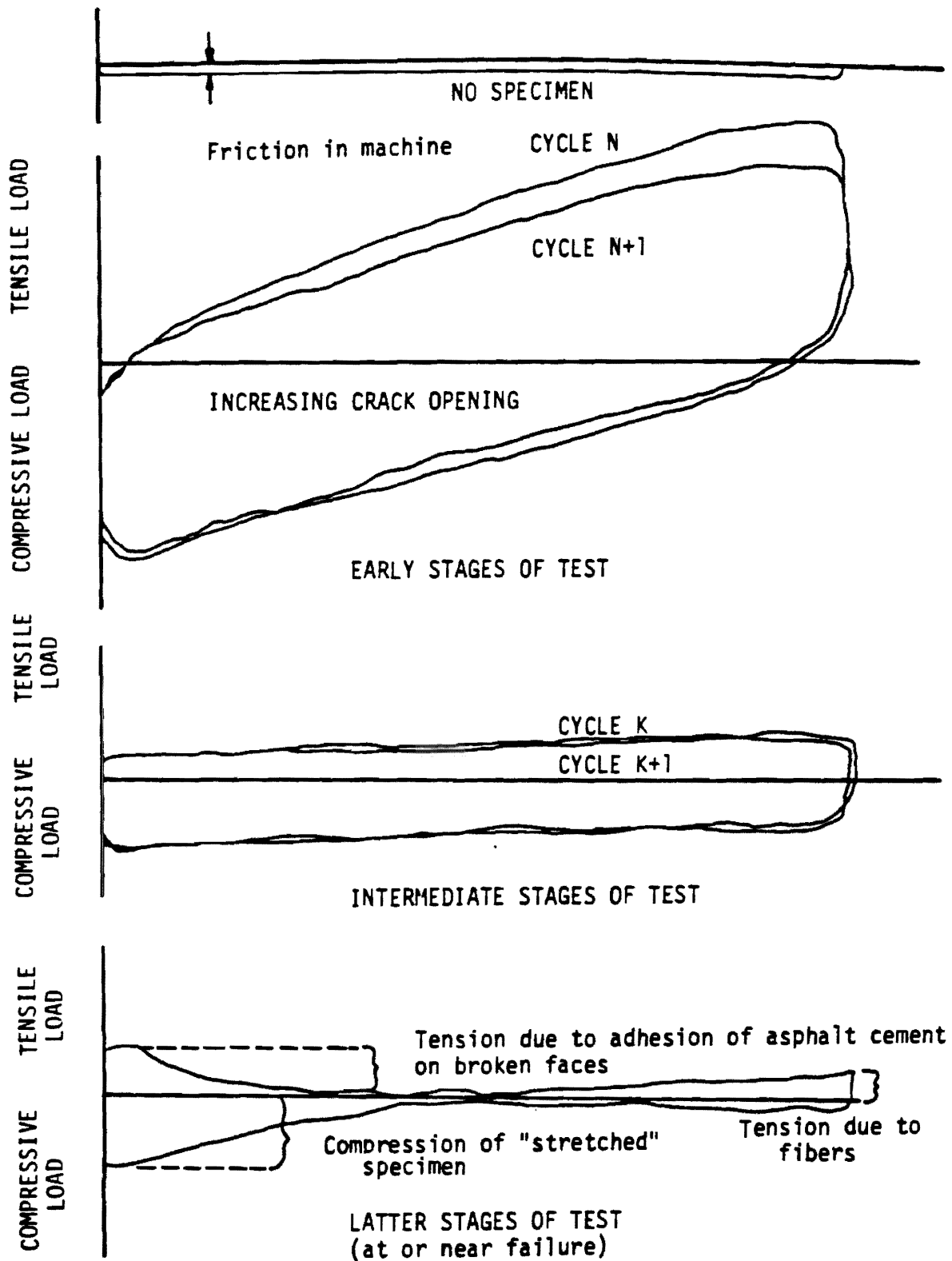
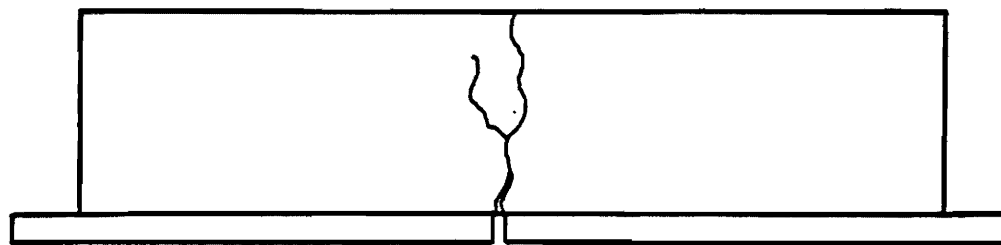
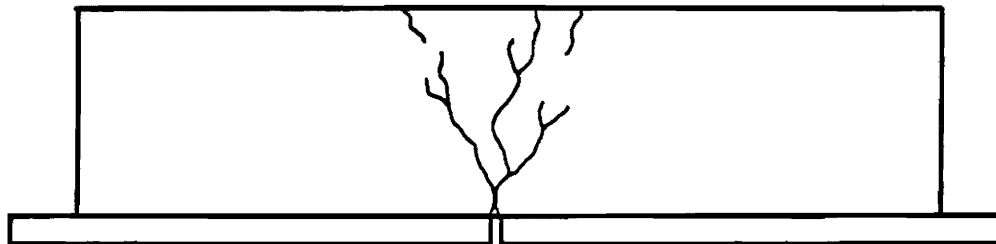


FIGURE D1. Typical Recordings of Load versus Deformation at Various Phases During a Test.



No Fibers (Control)



With Fibers

Figure D2 . Typical Cracking Patterns of Overlay Test Specimens With and Without Fibers.

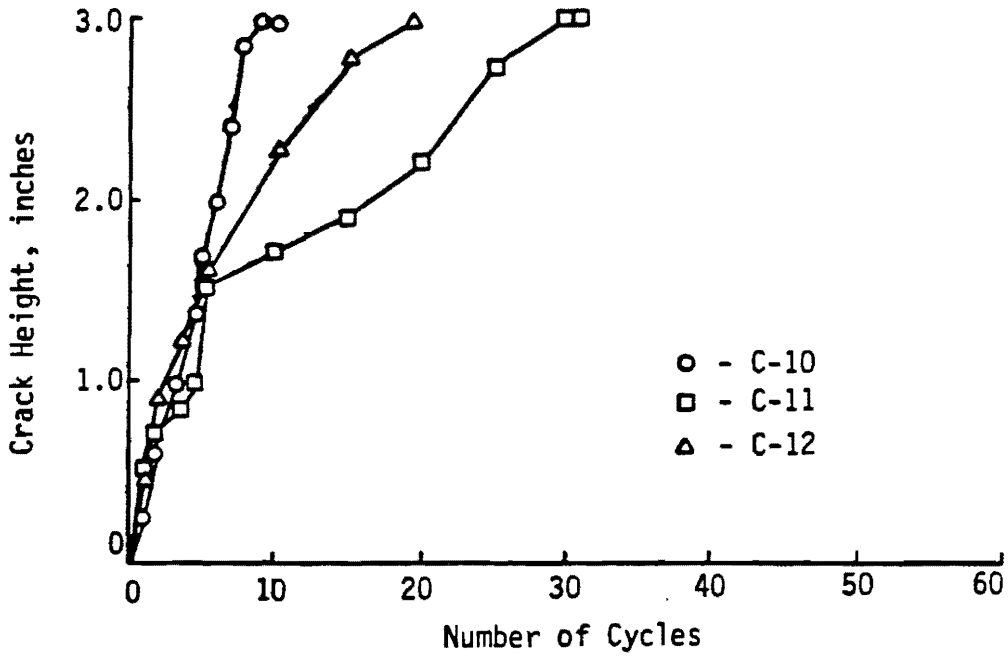


Figure D3 . Crack Height versus Number of Cycles for Control Overlay Specimens Tested at 77°F.

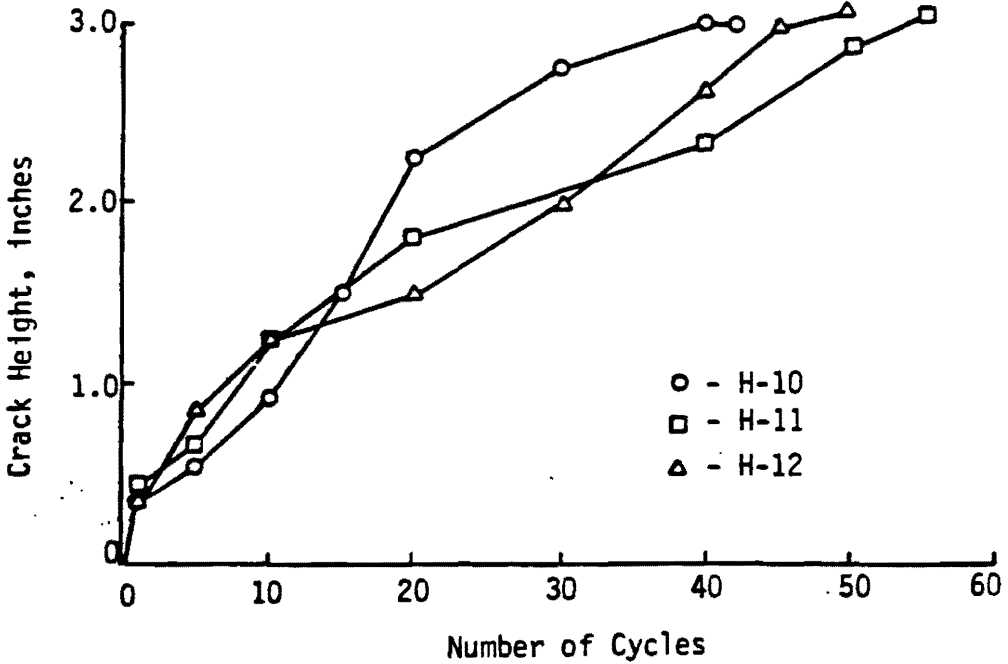


Figure D4 . Crack Height versus Number of Cycles for Hercules Overlay Specimens Tested at 77°F.

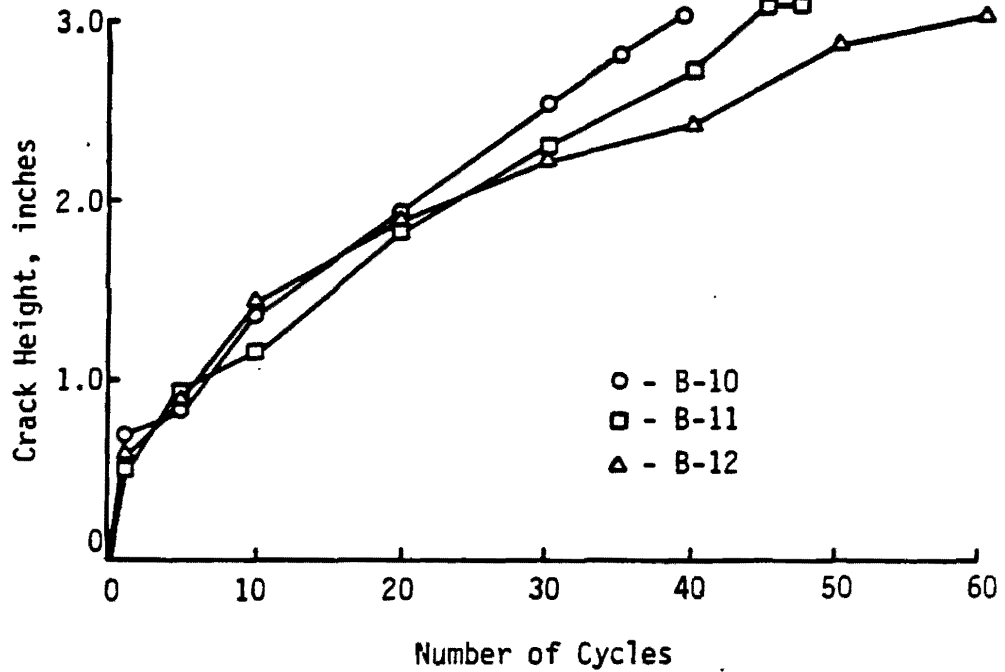


Figure D5. Crack Height versus Number of Cycles for BoniFiber Overlay Specimens Tested at 77°F.

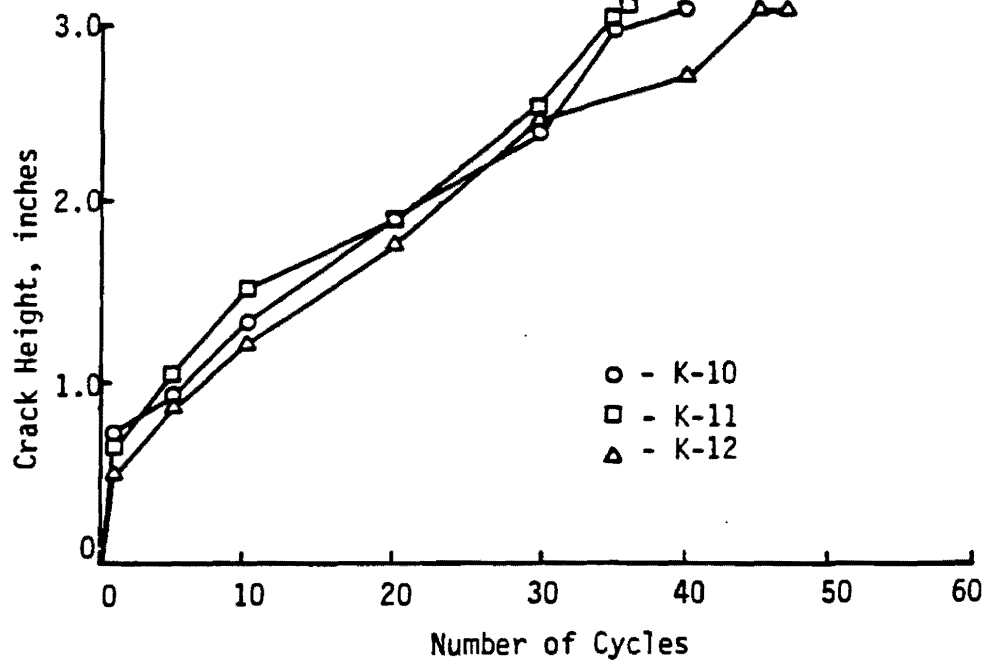


Figure D6. Crack Height versus Number of Cycles for Kevlar Overlay Specimens Tested at 77°F.

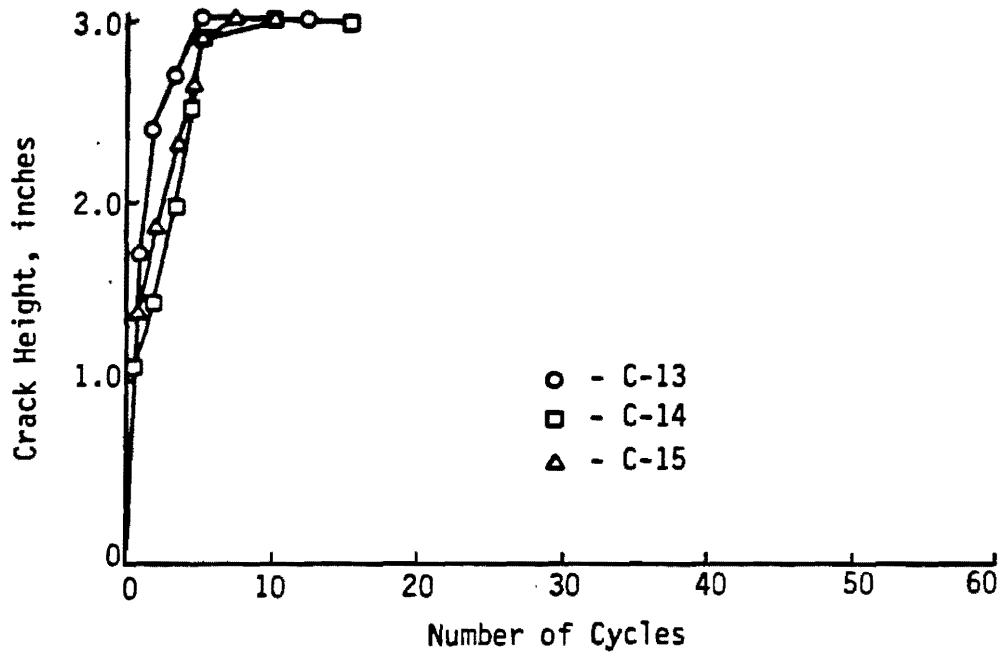


Figure D7. Crack Height versus Number of Cycles for Control overlay Specimens Tested at 33°F.

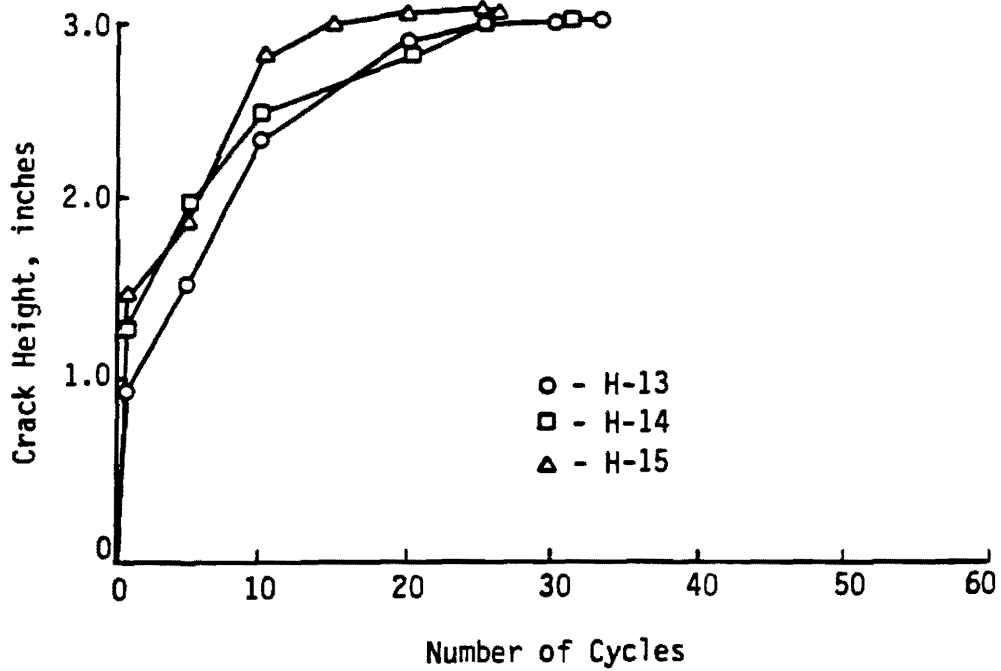


Figure D8. Crack Height versus Number of Cycles for Hercules Overlay Specimens Tested at 33°F.

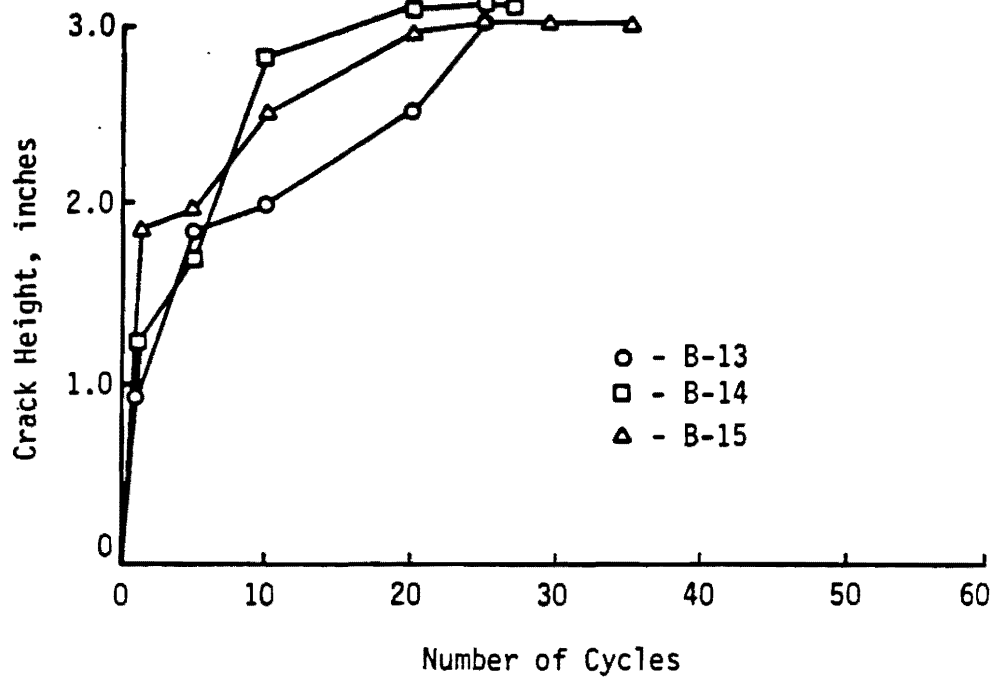


Figure D9 . Crack Height versus Number of Cycles for BoniFiber Overlay Specimens Tested at 33°F.

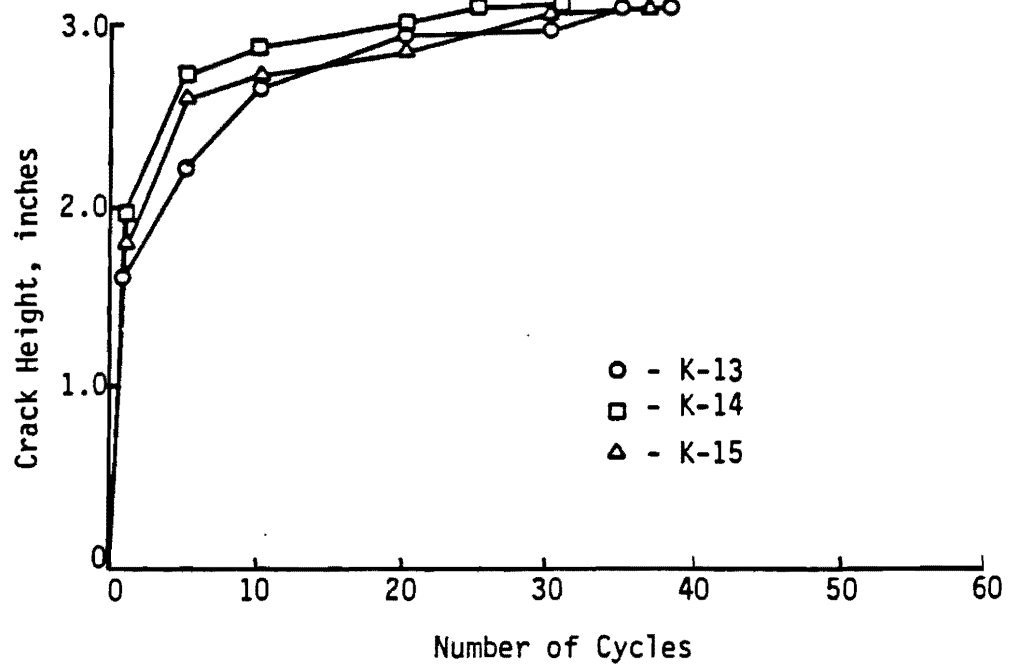


Figure D10 . Crack Height versus Number of Cycles for Kevlar Overlay Specimens Tested at 33°F.

APPENDIX E
Data from Direct Compression Tests

Table E1. Physical Properties of Direct Compression Test Specimens.

Test Temperature, °F	Sample ID	Sample Height, inches	Bulk Specific Gravity	Air Void Content, percent	Average Air Void Content	
40	C3	7.63	2.33	6.1	5.9	
	C4	7.55	2.34	5.5		
	C9	7.60	2.33	6.0		
	4.6-5	7.72	2.30	6.5	7.0	
	4.6-6	7.79	2.27	7.4		
	4.85-5	7.79	2.30	6.1	5.9	
	4.85-6	7.70	2.31	5.6		
	5.1-3	7.65	2.32	5.4	5.5	
	5.1-4	7.74	2.31	5.6		
	70	C1	7.55	2.34	5.5	5.6
		C2	7.55	2.33	5.8	
		C8	7.57	2.34	5.6	
4.6-1		7.68	2.31	6.1	6.2	
4.6-2		7.72	2.31	6.2		
4.85-1		7.73	2.31	5.8	6.0	
4.85-2		7.76	2.30	6.2		
5.1-1		7.73	2.31	5.5	5.5	
5.1-2		7.68	2.32	5.4		
100		C5	7.52	2.34	5.4	5.6
		C6	7.60	2.33	6.0	
		C7	7.59	2.35	5.4	
	4.6-3	7.66	2.31	5.9	6.3	
	4.6-4	7.74	2.29	6.7		
	4.85-3	7.63	2.32	5.1	5.4	
	4.85-4	7.67	2.31	5.6		
	5.1-5	7.65	2.32	5.3	5.2	
	5.1-6	7.61	2.32	5.1		

Table E2. Average Permanent Strain from the Incremental Static Compression Test.

Test Temperature, °F	Sample ID	Permanent Strain (in x 10 ⁻⁶ /inch) after Load Duration given below				
		0.1 sec	1 sec	10 sec	100 sec	1,000 sec
40	Control	0.291	1.75	4.17	13.2	65.7
	4.6	0.291	0.582	4.08	10.3	50.3
	4.85	*	0.146	0.291	5.53	44.6
	5.1	*	0.873	1.75	4.23	17.3
70	Control	0.582	5.82	47.9	202	737
	4.6	0.871	4.95	45.1	188	601
	4.85	*	1.75	37.9	195	725
	5.1	*	1.75	52.7	262	820
100	Control	17.9	101	283	642	1,580
	4.6	9.24	69	277	650	1,370
	4.85	30.4	87.1	281	601	1,335
	5.1	23.9	103	367	764	1,535

Table E3. Average Creep Compliance from 1,000 Second Creep Test.

Test Temperature, °F	Sample I.D.	Creep Compliance ($\text{psi}^{-1} \times 10^{-6}$) at Load Duration Given Below:									
		0.03	0.1	0.3	1	3	10	30	100	300	1,000
40	Control	0.22	0.26	0.31	0.37	0.45	0.63	0.86	1.35	2.14	3.89
	4.6	0.088	0.22	0.26	0.32	0.39	0.55	0.62	0.95	1.63	2.99
	4.85	0.10	0.25	0.29	0.34	0.43	0.58	0.78	1.10	1.92	3.34
	5.1	0.23	0.25	0.30	0.36	0.44	0.60	0.67	0.84	1.41	2.21
70	Control	0.47	0.95	1.57	2.79	4.85	8.60	13.4	19.7	28.4	40.5
	4.6	0.39	1.18	2.07	3.32	5.68	9.77	14.3	21.3	30.7	41.8
	4.85	0.41	1.18	1.88	3.18	5.37	9.79	14.2	22.1	32	46
	5.1	0.72	1.35	2.16	4.16	7.06	12.4	18.1	26.8	36.6	51.8
100	Control	2.16	7.26	16.7	28.5	38.6	47.9	56.1	65.1	76.5	95.3
	4.6	2.52	7.35	15.1	27.7	40.2	52.0	60.0	67.2	76.7	92.8
	4.85	2.78	8.07	17.7	32.0	45.9	57.2	65.5	74.8	85.8	102
	5.1	2.93	9.49	2.22	39.7	56.5	70.5	80.5	93.9	107	125

Table E4. Average Data from Dynamic Repetitive Loading Test.

Test Temperature, °F	Sample ID	Permanent Strain after No. of Load Repetitions given below					Dynamic Modulus @ 200 Repetitions, psi x 10 ⁶	Strain Amplitude @ 200 Repetitions, in x 10 ⁻⁶ /in
		1	10	100	200	1,000		
40	Control	0.290	0.971	1.55	1.75	1.80	6.5	3.4
	4.6	0.290	0.580	4.58	0.80	-	7.8	2.6
	4.85	0.29	0.436	0.73	1.02	-	7.3	3.7
	5.1	*	0.800	1.02	1.17	1.17	6.3	3.4
70	Control	2.72	11.9	24.1	27.2	34.9	1.7	12
	4.6	2.91	11.3	23.3	28.3	35.0	1.4	15
	4.85	2.42	6.70	25.3	40.8	-	1.4	14
	5.1	2.04	8.74	28.9	32.3	33.8	1.5	14
100	Control	33.7	114	360	453	995	0.15	140
	4.6	32.4	115	230	255	-	0.31	64
	4.85	34.5	118	240	302	550	0.29	70
	5.1	62.5	212	437	497	670	0.24	84

APPENDIX F
Test Results from Field Projects

Table F1. Individual Component of Project Design Gradation for Overlay Used on U. S. 83 District 8.*

Sieve Sizes	Coarse Aggregate	Crusher Screenings	Field Sand	Combined Gradation	SDHPT Type D Specification
Passing 1/2-inch sieve	100	100	100	100	100
Passing 3/8-inch sieve	95.1	100	100	97.0	85-100
Passing 3/8", retained on No. 4	60.9	0	0	37.8	21-53
Passing No. 4, retained on No. 10	31.3	7.2	0	21.3	11-32
Total retained on No. 10	97.1	7.2	0	62.1	54-74
Passing No. 10, retained on No. 40	1.0	50.5	2.1	14.0	6-32
Passing No. 40, retained on No. 80	0.3	17.7	62.3	12.3	4-27
Passing No. 80, retained on No. 200	0.5	12.6	33.3	7.6	3-27
Passing No. 200 sieve	1.1	12.0	2.3	4.0	1-8
Percent Combined	62	+ 26	+ 12	=	100 weight percent

*Data Supplied by District 8

Table F2. Properties of Asphalt Used in Overlay in District 8.
 (Data supplied by SDHPT District 8 personnel)

	<u>Shipped to Project 11-3-82</u>	<u>Approved 12-7-84</u>
Laboratory No.	C82374790	C82375940
Viscosity at 140 F, Stokes	864	929
Viscosity at 275 F, Stokes		2.5
Penetration at 77 F	90	93
Flash, C.O.C., F.	600+	600+
Specific Gravity at 77 F	1.025	1.027
Properties after T.F.O.T.:		
Viscosity at 140 F, Stokes		2264
Penetration at 77 F		50
Ductility at 77 F, cm		141*

Asphalt was AC-10, supplied by American Petrofina, Big Spring.

*Limit of test equipment without failure occurring.

Table F3. Aggregates Used in Surface Course Placed on SH 94 in District 11.*

Aggregates Used	Volume Percent	Weight Percent
Lightweight + #4**	23.0	17.0
Lightweight - #4**	39.0	29.0
Coarse Sand ***	24.0	34.3
Fine Sand ***	<u>14.0</u>	<u>19.7</u>
	100.0	100.0

- * Data supplied by SDHPT District 11 personnel
- ** Mostly retained on #10 sieve
- *** Mostly passing #10 sieve

Table F4. Project Design Gradation of Aggregates Used on SH 94 in District 11.*

Sieve Size	Percent Passing	
	Volume Percent	Weight Percent
1/2	100	100
3/8	98.9	98.6
4	63.3	65.9
10	38.4	54.3
40	32.2	45.5
80	15.9	22.2
200	4.4	5.9

- * Data supplied by SDHPT District 11 personnel

Table F5. Properties of Asphalt Used In Overlay in District 11.
 (Data supplied by SDHPT District 11 personnel)

	<u>Shipped to Project 4-22-83</u>	<u>Shipped to Project 4-27-83</u>	<u>Approved 5-3-83</u>
Laboratory No.	C83371601	C83371696	C83371893
Viscosity at 140 F, Stokes	2189	2137	1910
Viscosity at 275 F, Stokes			4.1
Penetration at 77 F	72	69	75
Flash, C.O.C., F	590	600+	600+
Specific Gravity at 77 F	1.032	1.030	1.031
Properties after T.F.O.T.:			
Viscosity at 140 F, Stokes			4253
Penetration at 77 F			50
Ductility at 77 F, cm			141*

Asphalt was AC-20, supplied by Texaco, Port Neches.

*Limit of test equipment without failure occurring.

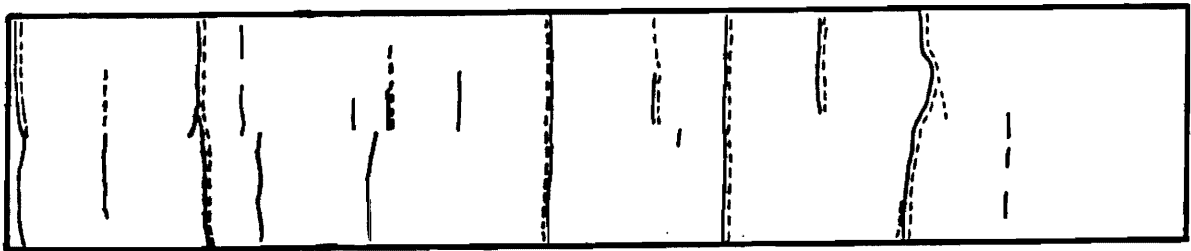
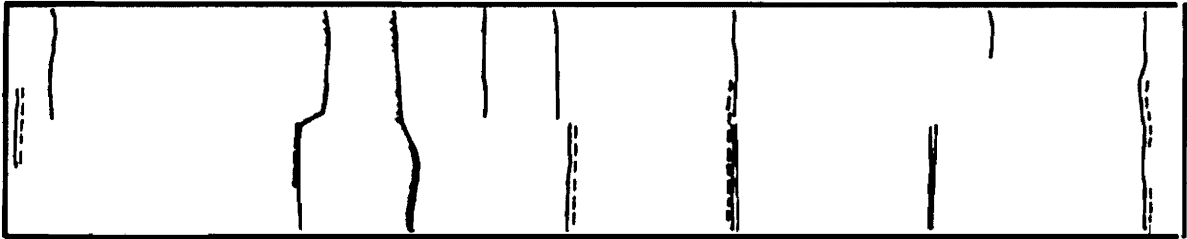
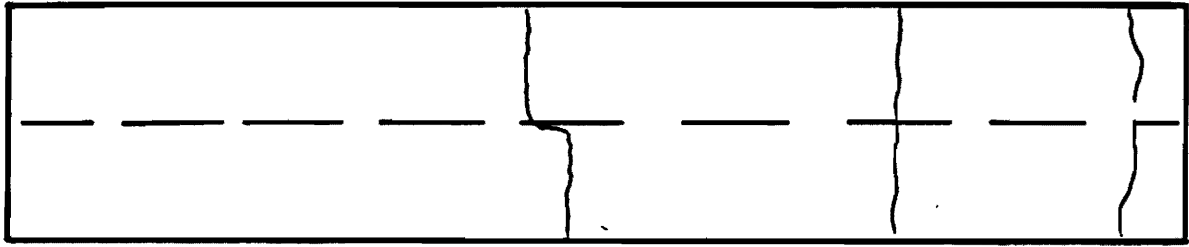


Figure F1. Typical Cracking Patterns Existing at Surface of US 83 Prior to Overlay (District 8).
(Dashed lines indicate cracks reflected through overlay.)

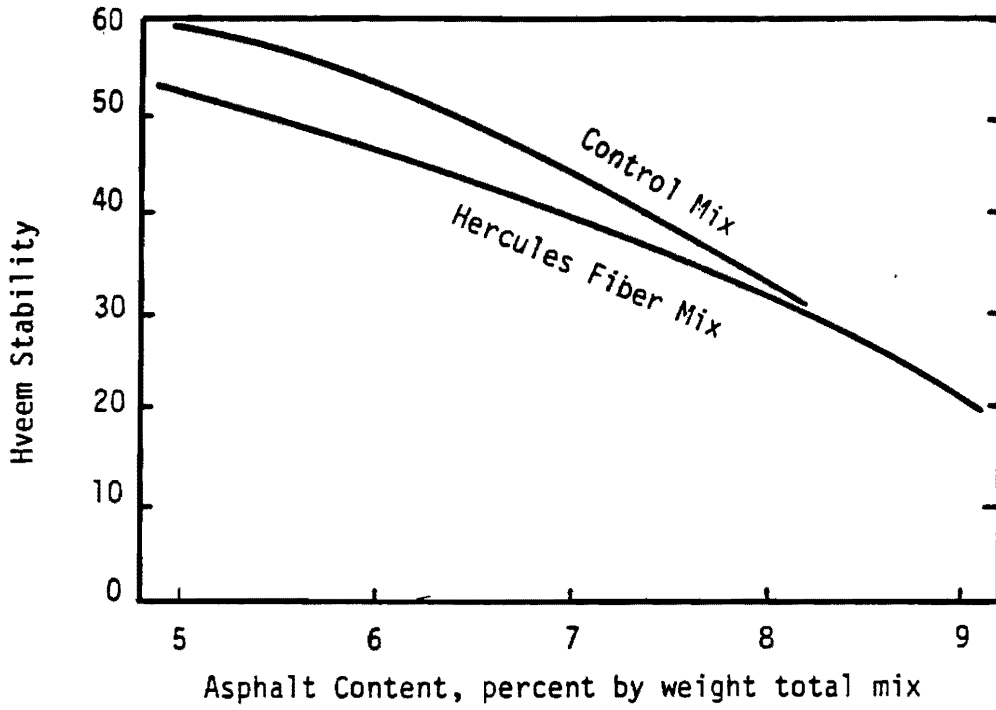


Figure F2. Hveem Stability Design Curves (data supplied by SDHPT, District 8).

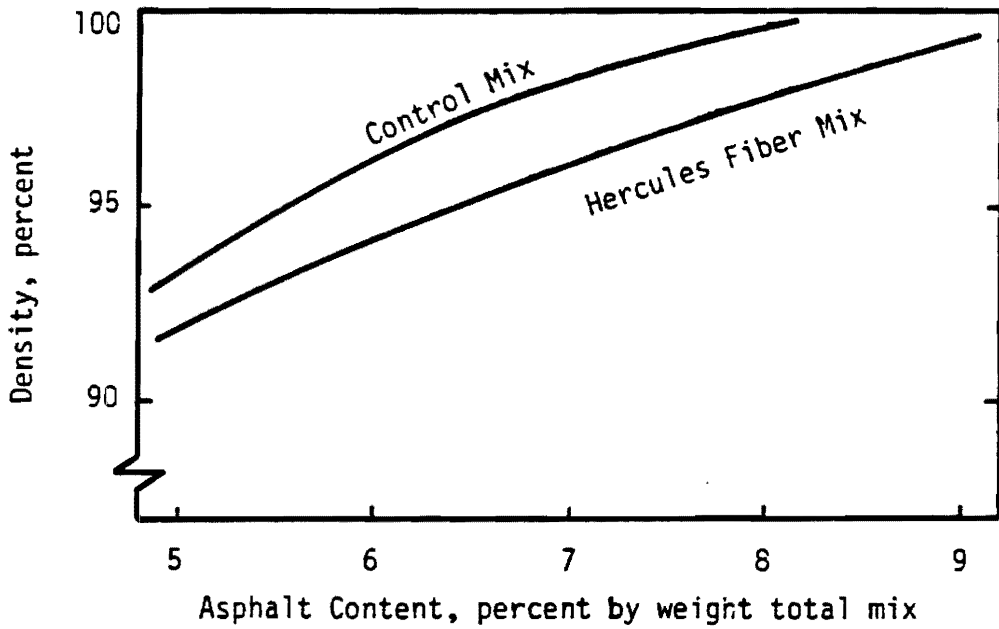


Figure F3. Design Curves - Percentage of Theoretical Maximum Density (data supplied by SDHPT, District 8).

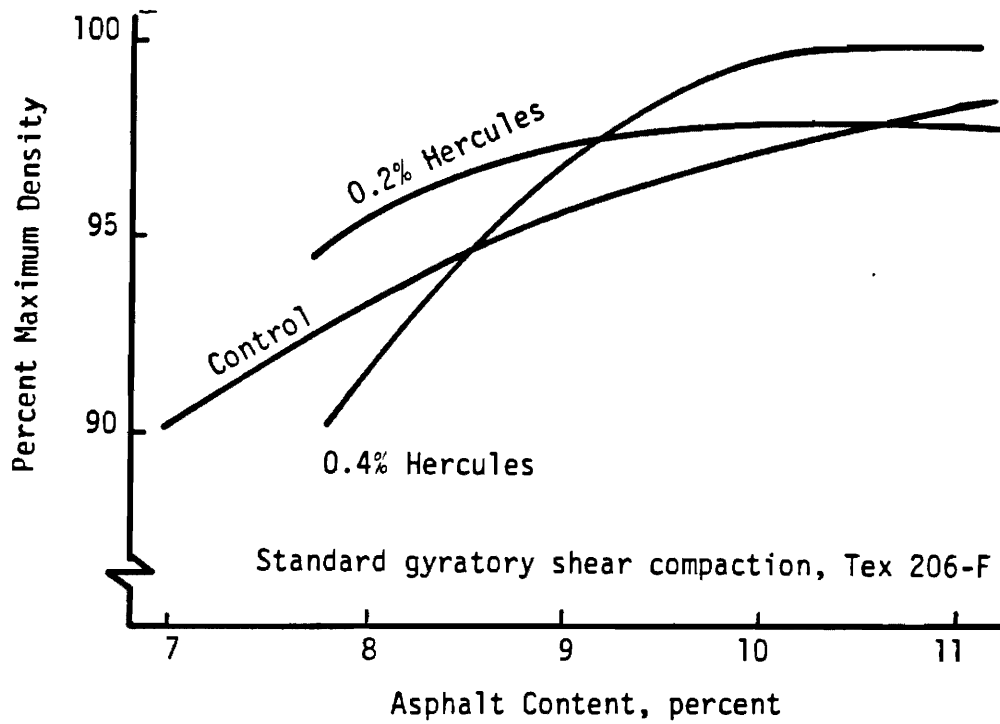


Figure F4. Density of Control and Hercules Fiber Mixtures as a Function of Asphalt Content - District 11.

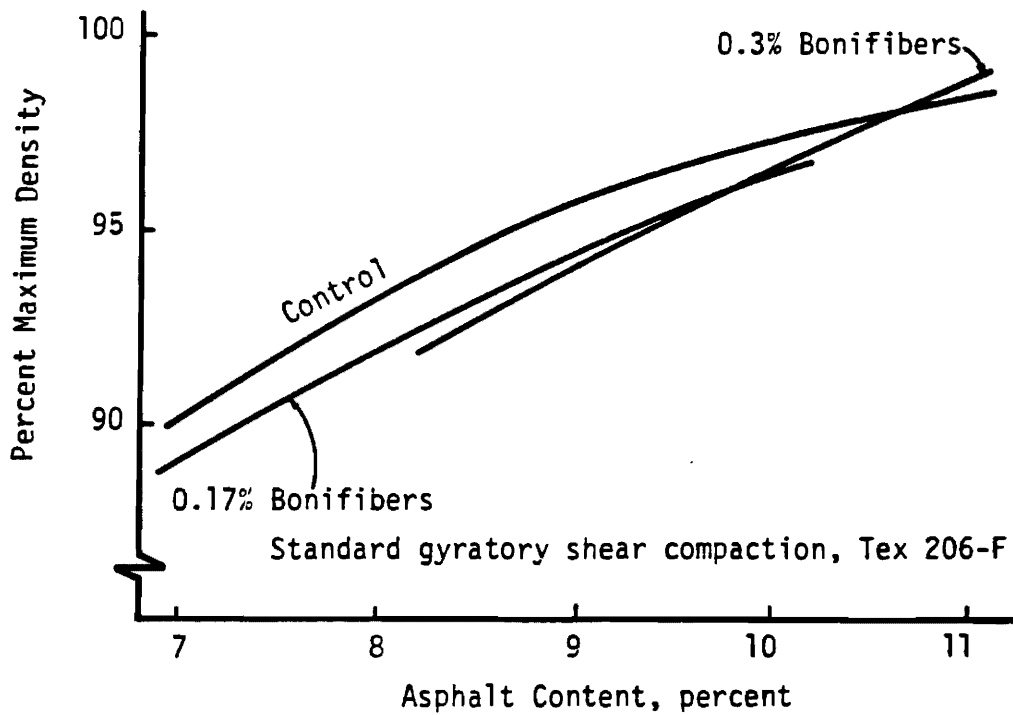


Figure F5. Density of Control and Bonifiber Mixtures as a Function of Asphalt Content - District 11.

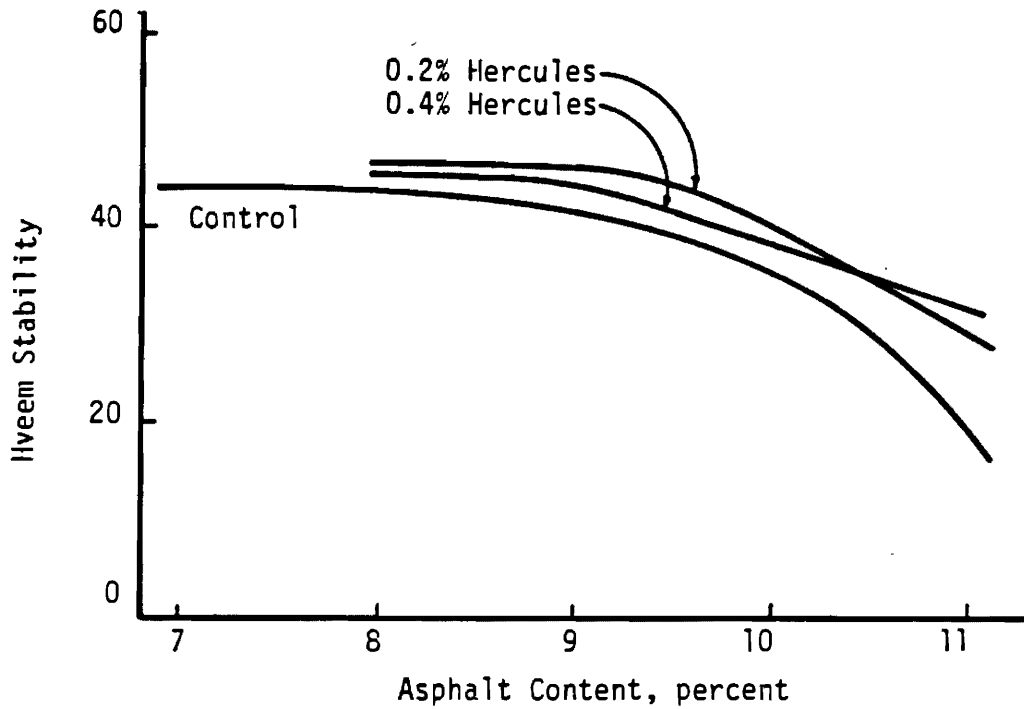


Figure F6. Hveem Stability of Control and Hercules Fiber Mixtures as a Function of Asphalt Content - District 11.

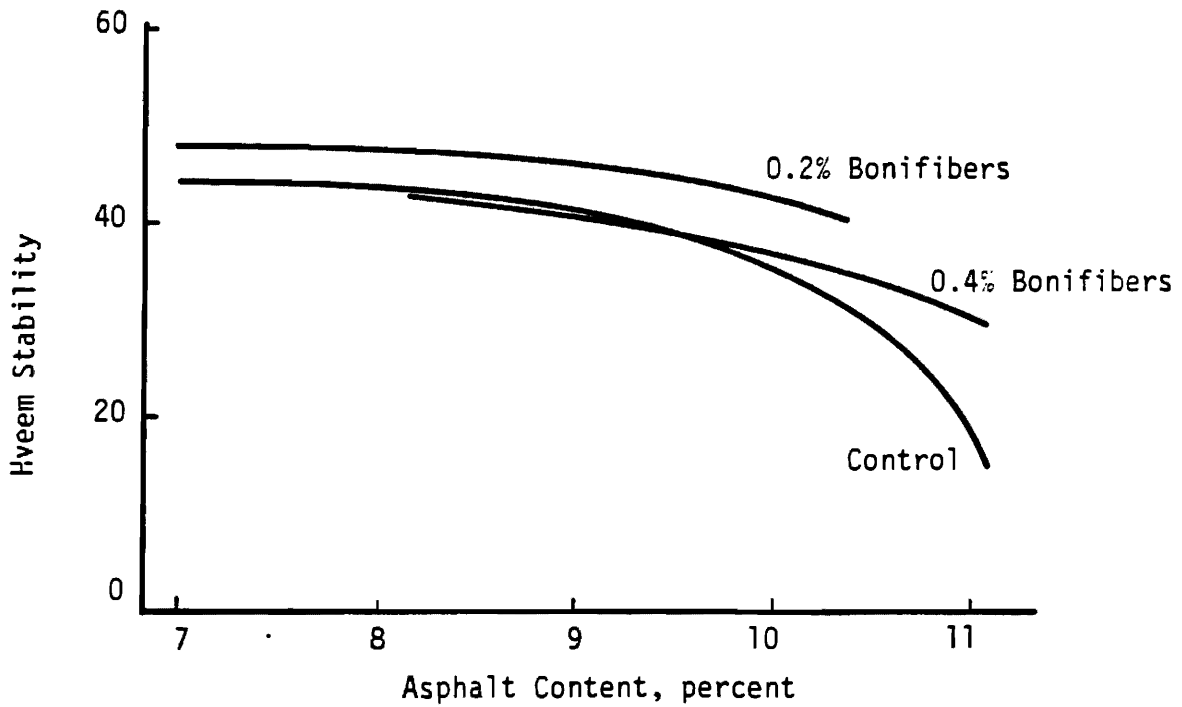


Figure F7. Hveem Stability of Control and Bonifiber Mixtures as a Function of Asphalt Content - District 11.

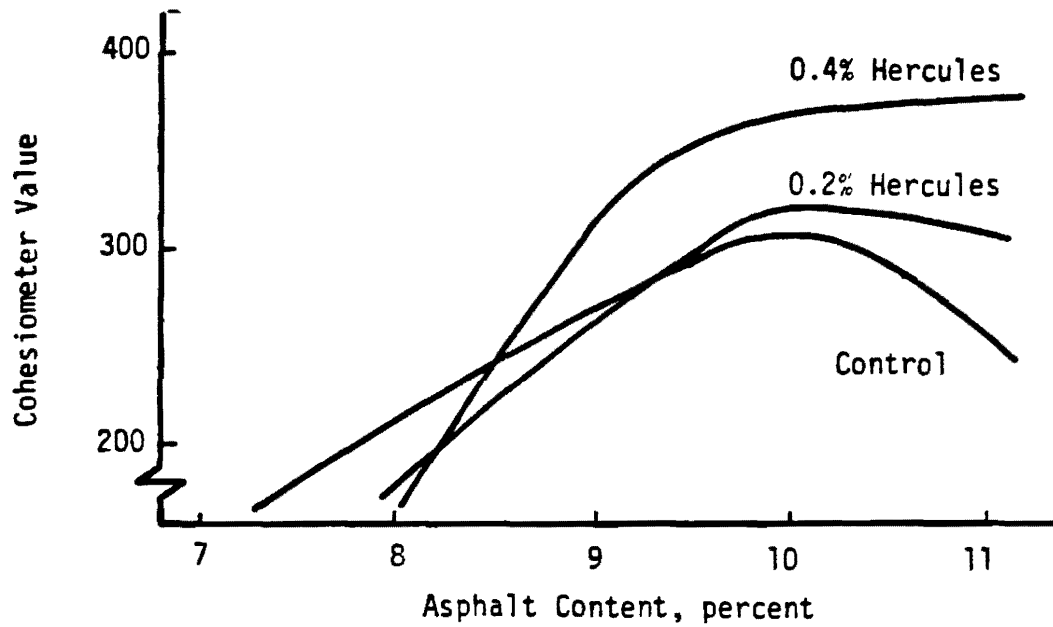


Figure F8. Cohesimeter Value as a Function of Asphalt Content for Control and Hercules Fiber Mixtures - District 11.

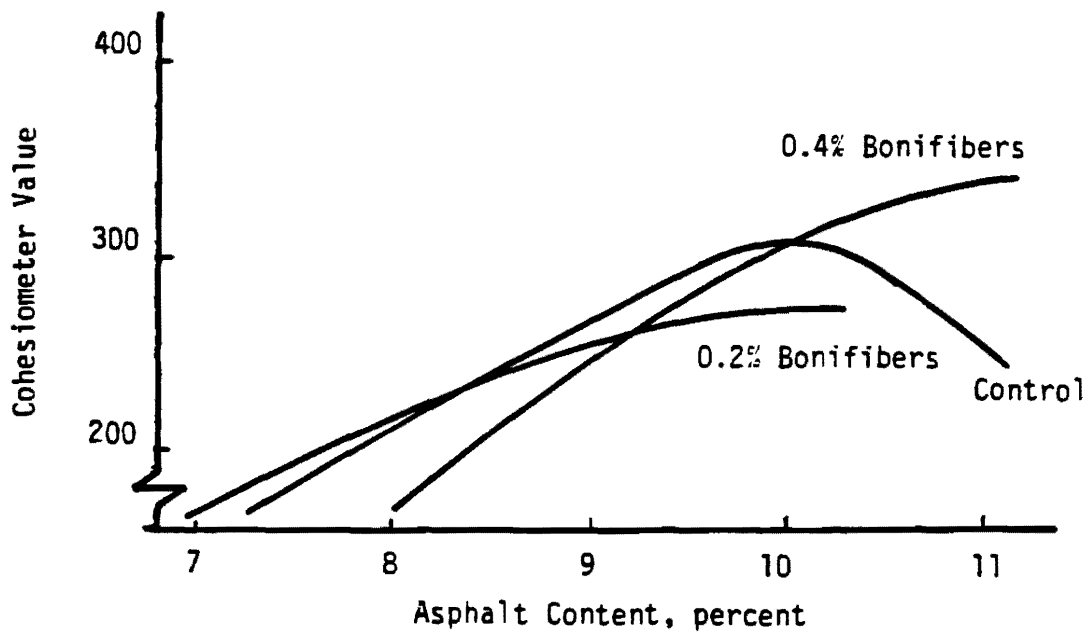


Figure F9. Cohesimeter Value as a Function of Asphalt Content for Control and Bonifiber Mixtures - District 11.